CeSMS2024

SAS2024 Satellite Meeting in Kitakyushu

～Fusion of Physics, Chemistry, Simulations, and Scattering～

Sponsor: U.S. ARMY
FSBL03XU
Kitakyushu City
QBAA (Quantum Beam Analyses Alliance)
The society of Polymer Science, Kyushu
Kitakyushu Convention & Visitors Association
The society of Polymer Science, Japan

Date: October 30, 2024 (Wed) 8:50～17:00

October 31, 2024 (Thr) 9:00～16:00

Venue: Kitakyushu International Conference Center

Advisory Board: Moonhor Ree, Mitsuhiro Shibayama, Hajime Tanaka, and Toshiji Kanaya

International Committee: Ian Hamley, Byeongdu Lee, and Hsin-Lung Chen

Local Committee: Shinichi Sakurai, Mikihito Takenaka, Satoshi Koizumi, Tsukasa Miyazaki, Katsuhiro Yamamoto, Maiko Nishibori, Tomoki Nishimura, Isamu Akiba, Yuichi Masubuchi, and Kazuo Sakurai (chair)

Contact us:
CeSMS2024 Organizing Committee: cesms2024@gmail.com

Program

CeSMS2024 Program

October 30, 2024 (Wed)

	Room A (International Conference Room)	Room B (Conference Room #21)
8:50	Opening Address (Kazuo Sakurai)	
	Chair : Isamu Akiba	
9:00－ 9:30	**Reidar Lund** Mechanism for Molecular Exchange Kinetics in Block Copolymer Micelles with Amorphous and Crystalline Cores	
9:30－10:00	**Quan Chen** Nonlinear Rheology of Associative Polymers: Role of Strain-induced Dissociation and Reassociation	
10:00－10:20	Coffee Break	
	Chair : Shinichi Sakurai	Chair : Tomoki Nishimura
10:20－10:50	**Cecilia Leal** Structural and Mechanical Properties of Phospholipid Membranes Hybridized with Synthetic Polymer Rafts	**Kazunori Sugiyasu** Precision Supramolecular Polymerization
10:50－11:20	**Shintaro Nakagawa** Structure-Mechanical Property Relationship in Highly Homogeneous Polymer Networks	**Kazuo Sakurai (10:50～11:10)** Monodisperse Micelles with Discrete Aggregation Numbers: Discovering the Platonic Micelle
11:20－11:40	**Atsushi Takano** Helical Microphase-Separated Structures formed from Multiblock copolymers	**Ramanathan Nagarajan (Invited 11:10～11:40)** Criterion for Forming Strucrurally Precise Nanoparticle by Self-assembly
11:40－12:00	**Ken Kojio** Deformation Behavior of Body-Centered Cubic Lattice Formed in ABA-type Triblock Copolymer	**Nobuyoshi Miyamoto** Monodisperse Nanosheet Mesophases
12:00－14:00	Lunch & Poster Session	
	Chair : Ken Kojio	Chair : Kazuo Sakurai
14:00－14:30	**Hironori Marubayashi** Structure and Dynamics of Crystalline Soft Materials Revealed by Diffraction and Scattering Techniques	**Byeongdu Lee** SAXS and SANS Studies on Competitive Adsorption of Polymer Chains onto Polymer Upcycling Catalysts
14:30－15:00	**Katsumi Hagita** MD Simulations of Spontaneous Crystallization and Scattering Images of Semicrystalline Polymers	**Emiko Mouri** Time Evolution of the Inner Structure of Colloidal Nanosheets Developing Structural Color
15:00－15:20	**Shinichi Sakurai** Synchrotron WAXD Studies on Strain-Induced Crystallization of Vulcanized Natural Rubber	**Mina Sakuragi** Deformation Behavior of Transfersomes Dispersed in Deep Eutectic Solvent during Stratum Corneum Penetration
15:20－15:40	**Yukiko Tamura** Selectively Remaining Outer Adsorption Layer on Top of Inner Adsorption Layer of SBR	**Yusuke Sanada** Reentrant Behavior of Bovine Serum Albumin with Multi-Valent Cation: Effects of Coexistence of Monovalent Cation
15:40－16:00	Coffee Break	
	Chair : Hironori Marubayashi	Chair : Isamu Akiba
16:00－16:20	**Yuichi Masubuchi** Phantom Chain simulations for the Rupture of Star-Polymer Networks	**Yuji Higaki** Double Hydrophilic Nano-Scale Compartment Produced by Microphase Separation of Zwitterionic Block Copolymers
16:20－16:40	**Filip Uhlik** Theory and Simulations of Branched Gels	**Shunji Kosaka** Synthesis and Function of Artificial Ion Channels Based on Thermoresponsive Amphiphilic Block Copolymers
16:40－17:00	**Ken Terao** Nanostructure Formation Behavior of Branched Poly(N-isopropylacrylamide) s in Water	**Akihito Hashidzume** Synthesis and Functions of Dense Triazole Polymers

18:00－	Banquet (Mikuni World Stadium)

October 31, 2024 (Thr)

	Room A (International Conference Room)	Room B (Conference Room #21)
	Chair : Kazuo Sakurai	
9:00－ 9:30	**Takaya Terashima** Precise yet Dynamic Self-Assembly of Amphiphilic Polymers into Nanostructured Soft Matter	
9:30－10:00	**Duyeol Ryu** Photoplastic and Photodielectric Properties in Microdomain Orientation using Self-healable Block Copolymer	
10:00－10:20	Coffee Break	
	Chair : Yuichi Masubuchi	Chair : Maiko Nishibori
10:20－10:50	**Ryohei Seto** Particle Simulation and Continuum Modeling for Dense Suspension Flows	**Arthi Jayaraman** Machine Learning-based Computational Analyses of Small-angle Scattering Results
10:50－11:20	**Qian Huang** The Influence of Chemical Side Groups and Molecular Architecture on Extensional Rheology of Polymer Melts	**Tsuyoshi Koga** Theoretical, Computational and Data Science Studies on Structure Formation of Polymers
11:20－11:40	**Satoshi Sawada** Evaluating crosslinking structures by small-angle neutron scattering measurement of sulfur crosslink-controlled rubber	**Daichi Ida** Wide-angle X-ray Scattering from Aqueous Solutions of Non-ionic Polymers
11:40－12:00	**Shigeru Deguchi** Baroplastics: Pressure-Resnponsive Block Copolymers as Sustainable Plastics	**Ying-Jen Shiu** Revealing the Solution Conformation and Hydration Structure of Type I Tropocollagen using X-ray Scattering and Molecular Dynamics Simulation
12:00－12:20	**Kakeru Obayashi** Analysis of Multiscale Structure of Epoxy Adhesive with Various Crosslink Density in the Single-lap Joint	**Hai Huang** Conformational Studies on Arabinogalactan by SAXS
12:20－14:00	Lunch & Poster Session	
	Chair : Mikihito Takenaka	Chair : Isamu Akiba
14:00－14:30	**Jaewook Nam** Rheological Insights and Coating Challenges in Battery Electrode Manufacturing	**Yoshinori Nishino** Damage-free 100-nm-Localized SAXS Analysis of Ionomers using X-ray Free-Electron Lasers
14:30－15:00	**Masanobu Naito** Data-driven Polymer Development toward Circular Economy	**Jia-Jhen Kang** Optimization of the in-line SEC-MALS-RI at the Small-Angle Neutron Diffractometer KWS-2
15:00－15:20	**Yu-Hung Cheng** Tuning the Complex Spherical Phase of Sugar-based Block Co-oligomer via Physical Blending	**Yuichi Takasaki** Introduction of Stat-of-the-art Laboratory SAXS System
15:20－15:40	**Mikihito Takenaka** Strain-Induced Enhancement of Density Fluctuation in Glassy Materials	**Maiko Nishibori** Structural Characterization of Food Materials through Small-angle X-ray Scattering at NanoTerasu
15:40－16:00	Closing & Poster Award Ceremony (Kazuo Sakurai)	

Poster Presentation

(Oct 30 12:00-14:00, Oct 31 12:20-14:00 at Hall next to the RoomA)

P01 Junsu Kim
Silicon- and fluorine-containing block copolymer films featuring sub-10 nm perpendicular lamellae and electric field induced directed assembly

P02 Mingeun Park
Defect-Free Block Copolymer Self-Assembly Facilitated by Structural Coloration for Providing Solar Cell Distributed Bragg Reflectors

P03 Kazuki Ito

P04 Yuki Nakama
Solvent Induced Chain Orientation of Cyclo Olefin Polymer Film

P05 Yasuhiro Eguchi
Microphase Separation of Dual Polysulfobetaine Diblock Copolymer Aqueous Solutions

P06 Miyu Sato
Phase behavior of aqueous solution of poly(N-vinylpyrrolidone-co-acrylic acid)

P07 Yasuyuki Maki
Preferential Solvation of Lysozyme in Aqueous Solutions of Sugars or Polyols Studied by Small-Angle X-ray Scattering

P08 Yuri Tanimura
Activation of Macrophage Glucose Metabolism by Cocktail Administration of Nucleic Acid Drugs

P09 Shotaro Shinoda
Evaluating Skin Permeation Mechanisms of Microemulsions Dispersed in Thymol-based Deep Eutectic Solvents

P10 Sota Yoshitake
Physical property evaluation of a polysaccharide-nucleic acid complex containing two DNA molecules by Small-Angle X-ray Scattering (SAXS)

P11 Yusuke Hayashida
Analysis of structural change of the skin lamellae induced by bicelle using small-angle X-ray scattering

P12 Takuma Kojima
Characterization of drug-loaded monodisperse nanoparticles using small-angle X-ray scattering (SAXS)

P13 Mina Tanigawa
Structural analysis of PEG-modified bicelles and their stratum corneum penetration mechanism

P14 Nanako Shimada
Fractionation analysis of micelles composed of polyglycerol mono fatty acid esters by field flow fractionation and small-angle X-ray scattering

P15 Aya Fujimoto
A microdomain Structure of Polystyrene-b-polyisoprene-b-polystyrene Copolymers Prepared by Shear Press and Injection Molding during Mechanical Deformation

P16 Tomoki Kosugi
Development of Nanoparticles Capable of Encapsulating Large Amount of Drugs and Elucidation of the Encapsulation Mechanism

Invited Speakers

Optimization of the *in-line* SEC-MALS-RI at the Small-Angle Neutron Diffractometer KWS-2

J. Kang[a,*], H. Iwase[b], G. Brandl[a], C. Lang[a], R. Biehl[c] and A. Radulescu[a]

[a]*Jülich Centre for Neutron Science at Heinz Maier-Leibnitz Zentrum (JCNS-4), Forschungszentrum Jülich, Garching 85748, Germany*

[b]*Neutron Science and Technology Center, Comprehensive Research Organization for Science and Society (CROSS), Tokai, Ibaraki, 319-1106, Japan*

[c]*Jülich Centre for Neutron Science (JCNS-1) & Institute of Biological Information Processing (IBI-8), Forschungszentrum Jülich, Jülich 52425, Germany*

An *in-line* size exclusion chromatography (SEC) setup is established at the small-angle neutron scattering (SANS) diffractometer KWS-2 as a new sample environment serving to deliver freshly eluted sample for SANS data collection. The present work describes the establishment and the performance of the *in-line* SEC option.

Given the spatial restriction around the KWS-2 hutch, the development of the *in-line* SEC instrument is challenging in the sense that SEC is located 2.5 meters away from the SANS sample stage. In order to test on such arrangement and to quantify the possible sample dilution effect of the additional dead volume by the long capillary, an additional UV detector is installed on the SANS sample stage to provide information on the chromatography performance and the protein concentration at the neutron exposure position. Based on the experimental result, a small dilution was found after the eluted sample from SEC instrument flows through the capillary and reaches the SANS stage, and, judging by the similar FWHM of the main elution peak, the chromatography resolution stays almost unchanged. Using 10 mg/ml of bovine serum albumin solution (injection volume 200 µl) for performance examination, a dilution factor for its monomer was found to be 3.4, which is comparable to other SEC-SAXS and SEC-SANS instruments worldwide.

The setup can be further combined with the multi-angle light scattering (MALS) machine followed with a refractive index (RI) detector, which envables the determination of molar mass of the eluted sample.

The presented examination measurements all together show that the described *in-line* SEC-MALS-RI at KWS-2 is ready for a testing with neutron in the near future, and it will be open to the user community soon after the testing.

Submitting Author: kathykang53@gmail.com

Structural and mechanical properties of phospholipid membranes hybridized with synthetic polymer rafts

Nurila Kambar, James Tallman, Antonia Statt and Cecilia Leal*

Department of Materials Science and Engineering, University of Illinois at Urbana-Champaign, USA

There is a long-term interest in creating artificial biomimetic membranes where self-assembled phospholipid bilayers are selectively permeabilized by synthetic channel-like molecules. One example is the co-assembly of amphiphilic block-copolymers with phospholipids into a hybrid membrane. Hybrid phospholipid block-copolymer bilayers display many properties seen in biomembranes such as selective transport phenomena, synergistic elastic properties, and structural phase transformations. Just like in biomembranes, these fundamental properties of hybrid bilayers are often regulated by lateral phase separation. Understanding the molecular and physical cues that determine the formation of rafts or domains in hybrid membranes, their size, and morphology is paramount to elucidating and programming their function. Employing a combination of coarse-grained molecular dynamics simulations and high-resolution cryogenic electron microscopy, we discovered that phosphatidylcholine-cholesterol bilayers hybridized with poly(butadiene-*b*-ethylene oxide) develop two distinct phase-separated morphologies. At molar fractions of polymer above 10 mol % the expected molecular distribution into lipid-rich and polymer-rich domains is observed. However, at low polymer content, a new structure develops in which the bilayer leaflets unzip (but remain continuous) to incorporate nanodomains of hydrophobic butadiene globules. We conjecture that unzipping is energetically more favorable than sustaining the hydrophobic mismatch between butadiene blocks and phospholipid acyl chains. These findings offer new insights into the morphology of biomembranes upon insertion of transmembrane proteins with bulky hydrophobic residues.

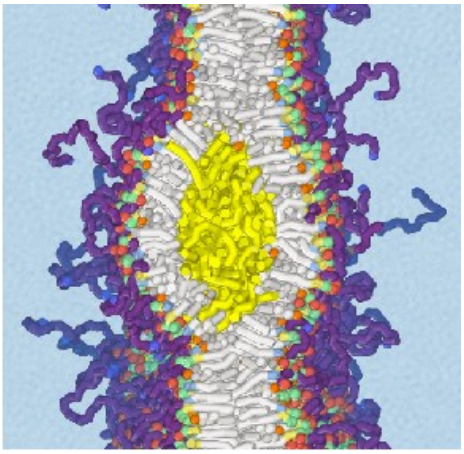

Figure 1: Polymer-lipid hybrid membrane.

Submitting Author: cecilial@illinois.edu

Exploring Competitive Adsorption Behavior of Polymer Chains in Silica Nanopores by Small Angle Neutron Scattering (SANS)

Xuchun Wang and Byeongdu Lee*

X-ray Science Division, Argonne National Laboratory, 9700 S. Cass Ave., Lemont, IL 60439, USA

Nowadays, the billions of tons of plastic production and mismanagement of end-of-life waste plastic, incinerated or landfilled, cause severe environmental pollution and safety issues for humans and wildlife. Chemical upcycling is one of the strategies to convert waste plastics into value-added products. Among numerous catalysts, processive hydrogenolysis catalysts, featuring metal nanoparticles (e.g., Pt) embedded at the base of cylindrical silica nanopores, exhibit the ability to repeatedly cleave polymer chains, yielding value-added hydrocarbon products with carbon number ranging from 10 to 30.[1-3] To enable the processive mechanism, the mesoporous shell should exhibit a preference for adsorbing longer polymers. This ensures that virgin chains (long polymers) remain at active sites for extended periods, increasing the likelihood of cleavage, while cleaved chains exit swiftly to avoid secondary cleavage. Thus, we hypothesize that competitive adsorption occurs among polymer chains of varying lengths within spatially constrained nanopores.

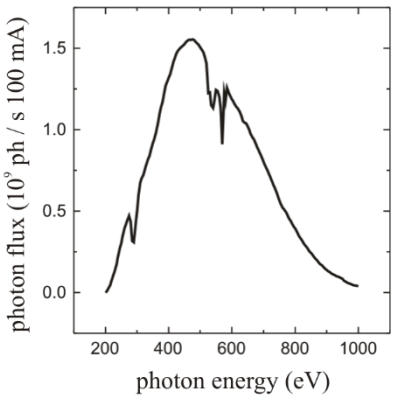

Figure 1: Example of a figure.

This research [3-4] presents a model study aimed at elucidating the competitive adsorption behavior of binary blends with distinct molecular weight in melting state, mimicking conditions akin to the intermediate stage of the catalytic reaction. Taking advantage of the contrast difference between hydrogenous and deuterated polymers in the neutron beam, we utilized small angle neutron scattering (SANS) to measure the relative composition of the polymers within the silica nanopores. Our findings demonstrate preferential adsorption of longer chains within the silica nanopores, which is consistent with the theoretical prediction in the literature for the case of the enthalpic attraction between polymers and pore walls.

References

[1] A. Tennakoon *et al.*, *Nat. Catal*. **3**, 893-901 (2020).
[2] X. Wu *et al*, *J. Am. Chem. Soc*. **144**, 5323-5334 (2022).
[3] X. Lyu *et al*, *ACS Appl Mater Interfaces* **15**, 27369–27379 (2023).
[4] X.Wang *et al*, *Macromolecules* ASAP (2024)

Submitting Author: blee@anl.gov

Rheological Properties of Battery Anode Slurry

Jaewook Nam[a, b*], Nayeon Park[a], Hyunjoon Jung[a] and Cheolheon Hyun[a]

[a] Department of Chemical and Biological Engineering, Seoul National University, 1 Gwanak-ro, Gwanak-gu, Seoul, 08826, Korea

[b] Institute of Chemical Process, Seoul National University, 1 Gwanak-ro, Gwanak-gu, Seoul, 08826, Korea

Understanding the rheological properties of lithium-ion battery slurries is crucial for optimizing electrode manufacturing processes. We present a comprehensive analysis of anode slurries, highlighting the significant influence of time and shear rate scales on their behavior. Our investigation reveals that these slurries exhibit a range of rheological phenomena, including yielding, thixo-viscoelastic, and shear-thinning or shear-thickening behaviors, depending on the applied stress and shear rate ranges. The Maxwell model, combined with thixotropic effects, provides valuable insights into both the short-term viscoelastic response and long-term thixotropic behavior of these materials [1]. While shear-thinning behavior was observed in the high shear rate ranges of model slurries with moderate solid content, it is noteworthy that highly concentrated graphite slurries exhibited shear-thickening behavior [2]. This shear-thickening phenomenon is closely related to anti-thixotropy and is attributed to the formation of a frictional contact network. Flow reversal tests indicate that this network partially persists even after flow cessation, possibly due to hydrophobic interactions. Our findings contribute to a deeper understanding of the intricate rheological behavior of battery slurries, encompassing yielding, thixotropy, viscoelasticity, and shear thinning or thickening. This comprehensive approach, emphasizing the roles of time and shear rate scales, allows for the extension of these insights to various types of battery slurries. The presented research lays a solid foundation for optimizing industrial electrode manufacturing processes and opens avenues for further detailed investigations in this critical field.

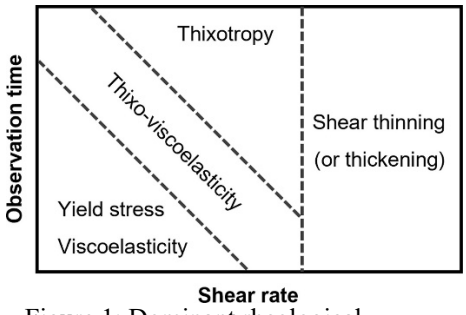

Figure 1: Dominant rheological properties of Li-ion battery anode slurry depending on time and shear rate scales.

References

[1] N. Park *et al., J. Power Sources*, **608** (2024).

[2] H. Jung *et al.,* Manuscript in preparation.

Submitting Author: jaewooknam@snu.ac.kr

Revisiting the Tensile Behavior of Dual Crosslinked Poly(vinyl alcohol) Gel

Jian Tang[a] and Quan Chen[*]

State Key Laboratory of Polymer Physics and Chemistry, Changchun Institute of Applied Chemistry, Chinese Academy of Sciences, Changchun, 130022, CHINA

The tensile test is a crucial method for assessing the mechanical properties of polymer gels. Prior research has shown that the initial strain rate significantly influences the tensile behavior of dual crosslinked gel. However, the connection between microscopic structural evolution and macroscopic tensile behavior has yet to be better understood. For example, Mayumi et al. found that the tensile behavior is highly strain-rate dependent for dual crosslinked poly(vinyl alcohol) (PVA) hydrogel containing chemical and physical crosslinks. They also observed the normalizable reduced stress representing the typical sticky Rouse behavior, i.e., stress scale with t^-0.5. In this study, we revisit the results of Mayumi et al. by examining the linear shear rheology and the nonlinear tensile properties of the same model system studied by Mayumi et al.. Our findings indicate that the relative values of the Hencky strain rate, the sticker dissociation rate, and the terminal relaxation rate of polymer chains govern the tensile behavior during the transition from nonlinear into linear viscoelastic regimes. This transition, as shown in Figure 1, is due to the decrease of the Hencky strain rate during the tensile test with the fixed engineering strain rate. Details will be presented on-site.

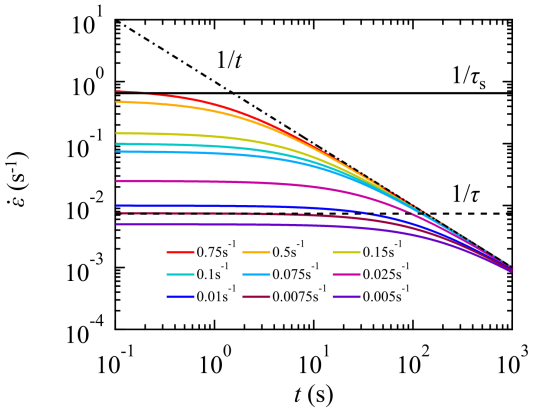

Figure 1: Predictions of time t dependences of Hencky strain rate $\dot{\varepsilon}(t)$ for samples with various intial strain rates. Solid and dashed lines represent the dissociation rate of the stickers and the relaxation rate of chains near equilibrium, respectively. Dashed-dotted-dashed line represents t dependence of $1/t$.

References

[1] K. Mayumi *et al.*, *ACS Macro Lett.* **2**, 1065–1068 (2013).
[2] X. Hu *et al.*, *Macromolecules* **50**, 652–659 (2017).
[3] Q. Chen *et al.*, *J. Rheol.* **57**, 1441–1462 (2013).
[4] L. G. Baxandall *et al.*, *Macromolecules* **22**, 1982–1988 (1989).

Quan Chen: qchen@ciac.ac.cn

Mechanism for Molecular Exchange Kinetics in Block Copolymer Micelles with Amorphous and Crystalline Cores

Reidar Lund [a] *

[a]Department of Chemistry, University of Oslo, 0314 Oslo, NORWAY.

Self-assembled systems, such as micelles, rely on various dynamic processes to achieve thermodynamic equilibrium. A primary mechanism for this equilibration process is molecular exchange, characterized by the continuous expulsion and insertion of unimers. However, this activated diffusion process is often slow or even arrested due to significant kinetic barriers, resulting in poorly defined, non-equilibrium structures in block copolymer systems. While the kinetics of micelle equilibration have been extensively studied, the focus has predominantly been on micelles with amorphous or liquid-like cores. When it comes to micelles with crystalline cores, additional challenges arise, including cooperative interactions, limited chain mobility, and confinement effects.

In this study, we employ two model systems: amorphous poly(ethylene-alt-propylene)-(polyethylene oxide) (PEP-PEO) and partly crystalline n-alkyl-PEO (Cn-PEO), both nearly monodisperse polymers in aqueous solutions. Early studies show that even low chain polydispersity gives rise to pseudo-logarithmic, extremely broad relaxation patterns, which can be related to the hypersensitivity of the chain length during the rate-determining expulsion step [1,2]. Utilizing small-angle X-ray scattering (SAXS/SANS), NMR, densitometry, and differential scanning calorimetry (DSC), we uncover a first-order phase transition in the micellar cores of Cn-PEO, analogous to the melting of a rotator-phase rather than a well-defined crystalline phase [4]. Fascinatingly, confinement induces a reduction in melting points that can be perfectly described by the Gibbs-Thomson equation [5].

Exploring molecular exchange kinetics through time-resolved small-angle neutron scattering (TR-SANS) [1,2,6], we elucidate the cooperative nature of the melting transition within confined micellar cores, contrasting with a decoupled, unimeric exchange process [7]. Crossing the melting point triggers a discrete change in activation energy. Furthermore, by co-assembling Cn-PEO with varying n-alkyl lengths, we demonstrate the tunability of melting points and, consequently, cooperativity, while the expulsion process remains non-cooperative.

Finally, we investigate "telechelic polymers" based on Cn-PEO-Cn, which form clustered micelles. [8] The results show that, unlike regular micelles, the kinetics occur in a multistep process involving a novel collision-induced single-molecule exchange mechanism. In this presentation, we will provide an overview of the major results from the last two decades, discuss these mechanisms in light of theoretical predictions, and outline future challenges.

References

[1] Lund, R. et al *Phys. Rev. Lett.* **2006**, *96* (6), 068302–068304.
[2] R. Lund, R.; Willner, L.; Richter, D. *Adv. Polym. Sci.* **2013**, *259*, 51–158.
[3] T. Zinn *et al*., *Soft Matter*, **2014**, 10, 5212.
[4] N. König et al. *Macromolecules* **2020**, *53* (23), 10686–10698.
[5] T. Zinn et al. *Phys. Rev. Lett.* **2014**, *113* (23), 238305–5.
[6] T. Zinn, et. Al *ACS Macro Lett.*, **2015**, 4, 651–655.
[7] N. König et al. Phys. Rev. Lett., **2019**, 122, 078001.
[8] N. König et al. *Phys. Rev. Lett.* **2020**, *124*, 197801.

Submitting Author: Reidar.lund@kjemi.uio.no

Scatteirng Pattern Analysis of Polymer Materials using Molecular Dynamics Simulations

Katsumi Hagita[a*]

[a]Department of Applied Physics, National Defense Academy,
1-10-20, Hashirimizu, Yokosuka, 239-8686, JAPAN

Two-dimensional scattering patterns (2DSPs) provide rich structural information regarding crystallization, domain formation, and void growth (fracture) in polymer materials as well as filler morphologies in polymer nano composites [1]. Molecular dynamics (MD) simulations are promising tools to reveal molecular level behaviors of polymer materials. Recent improvements in computer performance have made it possible to perform MD simulations on systems large enough to calculate 2DSPs that can be compared with the experimerimental results. Recently, we performed large scale simulations for polymer crystallizations and gel network fractures with uniaxial deformations and evaluated their 2DSPs with the circular average.

Figure 1**a,b** shows 2DSPs of crystallized *cis*-1,4-polyisoprene (PI) and *isotactic* polypropyrene (iPP) melts in our MD simulations [2]. To reproduce the cystallizatin of PI and iPP melts (Figure 1**a,b**), we performed united atom MD simulations with TraPPE-UA force field in order to maintain backbone structures that was crucial to the crystallization indudece by stretching. For both PI and iPP, immediately after stretching, only the peak spots due to orientation were observed, although the peaks due to crystallization were not observed. As isothermal crystallization proceeded, the brightness of the peaks due to crystallization increased. We concluded that "orientation" and "crystallization" are separate phenomena.

Figure 1**c** shows 2DSP of stretched polymer network like gels obtained by coarse grained MD simulations using Kremer-Grest model with bond brekage [3]. These bright spots were originated from voids growth under uniaxial stretching. Recently, we confirmed the CGMD simulations with bond brekage is one of the important factors for the generation of hysteresis loop in the SS curve under multicycle deformation. We also investigated the relationship between the progression of network failure and changes in 2DSPs.

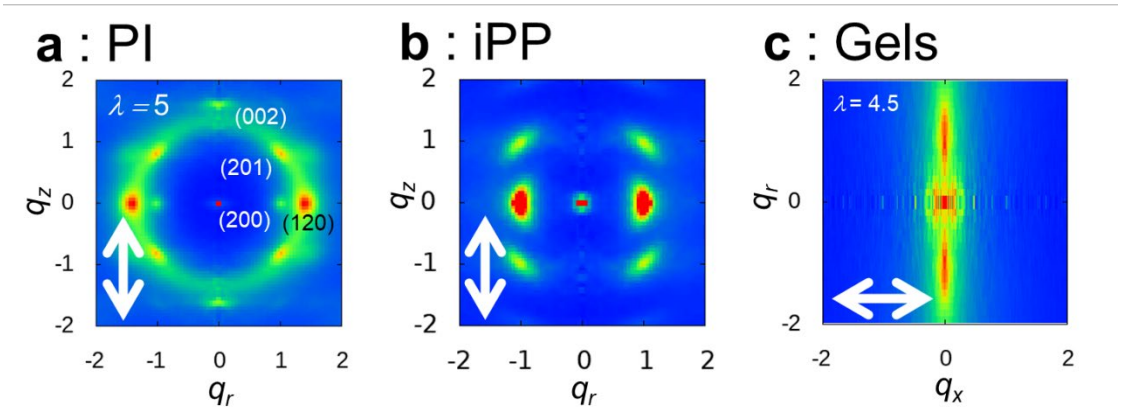

Figure 1: 2DSPs of the crystallized PI (a) and iPP (b), and polymer network (c) under uniaxial deformation.

References

[1] K. Hagita *et al.*, *Macromolecules* **56**, 4457–4467 (2023).
[2] K. Hagita *et al.*, *Under review.*
[3] K. Hagita *et al.*, *Under review.*

Submitting Author: hagita@nda.ac.jp

Machine Learning Based Computational Methods For Analyzing Small Angle Scattering Data From Soft Materials

A. Jayaraman[a,b], Z. Wu[a], C. Heil[a], N. Gupta[a,*] and S.V.R. Akepati[c,*]
[a]*Department of Chemical and Biomolecular Engineering, University of Delaware, Newark, DE 19716, USA*
[b]*Department of Materials Science and Engineering, University of Delaware, Newark, DE 19716 USA*
[c]*Master of Science in Data Science Program, University of Delaware, Newark, DE 19716 USA*

My research group's expertise lies in the development of physics-based molecular models and simulation methods as well as data-driven machine learning models for designing and characterizing soft macromolecular materials. In this talk, I will highlight examples from my group's recent work to showcase how we develop and use computational tools (e.g., CREASE [1-2], CREASE-2D [3], and PairVAE [4]) to interpret experimental characterization data from small angle scattering and electron microscopy. I will also show how we use these methods with experimental data that are either in the literature or shared by our collaborators in order to establish structure-property relationships (e.g., [5, 6]) for soft materials.

For interested researchers, we direct them to the *readme* documents for CREASE: https://crease-ga.readthedocs.io/en/latest/ and codes shared openly in https://github.com/arthijayaraman-lab

References

[1] C. M. Heil *et al.,* *ACS Central Science* **8**, 7, 996-1007 (2022).
[2] C. M. Heil *et al.*, *JACS Au* **3**, 3, 889–904 (2023).
[3] S.V.R. Akepati *et al., JACS Au* **4,** 4, 1570–1582 (2024).
[4] S. Lu and A. Jayaraman, *JACS Au* **3**, 9, 2510–2521 (2023).
[5] C. M. Heil *et al.*, *Science Advances* **9**, 21, 10.1126/sciadv.adf2859 (2023).
[6] A. Patil *et al.*, *ACS Materials Letters* **4,** 9, 1848–1854 (2022).

Submitting Author: arthij@udel.edu

Theoretical, Computational and Data Science Studies on Structure Formation of Polymers

Tsuyoshi Koga

Department of Polymer Chemistry, Kyoto University, Nishikyo-ku, Kyoto, 615-8510, JAPAN

In my presentation, I will talk about several research topics related to the characteristic structure formation and dynamics of polymer systems studied by using theoretical, computational and data science methods from the viewpoint of statistical-mechanical physics. Topics covered include the structure formation and rheological properties of associative polymers including self-sorting of amphiphilic polymers [1], the formation process of polyrotaxanes [2], the molecular mechanisms of baroplastics and so on.

[Associative Polymers] Hydrophobically modified water-soluble polymers (associative polymers) show characteristic properties due to the formation of various kinds of associated structures, such as intramolecular micelles, flower-type micelles, and physical gels. In the presentation, we will review recent developments in the study on the molecular origin of such structural and rheological properties by mainly using molecular dynamics simulations (Figure 1).

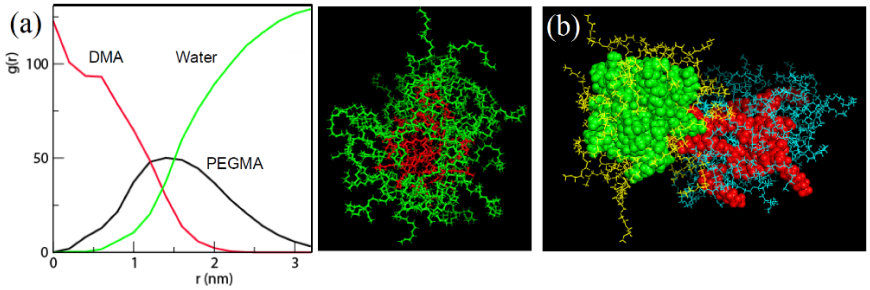

Figure 1(a) Number density profiles and a snapshot of intramolecular micelle of hydrophilic chains (PEGMA, green) with long hydrophobic side chains (DMA, red) by all-atom MD simulation. (b) Snapshot of a block copolymer of PEGMADMA (green) and PEGMA with short hydrophobic side chains (BMA, red).

[Polyrotaxanes] Cyclodextrin (CD) is capable of encapsulating various compounds in the hydrophobic space inside its ring structure, and this inclusion mechanism has been utilized in a wide range of applications, including drug transport, molecular recognition, and slide-ring gels. Polyrotaxanes have high filling ratio of CD that cannot be explained by a random inclusion process. To clarify the molecular mechanism behind this, we conducted research using statistical mechanical theory and molecular simulations, and found that hydrogen bonds between CDs play an important role in the formation of such inclusion complex (Figure 2) [2].

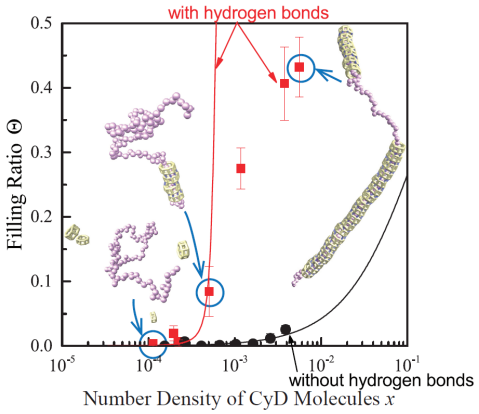

Figure 2 : The filling ratio in the presence (red) and absence (black) of hydrogen bonds. The symbols and solid lines show the results of the GCMC simulation and theoretical calculation, respectively. Pink spheres and cylinders indicate the polymer. Yellow cylinders and black lines indicate the CD molecules and the hydrogen bonds, respectively.

References

[1] Y.Hirai, T.Terashima, M.Takenaka, M.Sawamoto, *Macromolecules*., **49**, 5084-5091 (2016).

[2] T. Furuya, T. Koga, Polymer, 131, 193 (2017).

Tsuyoshi Koga: koga.tsuyoshi.6m@kyoto-u.ac.jp

Data-driven polymer design toward circular economy system

Masanobu NAITO[a] *

[a]National Instituete for Materials Science, 1-2-1 Sengen, Tsukuba, Ibaraki, 305-0047, JAPAN

The recent development of sequence-engineering in synthetic copolymers has led to the innovation of polymer materials. Short sequences, referred to as "codons" using an analogy to nucleotide triads, play crucial roles in expressing functions. However, the lack of efficient sequencing methods prevents the experimental determination of codon compositions, which hinders the integration of experiments and theories. To overcome this, a polymer sequencer based on mass spectrometry of pyrolyzed oligomeric fragments is proposed. Despite random fragmentation along copolymer main-chains, the characteristic fragment patterns of codons are identified and quantified through unsupervised learning of a spectral dataset of random copolymers. Codon complexities increase with length and monomer component number. By expanding the dataset, the data-driven approach accommodates the increasing complexities, enabling the quantification of codon compositions of binary triads, binary pentads, and ternary triads with small datasets (N<100). The sequencer can describe copolymers with their codon compositions/distributions, facilitating the sequence-engineering of innovative polymer materials. In this presentation, we will introduce our recent efforts to develop data-driven polymer materials using materials informatics and polymer smart labs.

References

1) Hibi Y, Uesaka S, Naito M.” A data-driven sequencer that unveils latent “codons” in synthetic copolymers”, Chem. Sci., 2023, **14**, 5619.

Submitting Author: cesms2024@gmail.com

Damage-free 100-nm-localized coherent SAXS analysis of fuel cell catalysts using X-ray free-electron lasers

Yusuke Ikuta[a], Akihiro Suzuki[a], Yoshiya Niida[a] and Yoshinori Nishino[a] *

[a]Research Institute for Electronic Science, Hokkaido University,
Kita 21 Nishi 10, Kita-ku, Sapporo 001-0021, JAPAN

The realization of a hydrogen society, where hydrogen serves as a clean and renewable energy source, is desired to reduce carbon dioxide emissions and achieve sustainable development. Polymer electrolyte fuel cells (PEFCs) are a key technology for automobiles in the hydrogen society. This study aims to analyze the nanostructures of the catalyst inks of PEFCs. In the catalyst layer, catalyst nanoparticles are supported on carbon and are thinly covered with an ionomer that facilitates proton conduction. We are particularly interested in examining the ionomer coating, which is important for PEFCs' performance but has been difficult to analyze.

We conducted coherent small-angle x-ray scattering (SAXS) measurements on PEFC catalyst inks using an 100-nm focused X-ray free-electron laser (XFEL) beam [1] with a photon energy of 4 keV at SACLA. The femtosecond XFEL pulses allowed us to perform radiation-damage-free measurements by outrunning major radiation-damage processes. Such damage-free measurements are highly valuable because radiation damage often poses challenges in high-resolution observation of ionomers using X-rays and electron beams. The measurements wer carried out for catalyst inks in both dried and solution states. The dried sample was prepared by dropping catalyst ink onto a silicon nitride membrane and air-drying it. The solution sample was enclosed in micro-liquid enclosure arrays [2] developed at Hokkaido University.

Experimental coherent SAXS data revealed contributions from the ionomer [3], which were previously thought to be difficult to capture due to strong X-ray scattering from the catalyst nanoparticles. Moreover, femto-second single-shot coherent SAXS data suggested spatial hetero-geneity in ionomer coating. To interpret the experimental data, we also performed simulations (Fig. 1) using an all-atom model based on reaction molecular dynamics calculations. To our knowledge, SAXS simulation on PEFC catalysts using an atomic model has notr been reported previously.

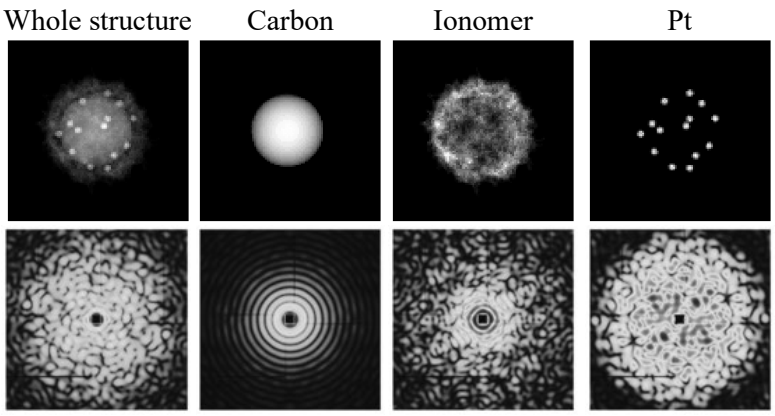

Figure 1: Simulation of coherent SAXS patterns (lower panel) of each component of catalyst ink (upper panel) using all-atom molecular dynamics calculation model.

References

[1] H. Yumoto, T. Koyama, A. Suzuki, Y. Joti, Y. Niida, K. Tono, Y. Bessho, M. Yabashi, Y. Nishino, and H. Ohashi, *Nature Commun.* **13**, 5300 (2022).
[2] T. Kimura, Y. Joti, A. Shibuya, C. Song, S. Kim, K. Tono, M. Yabashi, M. Tamakoshi, T. Moriya, T. Oshima, T. Ishikawa, Y. Bessho and Y. Nishino, *Nat. Commun.* **5**, 3052 (2014).
[3] Y. Ikuta *et al.*, *in preparation* (2024).

Submitting Author: yoshinori.nishino@es.hokudai.ac.jp

The Influence of Chemical Structures and Macromolecular Architectures on Extensional Rheology of Polymer Melts

Yiming Zhong[a], Yinrui Wang[a], Qian Huang[a*]

[a] *Polymer Research Institute, State Key Laboratory of Polymer Materials Engineering, Sichuan University, Chengdu 610065, CHINA*

Polymers are complex materials. While their monomers may have different chemical structures, the monomers can be further organized into different macromolecular architectures like linear, ring, star, comb, and dendritic shapes during synthesis. It is known that the rheological behaviour of polymer melts is very sensitive to macromolecular architectures. However, as the experimental data of nonlinear rheology especially the extensional rheology at large strains for model branched polymers is still rare, the link between the nonlinear rheological behavior and the macromolecular architectures is not fully understood. In addition, while the effect of chemical structures of the monomers is not considered in the classic tube model, a few experiments have already shown that chemical structures may influence the nonlinear extensional rheology significantly. But different even contrary explanations still exist.

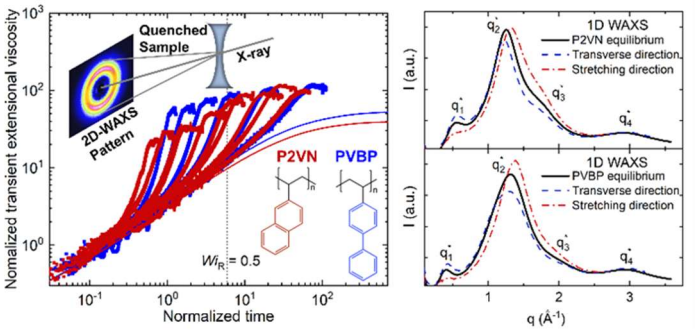

Figure 1: The transient extensional viscosity at different stretch rates of P2VN and PVBP melts (left), and the 1-D wide angle X-ray scattering results for the two melts at both equilibrium and stretched states (right).

Here we present two of our recent woks which study the influence of chemical structures and macromolecular architectures (i.e., at length scales smaller and bigger than an entangled strand, respectively) on extensional rheology of polymer melts [1, 2]. In the first work, we fix the macromolecular architecture to linear polymers, and investigate the influence of chemical structures. We compare polymer melts containing different aromatic rings in their side groups, where π-π stacking between neighbouring polymer chains may affect the rheological behaviour in extensional flow (Figure 1, left). The effect of π-π stacking is analyzed using *ex-situ* wide angle X-ray scattering (Figure 1, right). In the second work, we fix the chemical structure to polystyrenes (PS), and study the influence of macromolecular architectures.We start from the simplest branched architecture, i.e., star PS with one branch point only. We show that star PS melts with 8-10 arms behave differently from the star PS melts with 3 arms. Then the star PS melts are also compared with H and pom-pom PS melts which have two branch points.

References

[1] Y. Zhong *et al.*, *Macromolecules* **57**, 4833−4841 (2024).
[2] Y. Wang *et al.*, *ACS Macro Lett.* **13**, 812−817 (2024).

Submitting Author: qianhuang@scu.edu.cn

Criterion for forming structurally precise nanoparticle by self-assembly

Ramanathan Nagarajan

DEVCOM Soldier Center, Natick, MA 02461, USA

Multi-subunit proteins and enzymes are well known examples of structurally precise nanoparticles in the size range of 2 to 20 nm. The subunits may be identical as in alcohol dehydrogenase with 4 subunits or they may be different as in hemoglobin with 4 subunits of two kinds, aspartate carbamoyltransferase with 12 subunits of two kinds and G protein with 3 subunits of three kinds. The structural precision of these multi-subunit proteins (viewed here as nanoparticles) is enabled by the unique geometrical shapes of the subunits, the positioning of hydrophobic and hydrophilic regions on the surface, and the availability of hydrogen bonding and salt bridges formation that non-covalently link one subunit to another. Over the last decade, structurally precise aggregates formed from calix(n)arene amphiphiles, also referred to as Platonic micelles, have been reported in the literature. Their aggregation numbers are discrete, making them analogous to a multi-subunit protein. These aggregates are not stabilized by any non-covalent linkage between the molecules and their formation and stability is driven entirely by hydrophobic effect. Their structural precision, namely, their precise aggregation number is a consequence of how much of the hydrophobic surface of the amphiphile remains exposed to water when they self-assemble into aggregates. In this work, we explore how general this phenomenon of forming structurally precise amphiphilic aggregates can be, starting from common amphiphiles. The analysis of self-assembly of multi-tail amphiphiles each possessing multiple charges shows that by using the criterion of molecular packing and hydrophobic effect, structurally precise amphiphilic aggregates can be generally created via self-assembly.

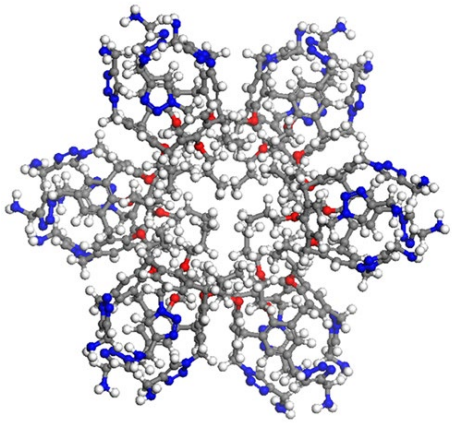

Figure 1: DFT based structure of micelle with aggregation number 6 from PACaL3, a calix[4]arene amphiphile, with primary amine head group and a propyl tail.

Ramanathan Nagarajan: ramanathan.nagarajan.civ@army.mil

.

Particle simulation and continuum modeling for dense suspension flows

Ryohei Seto

Wenzhou Institute, University of Chinese Academy of Sciences,
No.1 Jinlian Road, Longwan District, Wenzhou, Zhejiang, 325001, China

Viscoelastic fluids are non-Newtonian fluids characterized by their elastic structures and relaxation processes. However, what type of non-Newtonian fluid behavior emerges when solid particles are dispersed in a viscous liquid? Suspensions of fine solid particles, despite having much simpler components compared to polymer systems, have seen slow progress in the study of their rheology and constitutive modeling. This presentation aims to provide an overview of the current state of research on particle suspensions.

Particle suspensions have traditionally been studied within the framework of fluid mechanics. In dilute limits, a solid theoretical foundation exists based on hydrodynamics, making it a well-defined problem based on the Stokes equation—a comfortable starting point for applied mathematicians. However, when the volume fraction becomes finite, a crucial decision arises: should the particles be modeled as smooth spheres, which is a natural assumption? Typically, a no-slip boundary condition is applied at the particle surface. Under such idealization, the resistance coefficient diverges as particles approach each other, creating a singularity that has long hindered progress. Particularly for colloidal particles, it was once believed that the Brownian motion, considering the increasing viscous resistance in the limit of close particle approach, would prevent contact. The higher the Péclet number, the closer the system approaches this singularity, leading to an increase in the apparent viscosity—a phenomenon considered the mechanism behind shear thickening.

In reality, experimental evidence suggests that contact occurs even at finite Péclet numbers. Since real particle surfaces are not perfectly smooth, surface contact leads to interlocking, restricting tangential relative motion [1]. Even in systems without attractive forces that induce gelation, frictional contacts can create transient "bonds" during flow. This emergence of elastic structures from an otherwise freely moving particle system is the essence of the physics governing the flow behavior of dense suspensions.

Capturing the emergence of such elastic structures in a constitutive model is not straightforward. Existing models [2] for suspensions are rooted in the historical context mentioned above, involving components like affine deformations, hydrodynamic interactions, and closures that assume isotropy—all based on the fluid mechanical perspective. It is suggested that these models must explicitly address the emergence of elastic structures rather than the mere divergence of viscosity. Additionally, the volume fraction field acts as an internal degree of freedom within particle suspensions, and uniform dispersion cannot always be assumed under non-uniform flow.

Thus, there are still challenges to be addressed in the study of dense suspensions, which are of significant industrial relevance.

References

[1] C. Ness, R. Seto, and R. Mari. The physics of dense suspensions. Annu. Rev. Condens. Matter Phys., 13(1):97–117, March 2022.

[2] J. J. J. Gillissen, C. Ness, J. D. Peterson, H. J. Wilson, and M. E. Cates. Constitutive model for time-dependent flows of shear-thickening suspensions. Phys. Rev. Lett., 123:214504, Nov 2019.

Submitting Author: seto@wiucas.ac.cn

Repairable Cylindrical Microdomains from Block Copolymers Enabled by Photoplastic and Photodielectric Effects

Seungyun Jo, Hui Il Jeon, Seungbae Jeon, Taesuk Jun, and Du Yeol Ryu*

Department of Chemical and Biomolecular Engineering, 50 Yonsei-ro, Seodaemun-gu, Yonsei University, Seoul 03722, Republic of Korea

We present a *trans-cis* isomerization in cylinder-forming polydimethylsiloxane-*b*-poly((4(phenyldiazenyl)phenoxy)hexyl acrylate) (PDMS-*b*-PPHA) film that enables the generation of healable arrays over macroscopic distances. The *trans-cis* isomerization by UV light exposure brings about a significant increase in the dielectric constant and a dramatic decrease in the T_g of the PPHA block. Applying these photoplastic and photodielectric characteristics to an *in-plane* electric field, near-perfectly aligned cylindrical microdomains from *cis*-cast PDMS-*b*-PPHA film are obtained at low temperature of 40 ºC. To prevent dewetting of the BCP film at the ambient condition, visible light is exposed to cause *cis-trans* isomerization of the PPHA block, increasing the T_g to 54 ºC. Furthermore, the remarkable damage of 300-nm wide scratches on cylindrical arrays in *trans*-cast PDMS-*b*-PPHA film can be completely healed at 40 ºC upon UV light exposure and sequential electric-field application. [1]

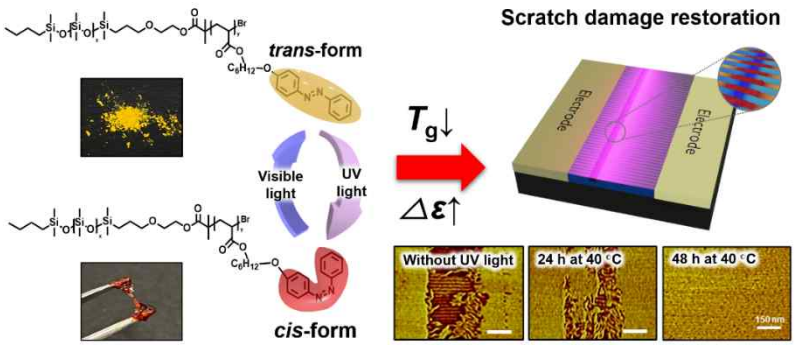

References

[1] H. I. Jeon, S. Jo, S. Jeon, T. Jun, J. Moon, J. H. Cho, H. Ahn, S. Lee, **D. Y. Ryu**, and T. P. Russell, "Repairable Macroscopic Monodomain Arrays from Block Copolymers Enabled by Photoplastic and Photodielectric Effects", *ACS Nano*, 17, 8367-8375 (2023)

Submitting Author: dyryu@yonsei.ac.kr

Living supramolecular polymerization as a tool for the syntheses of mesoscopic structures

Kazunori Sugiyasu*

Department of Polymer Chemistry, Kyoto University,
Kyotodaigaku-katsura, Nishikyo-ku, Kyoto 615-8510, Japan

Supramolecular polymers are expected in a variety of applications; nevertheless, its synthetic methodology had remained unestablished. In 2014, we demonstrated living supramolecular polymerization, a method to control supramolecular polymerization in a way similar to living polymerization [1]. Since then, we have achieved a variety of mesoscopic supramolecular structures with controlled size and shape [2].

During the course of this study, we discovered a unique mesoscopic structures: concentric toroids (Figure 1) [3]. Mechanistic insight into the propagation of concentric toroids suggested that it involves secondary nucleation as a rate-determining step. With this understanding, we succeeded in the synthesis of multi-componenent concentric toroids, which can be considered as two-dimensional block polymers, with tailored composition and sequence [4].

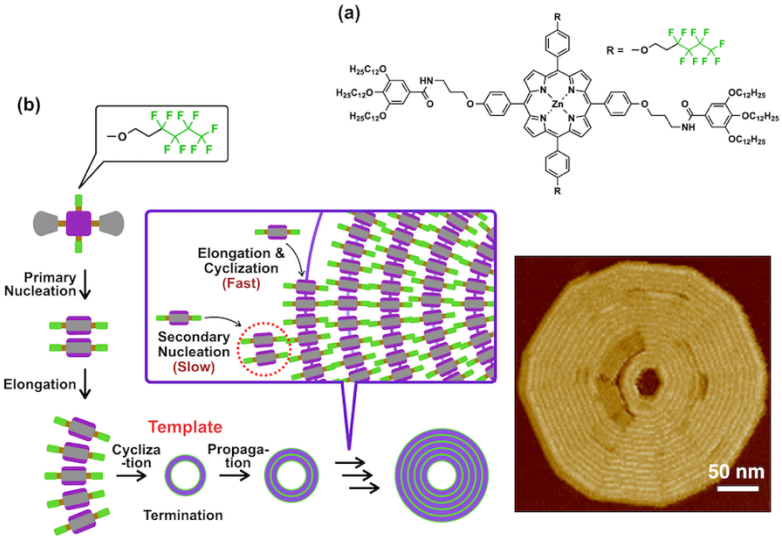

Figure 1. Propagation of supramolecular concentric toroids.

References

[1] S. Ogi, K. Sugiyasu, S. Manna, S. Samitsu, M. Takeuchi, "Living supramolecular polymerization realized through a biomimetic approach" *Nat. Chem.* **2014**, *6*, 188.

[2] K. Sugiyasu, "A case study of monomer design for controlled/living supramolecular polymerization" *Polymer J.* **2021**, *53*, 865.

[3] N. Sasaki, M. F. J. Mabesoone, J. Kikkawa, T. Fukui, N. Shioya, T. Shimoaka, T. Hasegawa, H. Takagi, R. Haruki, N. Shimizu, S.-i. Adachi, E. W. Meijer, M. Takeuchi, K. Sugiyasu, "Supramolecular double-stranded Archimedean spirals and concentric toroids" *Nat. Commun.* **2020**, *11*, 3578.

[4] N. Sasaki, J. Kikkawa, Y. Ishii, T. Uchihashi, H. Imamura, M. Takeuchi, K. Sugiyasu, "Multistep, site-selective noncovalent synthesis of two-dimensional block supramolecular polymers" *Nat. Chem*. **2023**, *15*, 922–929.

Kazunori Sugiyasu: sugiyasu.kazunori.8z@kyoto-u.ac.jp

Structure and Dynamics of Crystalline Soft Materials Revealed by Diffraction and Scattering Techniques

Hironori Marubayashi[a*]

[a]*Department of Biobased Materials Science, Graduate School of Science and Technology, Kyoto Institute of Technology, 1 Hashigami-cho, Matsugasaki, Sakyo-ku, Kyoto 606-8585, JAPAN*

Soft materials spontaneously form hierarchical microstructures ranging from subnanometers to micrometers by phase transitions such as crystallization and phase separation. In particular, crystallization has a significant effect on the structure formation of crystalline soft materials such as semicrystalline polymers, producing a variety of microstructures and properties. Wide-angle X-ray diffraction (WAXD)/small-angle X-ray scattering (SAXS) methods (SWAXS) are powerful techniques to study the hierarchical structure of materials and its dynamics. The author and collaborators have performed SWAXS on various crystalline soft materials and studied their structures and dynamics [1-7]. In this talk, some of the results will be presented.

Laboratory-scale SWAXS measuremsents were conducted by a NANO-Viewer (Rigaku) operating at 45 kV and 60 mA with Cu Kα radiation (λ = 0.1542 nm). An imaging plate BAS-IP SR 127 (Fujifilm) was used as a detector. Synchrotron SWAXS measurements were performed at BL-6A (λ = 0.1500 nm) and BL-10C (λ = 0.1488 or 0.1500 nm) in Photon Factory of KEK (Tsukuba, Japan). Various PILATUS detectors (Dectris) were used. Temperature-controlled sample stages were used: self-built or FP84HT TA Microscopy Cell (Mettler).

Bioplastics, polymers with low environmental impact, were targeted as homopolymers. The hierarchical structure and crystal polymorphism of novel bioplastics were clarified [3, 4, 7]. We also focused on the specially structured polymers—cyclic and cage-shaped polymers. The relationship between topology and hierarchical structure was studied [2]. In addition, the hexagonally packed structure of filamentous viruses and its orientation were analyzed and their effects on thermal diffusivity were evaluated [5].

In crystalline-crystalline diblock copolymers, it was revealed that crystal polymorphism can control the crystallization mode—simultaneous or sequential crystallization of two blocks—and the resultant morphology [6]. We also focused on ternary block copolymers that can be topologically converted from a star to a linear chain by introducing a rotaxane structure. The change in microphase-separated structure induced by topology transformation was clarified [1]. Crystallization/melting of crystalline blocks as well as glass transition of amorphous blocks had a great effect on the temperature dependence of the microphase-separated structure.

In addition to the above results, future prospective will be presented.

References

[1] Sato, H., Aoki, D., Marubayashi, H. *et al. Nat. Commun.* **12**, 6175 (2021).
[2] Mato, Y., Sudo, M., Marubayashi, H. *et al. Macromolecules* **54**, 9079–9090 (2021).
[3] Marubayashi, H., Ushio, T. & Nojima, S. *Macromolecules* **52**, 4624–4633 (2019).
[4] Marubayashi, H., Mizukami, R., Hamada, Y. *et al. Polym. Degrad. Stab.* **153**, 318–324 (2018).
[5] Sawada, T., Murata, Y., Marubayashi, H. *et al. Sci. Rep.* **8**, 5412 (2018).
[6] Osawa, S., Hijikawa, R., Marubayashi, H. & Nojima, S. *Polymer* **122**, 249–257 (2017).
[7] Marubayashi, H. *Sen'i Gakkaishi* **73**, 312–315 (2017).

Hironori Marubayashi: hmaru@kit.ac.jp

Precise yet Dynamic Self-Assembly of Amphiphilic Polymers into Nanostructured Soft Matter

Takaya Terashima[a*]

[a]Department of Polymer Chemistry, Graduate School of Engineering, Kyoto University, Katsura, Nishikyo-ku, Kyoto 615-8510, JAPAN

Precise yet dynamic self-assembly of amphiphilic polymers is important in creating nanostructured soft matter that is responsive to temperature, pH, salts in water or humidity in outer environments. Recently, we have developed self-assembly systems of amphiphilic random or alternating copolymers comprising hydrophilic poly(ethylene glycol) (PEG) and cationic groups and hydrophobic alkyl groups (Figure 1). Typically, the random or alternating copolymers induce chain-folding via the association of the hydrophobic groups in water to form small micelles (~10 nm).[1,2] Random copolymers carrying PEG and octadecyl groups form sub-10 nm lamellar structures via the crystallization of the octadecyl groups.[3]

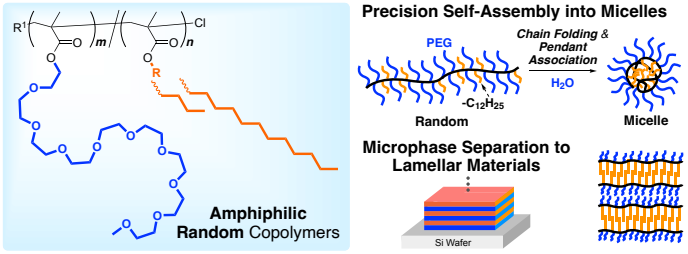

Figure 1: Self-assembly of amphiphilic random copolymers bearing PEG and alkyl groups into micelles in water and lamellar bulk or film materials.

In this paper, we report the recent advances of amphiphilic polymer self-assemblies: (1) design of amphiphilic random or alternating copolymer micelles in water;[1,2] (2) reversible control of co-self-assembly or self-sorting of binary amphiphilic copolymers into fused or discrete micelles in water (Figure 2a);[4] and (3) water-assisted microphase separation and morphology control by water absorption. For example, cationic alternating copolymers bearing imidazolium chloride and hydrophobic groups induce microphase separation via water-vapor annealing (Figure 2b).[5] The copolymers efficiently absorbed water into the cationic segments from the outer environments, depending on the relative humidity. The absorbed water modulates the weight faction of hydrophilic/hydrophobic units in the samples. Thus, the morphologies and domain spacing of the nanostructures are controlled by not only the side chains but also the amount of absorbed water.

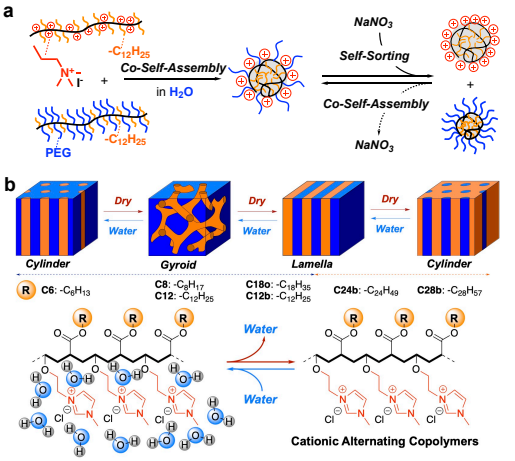

Figure 2: (a) Co-self-assembly and self-sorting of a cationic copolymer and a PEG copolymer in water. (b) Morphology contol of cationic alternating copolymers via water absorption.

The self-assembly of the cationic copolymers afforded universal access to various morphologies including lamella, gyroid, and cylinder, in addition to the precision control of the domain spacing.

References

[1] Imai, S.; Terashima, T. *et al.*, *J. Am. Chem. Soc.* **141**, 511–519 (2019).
[1] Kono, H.; Terashima, T. *et al.*, *Macromolecules* **56**, 6086–6098 (2023).
[3] Hattori, G.; Terashima, T. *et al.*, *J. Am. Chem. Soc.* **140**, 8376–8379 (2018).
[4] Kanno, R.; Terashima, T. *et al.*, *Macromolecules* **55**, 5213–5221 (2022).
[5] Sujita, R.; Terashima, T. *et al.*, *ACS Macro Lett.* **13**, 747–753 (2024).

Submitting Author: terashima.takaya.2e@kyoto-u.ac.jp

Structure-mechanical property relationship in highly homogeneous polymer networks

Shintaro Nakagawa[a*]

[a]Institute of Industrial Science, The University of Tokyo, 4-6-1 Komaba, Meguro-ku, Tokyo, 153-8505, JAPAN

Crosslinked polymers, such as rubber and gel, are conventionally fabricated via a random crosslinking reaction, which inevitably lead to various inhomogeneities in the polymer network structure, deteriorating the performance of the material (Fig. 1a). A promising way to precisely control the network structure is the *module-assembly* strategy, in which the network is constructed by end-linking of monodisperse star-shaped prepolymers (Fig. 1b) [1]. In this talk, I will introduce my recent studies on the structure-property relationship of precisely controlled polymer networks.

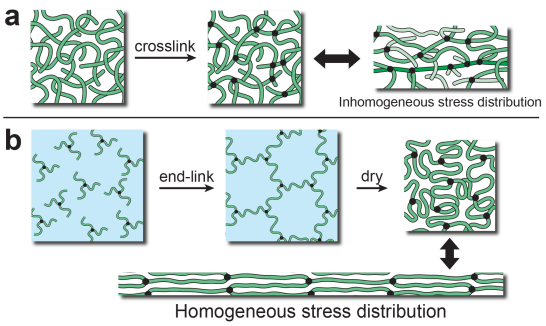

Fig. 1. (a) Conventional and (b) homogeneous elastomers.

Firstly, I synthesized and characterized a polyacrylate-based module-assembled elastomer [2]. Poly(*n*-butyl acrylate) (PBA), an amorphous polymer with a low glass transition temperature, was chosen as the main polymer component. A four-arm star PBA was synthesized by controlled radical polymerization, and the star PBA was end-linked in solution and the solvent was removed to obtain a PBA elastomer. The elastomer, which supposedly had a highly homogeneous network structure, was relatively weak, with the ultimate strength of ca. 0.17 MPa. This rather unexpected (and disappointing) result motivated me to further explore different main chain structures to achieve good mechanical properties of module-assembled elastomers.

Next, I developed a module-assembled elastomer consisting of bottlebrush (BB) polymers [3]. The backbone chain of BB polymers adopts a stretched conformation due to densely grafted long side chains. I hypothesized that this rigid conformation could lead to high elasticity. The module-assembled BB elastomer showed strain-stiffening at relatively small strains. The in situ small-angle X-ray scattering (SAXS) during tensile testing revealed that the preferential orientation of the rigid main chain was synchronized with the strain-stiffening behavior. However, the strength of the homogeneous BB elastomer was very low (~0.02 MPa).

Then, I constructed a module-assembled elastomer from an amorphous aliphatic polyester (poly(4-methyl-ε-caprolactone), PMCL), instead of polyacrylates with a relatively bulky side group [4]. Much different from the previous examples, the PMCL module-assembled elastomer showed high tensile strength (~25 MPa) and stretchability (strain at break ~ 1800%). Moreover, it exhibited an unusually large strain-stiffening capability, which has not been reached by any other soft materials known to date. From the in situ SAXS and wide-angle X-ray scattering (WAXS) during tensile testing, it was found that the unusual strain-stiffening and high strength was caused by the strain-induced ordering of the PMCL chains under an extreme strain. In the presentation, I will discuss about the above topics in more details.

References

[1] Nakagawa and Yoshie, *Polym. Chem.* **2022**, *13*, 2074.
[2] Huang et al. *Macromolecules* **2021**, *54*, 4070.
[3] Nakagawa and Yoshie, *Soft Matter* **2022**, *18*, 4527.
[4] Nakagawa et al. *Adv. Mater.* **2023**, *35*, 2301124.

Submitting Author: snaka@iis.u-tokyo.ac.jp

Organizing Committee

Structural characterization of food materials through small-angle X-ray scattering at NanoTerasu

R. Nishida[1], K. Ninomiya[1,2,3], T. Abe[4], N. Hoshino[4], T. Yamashita[4], Y. Tani[4], M. Nishibori[1,2,3]

[1]*Graduate School of Environmental Science, Tohoku University, Sendai, Japan*
[2]*International Center for Synchrotron Radiation Innovation Smart, Tohoku University, Sendai, Japan*
[3]*Institute of Multidisciplinary Research for Advanced Materials, Tohoku University, Sendai, Japan*
[4]*Riken Vitamin Co., Ltd., Tokyo, Japan*
Email: maiko.nishibori.d8@tohoku.ac.jp

Abstract

Bread, made from wheat, one of the world's three major grains, is an essential food in our diet. The properties of bread are controlled by the moisture-retaining ability of gluten and the crystallization of starch. While it is understood that emulsifiers play a crucial role in controlling these properties, the mechanisms behind this remain unclear. Therefore, we are investigating the mechanisms by which emulsifiers prevent the degradation of bread from the perspective of materials chemistry by using various synchrotron X-ray measurements. We focus mainly on "water" and are advancing our analysis using small-angle X-ray scattering combined with X-ray spectroscopy, exploring different structure and electronic structure scales. There have been very few studies applying synchrotron X-ray spectroscopy analysis to food, and we are attempting to discuss the mechanisms of emulsifier action by correlating the bulk structure and the electronic states of oxygen and nitrogen.

As an example of the results, Fig. 1(a) shows the changes in the WAXS profile with the preserved time measured for bread made without emulsifiers. The peak intensity associated with B-type starch increases with time, indicating that aging is occurring. In contrast, the SAXS profile shown in Fig. 1(b) does not exhibit any apparent trends, suggesting that structural changes at different hierarchies may occur independently.

Acknowledgment: WAXS/SAXS and soft X-ray XAS measurements were performed at NanoTerasu BL08W and BL07U, respectively. The authors thank Dr. K. Kamiya and Dr. H. Meguro of PhoSIC and Dr. H. Kiuchi of the University of Tokyo.

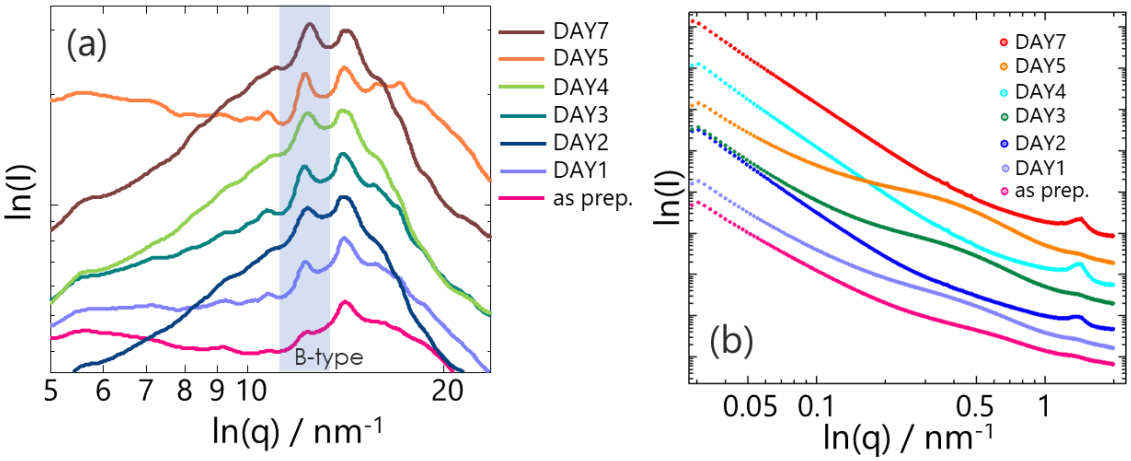

Fig.1 (a) WAXS and (b) SAXS observation of aging due to storage duration. Measurements were performed at NanoTerasu BL08W.

Synchrotron WAXD Studies on Strain-Induced Crystallization of Vulcanized Natural Rubber

Y. Jotatsu[1], T. Uemura[1], R. Tanaka[1], Yuji Kitamura[2], Katsuhiko Tsunoda[2], H. Masunaga[3], K. Urayama[4] and S. Sakurai[1]

[1]*Department of Biobased Materials Science, Kyoto Institute of Technology, Kyoto, Japan*
[2]*Bridgestone, Kodaira, Tokyo, Japan*
[3]*High Energy Accelerator Research Organization, Tsukuba, Ibaraki, Japan*
[4]*Department of Material Chemistry, Kyoto University, Kyoto, Japan*
Email: shin@kit.ac.jp

Abstract

Natural rubber (NR) is a biopolymer and an important material utilized for many different kinds of usage supporting our daily life. One of the most significant applications of NR is tire for vehicles. Among them, the tire for aircrafts should have the highest safety and reliability to avoid tragic accidents due to burst of the tires. To contribute to the safety and reliability of the tire through the prevention of crack growth, strain-induced crystallization (SIC) plays a very important role [1]. Although there are a bunch of research works of the SIC, they are limited in the case of the uniaxial elongation and very few works are available for the case of the multiaxial elongation, which is more important to consider the realistic case of the tire deformation. Therefore, we have studied the SIC behaviors upon the biaxial elongation of NR by measuring the wide-angle X-ray scattering (WAXS) patterns to detect the crystalline reflection peaks at the Japanese synchrotron facility (SPring-8).

Figure 1 displays a state diagram of SIC in the plot of strains ε_X and ε_Y, found for the case of the two-step elongation whereby the specimen was first elongated in Y direction then it was fixed at the elongated state. Further, it was elongated in X direction. In the "No SIC" region for $\varepsilon_Y > 3$, the crystal formed in the first-step elongation in Y direction completely melted away upon the second-step elongation in X direction. This complexity may stem from mismatches of the molecular chain orientation in the amorphous phase as compared to the orientation of the crystallites. Such situation is a characteristic of the chain molecule, very much unusual compared to the case of low-molecular weight compound. The study of SIC in the case of the uniaxial elongation is relevant to the complete matching of these orientation, so that such complexity has never been found.

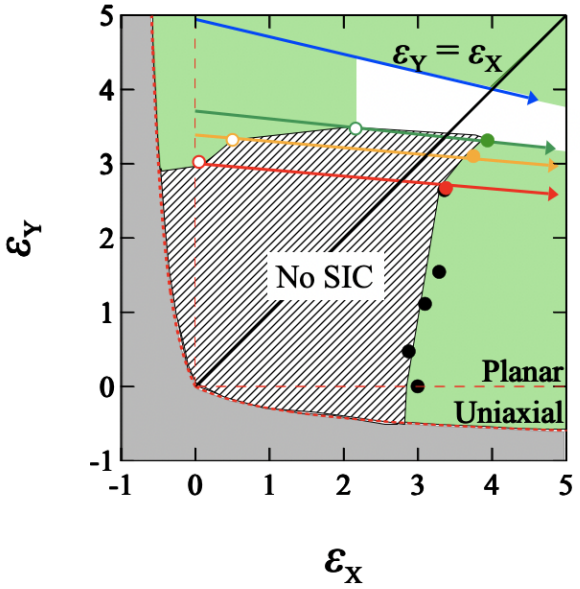

Figure 1. State diagram of SIC in the plot of e_X and e_Y where the specimen was first elongated in Y direction then it was fixed at the elongated state. Further, it was elongated in X direction.

Acknowledgement: This work is financially supported by Japan Science and Technology Agency JST Grant Number JPMJPF2114.

1. T.-Tam Mai et al., Advanced Science, 2024, 11, 2307741.

Structural Analyses of Phospholipid-Surfactine Mixtures by using SAXS and SANS in combination with Field-Flow-Fractionation

Isamu Akiba*, Hiroki Miwa and Ryosuke Nagao

Department of Chemistry and Biochemistry, The University of Kiatakyushu, 1-1 Hibikino, Wakamatsuku, Kitakyushu, Fukuoka, 808-0135, JAPAN

Mixing surfactant micelles into phospholipid liposomes results in significant structural changes, such as the formation of bicelles, and imparts new and novel functions to the liposomes. Consequently, phospholipid-surfactant mixtures have garnered considerable attention in the medical and cosmetic fields. For applications involving human contact, biologically derived substances are preferred as surfactants. Therefore, we focus on surfactin (SFNa), an amphiphilic cyclic peptide produced by *Bacillus subtilisra*, as a surfactant in these mixtures.

We found that the addition of an aqueous solution of SFNa micelles to a turbid aqueous solution of vesicles of DOPC, a phospholipid transformed it into a transparent solution. This result suggests that SFNa and DOPC have formed a complex. Analyses of small-angle X-ray scattering (SAXS) combined with field-flow-fractionation (FFF) techniques showed that SFNa-DOPC complex has a 1 : 1 molar ratio of SFNa to DOPC. To reveal the associating structures and the arrangement of the moleculars of SFNa-DOPC complex, SAXS and small-angle neutron scattering (SANS) analyses were performed.

Figure 1 displays the SAXS (red) and SANS (blue) profiles of the SFNa-DOPC(0.5) complex in H_2O and D_2O, respectively. The number in parentheses indicates the mole fraction of SFNa in the SFNa-DOPC complex. Due to differences in scattering contrast between SAXS and SANS, these profiles reveal different structural information. SANS, performed on the SFNa-DOPC(0.5) complex in D_2O, suggests that the internal composition of the complex forms uniform lipid nanodisks. Conversely, in SAXS, the SFNa-DOPC(1.0) complex appears as core-shell particles. Numerical analyses using core-shell particle models for SAXS and solid particle models for SANS were conducted. The solid lines in Figure 1 represent the best-fit results of the calculated scattering curves for both SAXS and SANS profiles. The SANS profile aligns well with the solid disk model with the same membrane thickness as DOPC vesicles, indicating that the complex resembles a fragment of a DOPC membrane. Additionally, the SAXS profile corresponds well with the theoretical curve calculated on a model of a core-shell disk with a rim composed of SFNa. In summary, SFNa and DOPC were found to form bicelles with a 1:1 molar ratio of SFNa to DOPC quite easily by simply mixing.

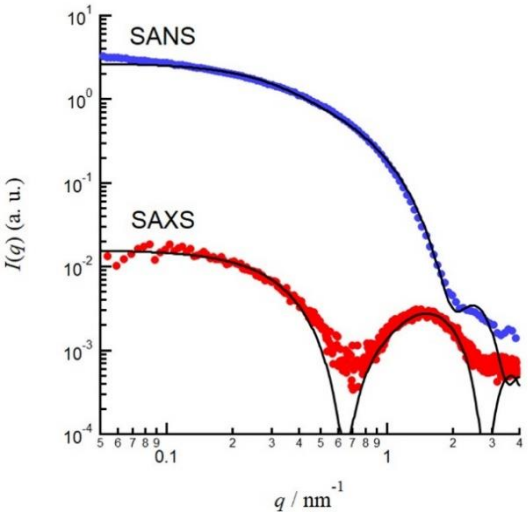

Figure 1: SAXS and SANS profiles of DOPC-SFNa mixture at 1 : 1 molar ratio.

Submitting Author: akiba@kitakyu-u.ac.jp

Discovery of the platonic micelles that have a discreet aggregation number chosen from 4, 6, 8, 12, and 20

Kazuo Sakurai

Department of Chemistry and Biochemistry, University of Kitakyushu,
Hibikino, Kitakyushu 808-0135, Japan.

The concept of micelles was first proposed in 1913 by McBain and has rationalized numerous experimental results of the self-aggregation of surfactants. It is generally agreed that the aggregation number (N_{agg}) for spherical micelles has no exact value and a certain distribution. However, our studies of calix[4]arene surfactants showed that they were monodisperse with a defined N_{agg} whose values are chosen from 4, 6, 8, 12, 20, and 32. Synchrotron small-angle X-ray scattering patterns exhibited a sharp intensity dump, indicating high symmetry and shape monodispersity. The size monodispersity of the micelles was confirmed with analytical ultracentrifugation. Interestingly, some of the observed N_{agg} coincide with the face numbers of Platonic solids, thus we named them "platonic micelles". The preferred N_{agg} values were explained in relation to the mathematical Tammes problem: how to obtain the best coverage of a sphere surface with multiple identical circles. The coverage ratio $D(N)$ can be calculated and produces maxima at $N = 6, 12, 20, \text{and } 32$, coinciding with the observed N_{agg} values. We presume that this "platonic nature" may hold for any spherical micelles when N_{agg} is sufficiently small. Now, we are in the middle of applying this new micellar nature to construct a new drug delivery system.

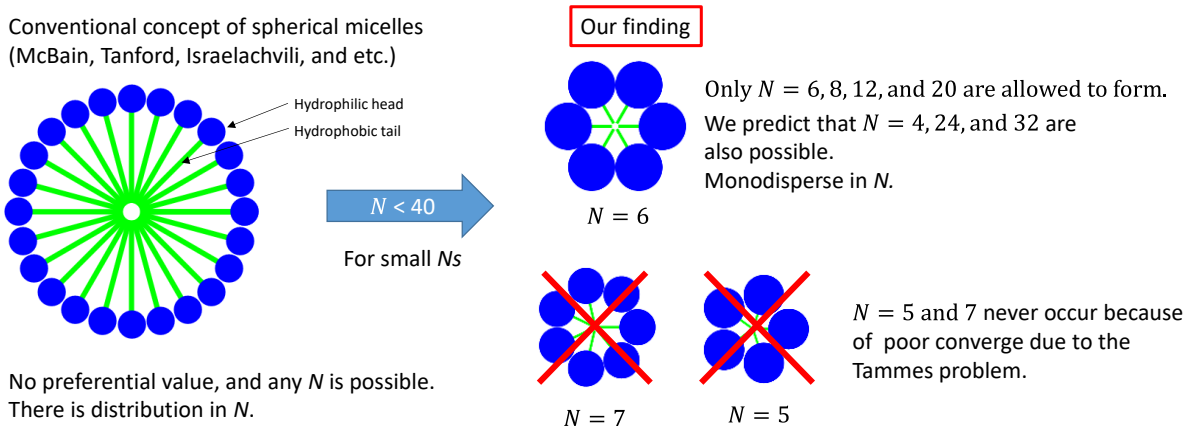

References
Langmuir, *28*, 3092–3101, (2012)
Langmuir, 29, 13666-13675, (2013)
Chem. Comm., 49, 3052-3054 (2013)
Bull. Chem. Soc. Jpn., 354-359 (2012)
Scientific Report 7, 44494; doi: 10.1038/srep44494 (2017)

Phantom chain simulations for the rupture of star-polymer networks

Yuichi Masubuchi *

Department of Materials Physics, Nagoya University, Nagoya 4648603, JAPAN

Despite many attempts, the structure-property relationship of network polymers is yet to be clarified. For instance, the effect of network node functionality on the network fracture has yet to be understood. This study [1,2] conducted coarse-grained simulations for polymer networks with various node functionalities and conversion rates. Figure 1 represents a schematic of the model and the simulation scheme employed. Sols of bead-spring chains without excluded volume were equilibrated and gelated via the Brownian dynamics scheme, and the resultant networks were validated regarding cycle rank, which was fully consistent with the mean-field theory. The networks were stretched until the break via the energy-minimization scheme, and the fracture behavior was characterized by strain and stress at the break and work for fracture. For the networks with monodisperse strand length but various node functionalities and conversion rates, the fracture characteristics as functions of cycle rank lie on master curves when the values are normalized according to the branch point density. The same master curves have been confirmed for networks created from mixtures of prepolymers with different node functionalities [3]. Further, the data draw the same curves for mixtures of linear prepolymers and multi-functional linkers, even though primary loops are included [4]. These results imply that the fracture behavior of polymer networks is dominated by cycle rank.

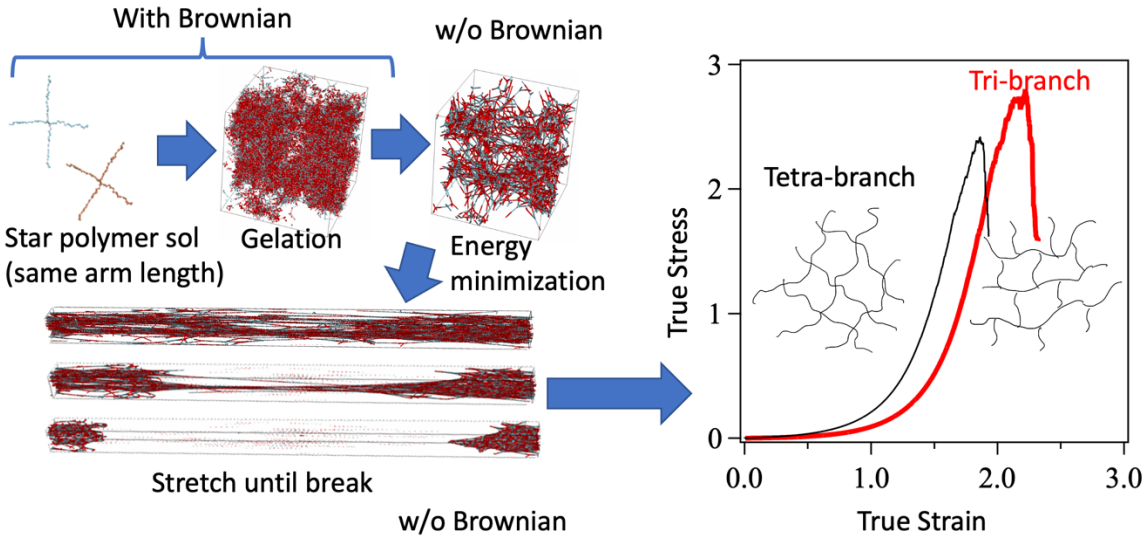

Figure 1 Schematic of the model and the simulation

References

[1] Y. Masubuchi, *et al.*, *Macromolecules*, **56**, 2217 (2023).
[2] Y. Masubuchi, *et al.*, *Macromolecules*, **56**, 9359 (2023).
[3] Y. Masubuchi, *Polymer J*, **56**, 163 (2024).
[4] Y. Masubuchi, *Polymer*, **297**, 126880 (2024).

mas@mp.pse.nagoya-u.ac.jp

Strain-Induced Enhancement of Density Fluctuations in Glassy Materials

Mikihito Takenaka[a,b], Syuhei Fujita[a,b], Ryuta Izumi[a],
Shotaro Nishitsuji[c], and Shin'ya Yoshioka[d]

[a]Institute for Chemical Research, Kyoto University, Uji, Kyoto 611-0011, Japan.
[b]Structural Materials Science Laboratory, SPring-8 Center, Sayo-cho, Sayo-gun, Hyogo 679-5148, Japan.
[c]Department of Polymer Science and Engineering, Graduate School of Science and Engineering, Yamagata University, Yonezawa, Yamagata, 992-8510, Japan.
[d]Department of Mechanical & Physical Engineering, Graduate School of Engineering, Osaka City University, Sugimoto, Osaka, 558-8585, Japan

Polymer glass cannot deform isothermally because, by definition, micro-Brownian motion will be limited in the glass state. However, plastic flow in polymer glass can easily occur under conditions of stress. Many researchers claimed that the spatially heterogeneous dynamics occurs after flow onset and it is expected that the spatial heterogeneous structure causing the spatially heterogeneous dynamics is induced by deformation. We have investigated the changes in density fluctuations in polymethylmethacrylate (PMMA) below glass transition temperature with strain by using small-angle X-ray scattering (SAXS) and observed that the enhancement of the density fluctuation induced by strain around the yield point of the stress-strain curve of PMMA. We have concluded that the enhancement was a result of coupling between the velocity field and density fluctuations that stemmed from a strong density dependence of viscosity that was characteristic of polymer glass that was being deformed. Here we aim at clarifying the universality of the enhancement in other glassy polymers such as polycarbonate (PC) and polystyrene (PS). Figure 1(a) shows two-dimensional (2D) SAXS patterns of PC sample before stretching. The scattering pattern before stretching was isotropic. We stretched PC to the strain $\varepsilon = 0.12$ at temperature T=412K with strain rates $\dot{\varepsilon} = 1.00 \times 10^{-3}$ to 1.00×10^{-5} s^{-1}. At 1.00×10^{-4} (Figure 1 (b)) and 1.00×10^{-4} s^{-1} (Figure 1 (c)), the scattering patterns become anisotropic, thereby exhibiting the so-called abnormal butterfly pattern. On the other hand, at 1.00×10^{-5} s^{-1}, the enhancement of the scattering patterns along the stretch direction is not observed. These results suggest that the density fluctuations are not enhanced by the stretch at 1.00×10^{-5} s^{-1} and that the critical strain rate $\dot{\varepsilon}_c$ of the strain-induced enhancement of density fluctuations exists between 1.00×10^{-4} and 1.00×10^{-5} s^{-1} at 412K. We also found the strain-induced enhancement of density fluctuations occurs in PS. $\dot{\varepsilon}_c$ increases with temperature. Similar tendency can be observed in PMMA and PS. These results indicate that the strain-induced enhancement of density fluctuations is a universal feature in glassy polymers.

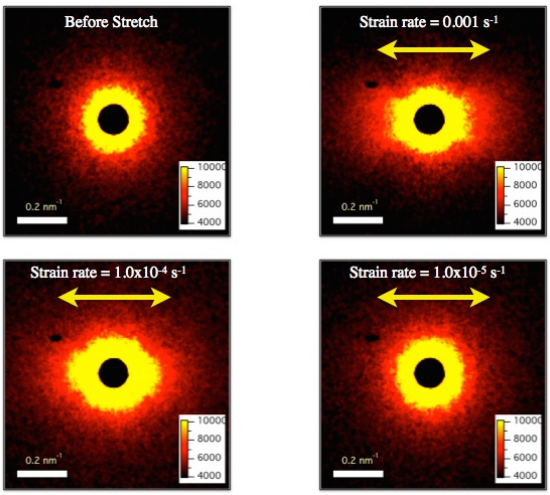

Figure 1 SAXS patterns at various strain rate for PC at 412K and ε = 0.12. (a) 2D SAXS pattern of PMMA before stretching. (b) 2D SAXS pattern at $\dot{\varepsilon} = 1.00 \times 10^{-3}$ s^{-1}. (c) 2D SAXS pattern at $\dot{\varepsilon} = 1.00 \times 10^{-4}$ s^{-1}. (d) 2D SAXS pattern at $\dot{\varepsilon} = 1.00 \times 10^{-5}$ s^{-1}. Arrows indicate stretch

References

[1] A. Furukawa, H. Tanaka, *Nature*, **443**, 434 (2006).

Submitting Author: takenaka@scl.kyoto-u.ac.jp

Oral Presentation

Tuning the Complex Spherical Phase of Sugar-based Block Co-oligomer via Physical Blending

Yu-Hung Cheng [1], Hsin-Lung Chen[1] *, Takuya Isono[2], aned Toshifumi Satoh[2]

[1] *Department of Chemical Engineering, National Tsing Hua University, Hsinchu 300044, Taiwan*

[2] *Faculty of Engineering, Hokkaido University, Sapporo 060-8628, Japan*

hlchen@che.nthu.edu.tw

Our previous study demonsteated that a full spectrum of Frank-Kasper (FK) phase and dodecagonal quasicrystal (DDQC), previously discovered in different block copolymers, can be accessed in a single sugar-based AB_2 star block co-oligomer (BCO) system composed of an oligosaccharide (Glc_n) block attached with two solanesol (Sol) blocks (denoted as Glc_n-$(Sol)_2$), where a discrete increase of the number of glucose monomer (n) in the Glc_n block led to the transition of the micelle packing from DDQC/body centered cubic (BCC) (n=1) to FK σ (n=2) and then to FK A15 (n=3) phase. Additionally, Laves C15/C14 phase emerged from the high-temperature σ phase in Glc_2-$(Sol)_2$ upon stepwise cooling. While the synthetic approach of tuning the oligosaccharide length can be laborious, this study reveals that these complex spherical phases can also be accessed through binary blending of Glc_n-Sol BCOs. Specifically, blends of Glc_1-$(Sol)_2$ and Glc_4-$(Sol)_2$ exhibited FK phases, including the σ and C14, along with complex phase transition pathways, even though neither individual component exhibited FK phases on its own (Figure 1). Blending Glc_1-$(Sol)_2$ with a $(Glc_2)_2$-$(Sol)_2$ BCO, which bears an A_2B_2 architecture, yielded both the A15 and σ phases (Figure 2). The tuning of micelle packing structures relies on the intimate mixing of BCO molecules within micelles, leading to variable core sizes depending on the overall blend composition and thermal processing conditions. Our findings highlight sugar-based amphiphiles as a promising soft matter system for accessing FK and quasicrystal phases, offering an expandable phase window through binary blending and thermal processing.

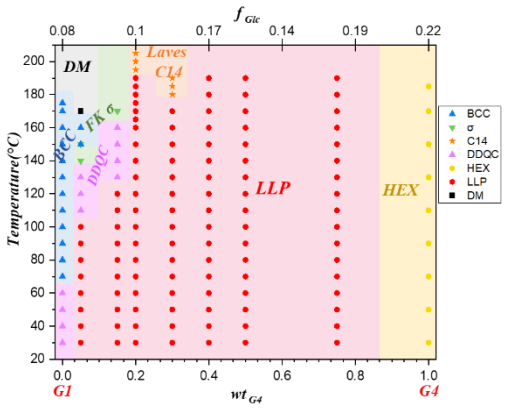

Figure 1. Morpholoical diagram of Glc_1-$(Sol)_2$/ Glc_4-$(Sol)_2$ blend blends

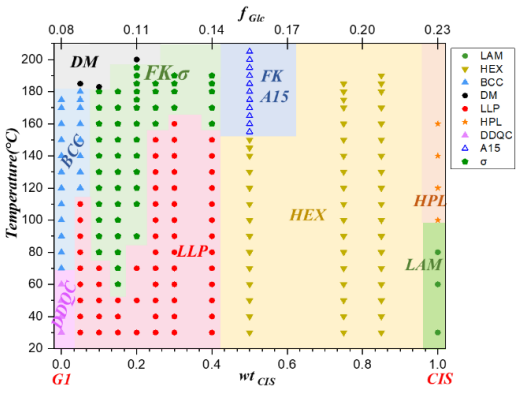

Figure 2. Morpholoical diagram of Glc_1-$(Sol)_2$/ $(Glc_2)_2$-$(Sol)_2$ blend

References

[1] M. W. Bates *et al.*, PNAS **2019**, *116*, 13194-13199.

[2] F. S. Bates, *et al.*, Macromolecules **2021**, *54*, 2647-2660.

Deformation Behavior of Transfersomes Dispersed in Deep Eutectic Solvent during Stratum Corneum Penetration

Mina Sakuragi[a*], Amika Takada[a], Misato Matsuoka[a]

[a]*Department of Nanoscience, Faculty of Engineering, Sojo University*
4-22-1 Ikeda, Nishi-ku, Kumamoto, 860-0082, JAPAN

The stratum corneum (SC), outermost layer of the skin, is known as a skin barrier. SC consists of corneocytes and intercellular lipid lamellar. Various drug carriers, such as microemulsions, bicelles, liposomes, and transfersomes (TFs), have been used to improve the skin permeability of drugs. Liposomes are vesicles comprising unilamellar and multilamellar lipid membranes. However, their skin permeability is low because of their large size, which makes it challenging to permeate through intercellular lipids in the SC. TFs comprise phospholipids and a single-chain surfactant that acts as an "edge activator." Consequently, TFs can penetrate the narrow intercellular spaces of the SC. Recently, transdermal delivery using deep eutectic solvents (DESs) has gained attention because DESs enhance the solubility and skin permeability of some drugs. DESs are formed by the self-association of two or more components that self-associate through hydrogen bonding interactions. Hydrated DESs are produced by the incorporation of water. Compared to unhydrated DESs, the hydrated counterparts exhibit significantly reduced viscosity. Furthermore, they improve long solvent-transfer times and slow molecular diffusion In this study, TFs dispersed in hydrated DESs were prepared. This system is presumed to improve skin permeability through two mechanisms: the deformation of TFs and the disruption of the SC lipid structures by DESs. As a model drug, we selected an antioxidant compound, β-carotene, renowned for its health benefits, which include deactivating highly reactive oxygen species under ultraviolet (UV) irradiation. The concentration of β-carotene in TFs and liposomes that penetrated hairless mouse skin was evaluated. β-carotene did not thoroughly pass through the skin. The results clearly indicate that the topical delivery of β-carotene through TFs was higher compared to that through liposomes. TFs dispersed in DES/water = 8/2 accumulated the most in the SC among all the prepared samples. Therefore, in subsequent studies, DES/water = 8/2 was selected as the sample solvent. Small angle X-ray scattering (SAXS) results showed that TFs and liposomes dispersed in DES/water = 8/2 formed multilamellar structures with a repeat distance of around 6.9 nm. Dynamic light scattering (DLS) and transmittance electron microscopy (TEM) results showed that the diameters ranged from approximately 250 to 500 nm for liposomes and > 500 nm for TFs. Finally, structural changes in the TFs and liposomes after application to the SC were observed. We examined six positions where strong peak intensities of TFs and liposomes were detected. In the case of TFs, the peak area varied significantly depending on the irradiation time and position (Fig.1 top). Conversely, the peaks of liposomes exhibited less changes compared to those of TFs (Fig.1 bottom). These findings indicate that TFs penetrate the SC while being deformed, while liposomes undergo minimal deformation. Consequently, the topical delivery of β-carotene through TFs was higher than through liposomes.

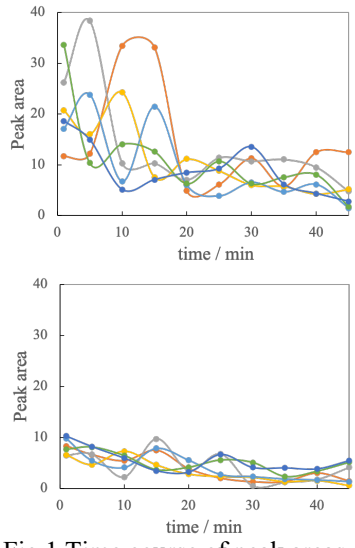

Fig.1 Time course of peak areas of TFs (top) and liposomes (bottom) from 1 to 45 min after application to the SC.

Mina Sakuragi: d08b0101@nano.sojo-u.ac.jp

Helical Microphase-Separated Structures formed from Multiblock Copolymers

Kyoka Kusano, Tsuyoshi Orido and Atsushi Takano

Research Institute for Quantum and Chemical Innovation, Nagoya University
Furo-cho, Chikusa-ku, Nagoya, Aichi 464-8603, Japan

Hexagonally-packed double-stranded helical domain structure having a homochiral single row but with alternating chirality inversion was observed from a tetrablock terpolymer of the S_1IS_2P type, where S, I and P denote polystyrene, polyisoprene and poly(2-vinylpyridine), respectively.

SISP tetrablock terpolymer was synthesized by a living anionic polymerization.[1],[2] Molecular characteristics for the S_1IS_2P terpolymer are summarized in Table 1, and two kinds of structure parameter are used as $\alpha\,(=\phi_{S1}/\phi_{S2})$ and $\beta\,(=\phi_P/\phi_I)$, where ϕ_{S1}, ϕ_{S2}, ϕ_P and ϕ_I are volume fractions of components S_1, S_2, P and I, respectively.

Table 1 Molecular characteristics of tetrablock terpolymer.

Sample	$10^{-3}M_n$ [a]	Volume fraction[b]				M_w/M_n [c]	α	β
		S_1	I	S_2	P			
S_1IS_2P	119	0.657	0.114	0.053	0.176	1.04	12.5	1.53

[a] Determined by SEC-MALS and ^{1}H NMR.
[b] Estimated from ^{1}H NMR.
[c] Measured from SEC.

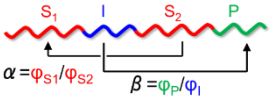

Figure 1a and 1b show the 2D-TEM image and 3D-reconstructed image of I domains stained selectively by OsO_4, respectively, it has been confirmed that the I domains have double-stranded helical structure. While from the 2D-TEM image of P domains stained selectively by I_2 as shown in Figure 1c, it has been confirmed that P domains have hexagonally-packed helical structure. Summarizing these experimental facts, it has been confirmed that the SISP terpolymer shows hexagonally-packed structures having helical domains of P component surrounded with double-stranded helices of component I embedded in the matrices of component S as shown in Figure 1d. Figure 2 reveals a 3 dimensional reconstructed image of the SISP terpolymer by TEM tomography, in which the blue helices are right-handed double helix and the red helices are left-handed ones. This image clearly shows that helices in one row is homogeneous, however handedness is totally inverted in the adjacent row and so on.

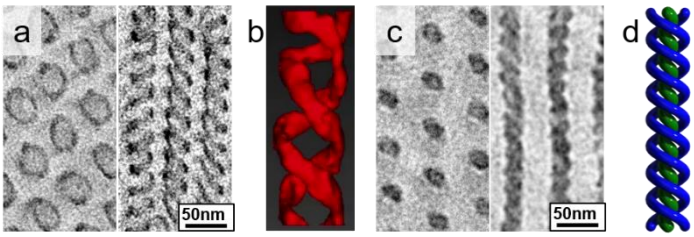

Figure 1. (a) TEM images of I domain stained by OsO_4, (b) 3D TEM images of I domain, (c) TEM images of P domain stained by I_2, (d) Schematic drawing of I/P domains.

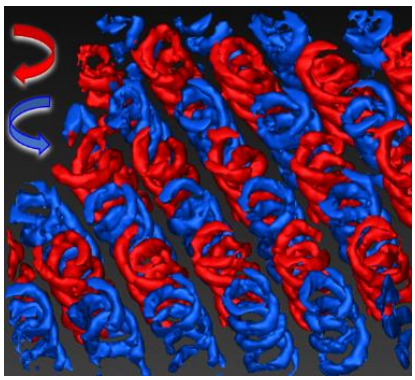

Figure 2. A projected view of a 3D-constracted image. The right-handed helices are painted with blue, while the left-handed helices are in red

References

[1] Y. Miyamori, et al., *ACS Macro Lett*. **2020**, 9, 32−37
[2] Y. Miyamori, et al., *ACS Macro Lett*. **2021**, 10, 978−983

Reentrant Behavior of Bovine Serum Albumin with Multi-Valent Cation: Effects of Coexistence of Monovalent Cation

Yusuke Sanada, Takafumi Ise, Ryutaro Inoue, Yuka Nagano, and Yukiteru Katsumoto

Department of Chemistry, Faculty of Science, Fukuoka University, 19-1 Nanakuma, Jonan-ku, Fukuoka, Fukuoka, 814-0180, JAPAN

Some hydrophilic proteins are regarded as "charged particles" due to their positive/negative charge(s) on their surfaces. Reentrant phenomenon is an interesting behavior for the solutions of these "charged particles" that the solubility of particles depends on concentration of multi valent ions; (i) the particles are soluble with lower concentration, (ii) insoluble in middle concentration, and (iii) soluble (reentrant) in higher concentration (Zhang et al. 2008)[1]. This phenomenon should be related with the protein's in vivo behavior such as peptide folding, aggregation/segregation. Toward quantitative discussion of this reentrant phenomenon, we explored aggregation behavior of bovine serum albumin (BSA) solution with multi valent cation Yttrium chloride (YCl_3) using light scattering technique.

Static light scattering (SLS) measurements were carried out with Strutt (our self-making light scattering spectrometer) with a laser of wavelength as 633 nm. Scattering angle was set at 90 °. YCl_3 concentrations were varied in the range of 0.05 – 100 mM. Monovalent salt NaCl was added as an additional salt at a concentration of 0 or 50 mM.

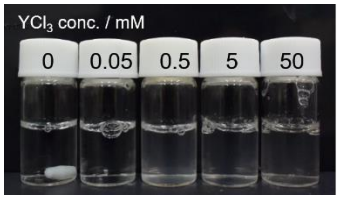

Figure 1: Picture of the sample vials with increase of YCl_3 concentration (BSA concentration was set at 50 mM).

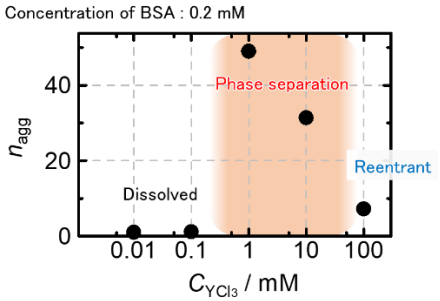

Figure 2: Relative scattering intensity of the solutions of BSA/BSA aggregates against YCl_3 concentration.

Figure 1 shows the visual observation of the solution with five YCl_3 concentrations, and aggregation numbers (n_{agg}), which are calculated from the relative scattering intensities, shown in the Figure 2. With YCl_3 concentration of 1 or 10 mM, the solutions were slightly turbid and the relative scattering intensities were about 50 times higher than the ones of lower YCl_3 concentrations. Above the concentrations of 10 mM, relative intensities were decreased with increase of YCl_3 concentration. It means decrement of aggregation number, and this is the first quantitative report of reentrant phenomenon. In the solution of monovalent salts added, the concentration range of YCl_3 accompanied with aggregation narrowed. However, in this region aggregation occurred, the turbidity became stronger and larger aggregation numbers were observed.

Reference

[1] Zhang, F. et al. Reentrant Condensation of Proteins in Solution Induced by Multivalent Counterions. *Phys. Rev. Lett.* **2008**, 101 (14), 148101.

Yusuke Sanada: sanada@fukuoka-u.ac.jp

Wide-angle X-ray Scattering from Aqueous Solutions of Non-ionic Polymers

Ryo Watanabe,[a] Daichi Ida,[a*] and Keiji Numata[b]

[a]Department of Polymer Chemistry, Kyoto University, Katsura, Kyoto 615-8510, JAPAN
[b]Department of Material Chemistry, Kyoto University, Katsura, Kyoto 615-8510, JAPAN

In the field of polymer solution science, small-angle X-ray (or neutron) scattering (SAXS or SANS) measurements have been made to determine the scattering function $P(k)$ as a function of the magnitude k of the scattering vector in the range of $k/\text{Å}^{-1} \lesssim 2$ for a single polymer chain in solutions. The analyses of $P(k)$ on the basis of the Kratky–Porod wormlike chain or the helical wormlike chain model[1] lead to the molecular-level information of a polymer chain in solutions, the mean-square radius of gyration $\langle S^2 \rangle$, stiffness parameter λ^{-1} (or persistence length q), and diameter d of the cross section of the chain contour.

Recently, synchrotoron radiation facilities have become readily available, enabling accurate measurements of X-ray scattering in a wider range of k. Hirai *et al.*[2] have measured X-ray scattering from aqueous solutions of proteins in the range of $0.01 \lesssim k/\text{Å}^{-1} \lesssim 2.5$ and proposed a procedure for estimate the excess scattering intensity $\Delta\hat{I}(k)$ of solutions in such a high-k range, where $\Delta\hat{I}(k)$ is defined by

$$\Delta\hat{I}(k) = \Delta I_{\text{soln}}(k)/I'_{\text{soln}} - \Delta I_{\text{solv}}(k)/I'_{\text{solv}} \tag{1}$$

with $\Delta I_\alpha(k)$ (α =soln or solv) the (excess) scattering intensity of solution or solvent, respectively, and I'_α the scattering intensity of the higher peak corresponding the intermolecular correlation between solvent molecules in solution or solvent, respectively. By the use of their procedure, the hierarchical structure of proteins in solutions, from the mean-square radius of gyration to the packing structure of side chains, may be simultaneously elucidated.

In this study, the wide-angle X-ray scattering (WAXS) measurements were carried out for aqueous solutions of poly(*N*,*N*-diethylacrylamide) (PDEA), as a example of the systems exhibiting the normal lower-critical-solution-temperature (LCST) phase behavior (Θ = 29.5 °C), and then examined the dependence on temperature of $\Delta\hat{I}(k)$ in the range of $1 \lesssim k/\text{Å}^{-1} \lesssim 3$ obtained using with the procedure by Hirai *et al.* Figure 1 shows plots of $\Delta\hat{I}(k)$ against k for the aqueous solution of PDEA of weight-average molecular weight 1.77×10^5 with weight fraction 1.901 %. In the range of $1 \lesssim k/\text{Å}^{-1} \lesssim 1.5$, the temperature dependence of $\Delta\hat{I}(k)$ is observed. The origin of this temperature dependence is elucidated by the molecular dynamics simulations using a full-atom model. The details will be explained on the day of the presentation.

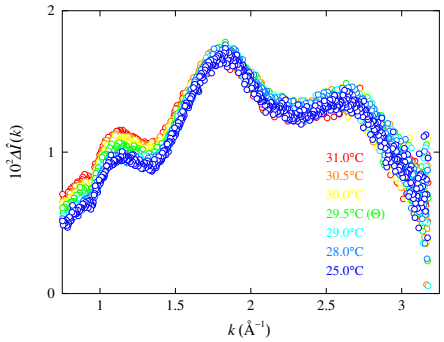

Figure 1. Plots of $\Delta\hat{I}(k)$ against k for the aqueous PDEA solution.

[1] H. Yamakawa and T. Yoshizaki, *Helical Wormlike Chains in Polymer Solutions*, 2nd Ed. (Springer, Berlin, 20016).

[2] M. Hirai, H. Iwase, T. Hayakawa, K. Miura, and K. Inoue, *J. Synchrotron Rad.*, **9**, 202 (2002).

Submitting Author: ida@molsci.polym.kyoto-u.ac.jp

Introduction of State-of-the-art Laboratory SAXS system

Yuichi Takasaki[a] *

[a]*Bussine Unit Characterization SAXS&XRD, Anton Paar Japan K.K., 1-19-9 Tsutsumidori, Sumidaku, Tokyo, 131-0034, JAPAN*

The fist commercial SAXS camera was developed by Otto Kratky and Anton Paar in 1957, and this type of instrument was improved as Kratky compact camera system in 1981. (Figure 1) Anton Paar was working as a manufacture of Kratky-type SAXS instruments, and developed a laboratory line-collimation SAXS system (SAXSess) in cooperation with Otto Glatter in 2003. SAXSess system was widely used in research fields of soft material such as colloidal science and pharmaceutical industry. Due to the simultaneous SAXS-WAXS measurement with using an imaging plate detector, the users can obtain a wide q-range data ($0.05 < q < 28$ nm^{-1}) in one measurement, which was one of the key features of the Anton Paar's SAXS instrument.

Anton Paar also developed a prototype point-collimation SAXS system (SAXSpoint 1.0) in 2015, and improved this system to a high-resolution and fully automated system as SAXSpoint 5.0 in 2020. SAXSpoint 5.0 achieved a better SAXS resolution (q_{min}~0.01 nm^{-1}) and motorized-detector moving system (SlideMaster) in compact foot print. (Figure 2) Using this moving detector feature, users can automatically obtain a wide q-range data ($0.01 < q < 40$ nm^{-1}) without a manual operation.

In March 2024, SAXSpoint 5.0 system was installed in NanoTerasu BL08W for the first time as a combination of laboratory-SAXS system and synchrotron X-ray beam. The collimated X-ray beam enters into the beam path of SAXSpoint 5.0 housing where the whole area is evacuated for reducing air-scattering. BL08W user can complete one measurement within a few minuates, and freely change the sample-to-detector distances (SDD) within several seconds by entering the desired SDD values.

SAXSpoint 5.0 can also adapt for GISAXS, USAXS, and RheoSAXS measurement modes by changing the sample stages to the corresponding modules, which enables the highest measurement flexibility for the users.

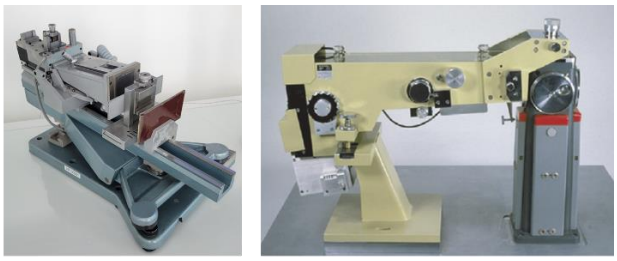

Figure 1: Early laboratory SAXS instruments.Photos were taken in Anton Paar GmbH.

Figure 2: Exterior of SAXSpoint 5.0 system. Its foot print is 3.6 × 0.9 m.

Yuichi Takasaki: yuichi.takasaki@anton-paar.com

Growth behavior of styrene-butadiene rubber adsorption layer using reflectometry and AFM

Yukiko Tamura[1,2], Masato Arakawa[2], Mikihito Takenaka[2], Katsuhiro Yamamoto[3], So Fujinami[4], Tsukasa Miyazaki[4]

[1] ENEOS Materials Corp., 100 Kawajiricho, Yokkaichi-shi, Mie 510-0871, Japan

[2] Institute for Chemical Research, Kyoto University, Gokasho, Uji, Kyoto 611-0011, Japan

[3] Department of Life Science and Applied Chemistry, Gradual School of Engineering, Nagoya Institute of Technology, Gokiso-cho, Showa-ku, Nagoya, 466-8555, Japan

[4] Office of Society-Academia Collaboration for Innovation, Kyoto University, Sakyou-ku, Kyoto 606-8501, Japan

【Introduction】 The mechanical properties of polymer composites, such as filler-filled vulcanized rubber, are generally said to be controlled by two factors: (1) enhancing the wettability of the filler surface with the matrix polymer and (2) introducing functional groups into the rubber or filler to enhance the interaction at the rubber/filler interface, thereby modifying the structure of the adsorption layer. In this study, we conducted a structural analysis of the adsorption layer of styrene-butadiene rubber (SBR) formed on a silicon substrate, focusing on the observation of the thickness and surface morphology of the adsorption layer.

【Experiment】 The SBRs were synthesized by living anionic polymerization. The weight-average molecular weights of the four types of polymers used in this study were 50,000, 102,000, 189,000, and 343,000 g/mol, respectively. The molecular weight distributions (Mw/Mn) of these polymers were 1.06, 1.06, 1.11, and 1.07, respectively. The SBRs were dissolved in toluene and spin-coated onto Si wafers. The SBR formed on a silicon substrate was annealed at 60°C for 3, 6, 24, and 48 hours, respectively, followed by leaching in toluene, and neutron reflectivity (NR) measurements were performed using BL16 SOFIA installed in the Japan Proton Accelerator Research Complex, Material and Life Science Experimental Facility . Additionally, atomic force microscopy (AFM) measurements were conducted on the same samples to observe the surface morphology .

【Result and discussion】 NR data of the samples annealed for 3 and 6 hours were fitted using a simple two-layer model, consisting of an SBR layer and a native oxide layer on the substrate. The scattering length density profiles obtained from the fitting calculations indicated that an extremely thin SBR layer of approximately 1 nm remained on the native oxide layer. This thin layer is presumed to be the inner adsorption layer of the SBR. The AFM image of the sample annealed for 3 hours also showed a uniform and flat surface structure of the inner adsorption layer (Figure 1a). For the samples annealed for 24 and 48 hours, AFM observations revealed the partial presence of a terrace structure on top of the inner adsorption layer, as shown in Figure 1b for the sample annealed for 24 hours. We speculate that the terrace structure was an energetically stable outer adsorption layer that was not leached by toluene. Furthermore, as the annealing time increased, the area covered by the terrace structure expanded, and it was confirmed that the surface coverage varied depending on the annealing time.

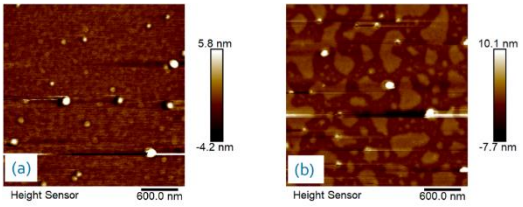

Figure 1:AFM morphological images of the adsorption layers leached in toluene after annealing at 60 °C for 3(a), 24 hours(b).

Baroplastics: Pressure-Resnponsive Block Copolymers as Sustainable Plastics

Shigeru Deguchi[a*], Ikuo Taniguchi[b] and Tsuyoshi Koga[c]

[a]Research Center for Bioscience and Nanoscience, Japan Agency for Marine-Earth Science and Technology (JAMSTEC), 2-15 Natsushima-cho, Yokosuka 237-0061, JAPAN
[b]Graduate School of Science and Technology, Kyoto Institute of Technology, Matsugasaki, Sakyo-ku, Kyoto 606-8585, JAPAN
[c]Graduate School of Engineering, Kyoto University, Katsura, Nishikyo-ku, Kyoto 615-8510, JAPAN

Pressure is one of the state quantities that determines the thermodynamic state of a system but is often treated as a constant, implicitly fixed at 0.1 MPa. Unlike temperature, pressure propagates instantaneously and uniformly throughout a system, making pressure-responsive systems dynamic, manageable, and scalable. In addition, generating and maintaining high pressures equivalent to deep-sea hydrostatic pressures does not require much energy. Thus, materials that respond to deep-sea high pressures could be useful for developing sustainable solutions, such as for materials processing with reduced energy consumption and CO_2 emissions [1].

Baroplastic diblock copolymers exhibit order–disorder transitions (ODTs) and melt upon compression, in some cases even at ambient temperatures (**Figure 1**). The baroplastic behavior is typically observed in block copolymers consisting of a rubbery and a glassy segment. The compressibility mismatch between the two segments plays a critical role in the emergence of the pressure-responsive ODT. We are exploiting the properties of baroplastics to develop sustainable polymers. In this talk, the molecular mechanism of pressure-induced phase transitions and on-demand polymer degradation by pressure will be presented [2].

This work is supported by JST CREST JPMJCR21L4.

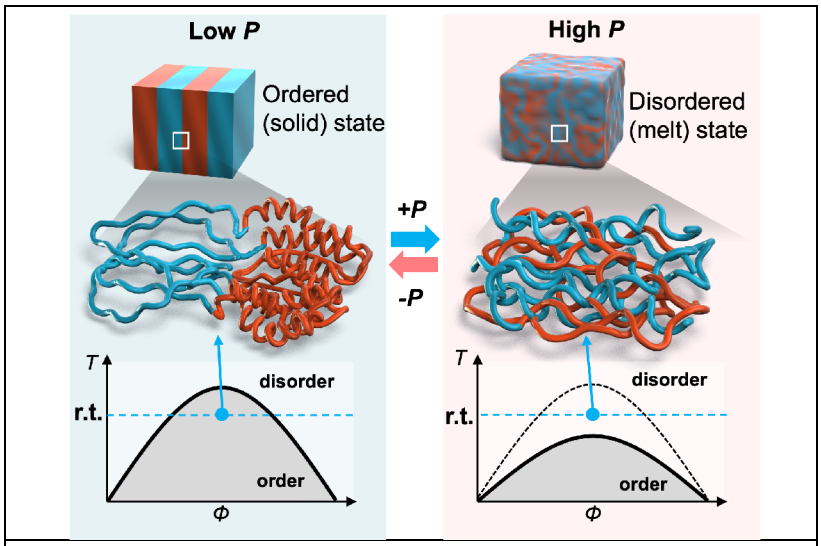

Figure 1. Schematic of pressure-induced ODT of baroplastic block copolymers. Reproduced with permission from ref [1].

References

[1] S. Deguchi *et al.*, *Langmuir* **39**, 7987–7994 (2023).
[2] H. Degaki *et al.*, *Soft Matter* **20**, 3728–3731 (2024).

Submitting Author: Shigeru.deguchi@jamstec.go.jp

Synthesis and Functions of Dense Triazole Polymers

Akihito Hashidzume[a]*, Masaki Nakahata[a] and Yuri Kamon[a]

[a]Graduate School of Science, Osaka University,
1-1 Machikaneyama-cho, Toyonaka, Osaka 560-0043, JAPAN

Copper(I)-catalyzed azide-alkyne cycloaddition (CuAAC) yields 1,4-disubstituted 1,2,3-triazoles from azides and alkynes in the presence of copper(I) compounds. Recently, we have been focusing on dense 1,2,3-triazole polymers as new functional polymers, which are synthesized by CuAAC polymerization of 3-azido-1-propyne (AP) derivatives. The dense 1,2,3-triazole polymer of AP is insoluble in common organic solvents presumably because of strong dipole–dipole interactions of the dense 1,2,3-triazole backbone. Thus, we synthesized a new AP derivative, *t*-butyl 4-azido-5-hexynoate (tBuAH), which has a *t*-butyl (tBu) ester side chain, and polymerized by CuAAC to yield a dense 1,2,3-triazole polymer which is soluble in many organic solvents. tBuAH can be utilized for synthesis of stereoregular and sequence-controlled polymers because of the following features: (1) tBuAH possesses a chiral carbon at the 4-position, and the R- and S-isomers can be prepared by asymmetric reduction. (2) The tBu ester of tBuAH can be converted to 4-azido-5-hexynoic acid (AH) derivatives carrying various side chains. (3) Precursors of AH derivatives carrying a hydroxyl group, i.e., the precursor of azide residue, and a silyl-protecting group on the alkyne, can be used for stepwise CuAAC. In this paper, we will review four generations of dense 1,2,3-triazole polymers we have synthesized recently (Figure 1) [1-8].

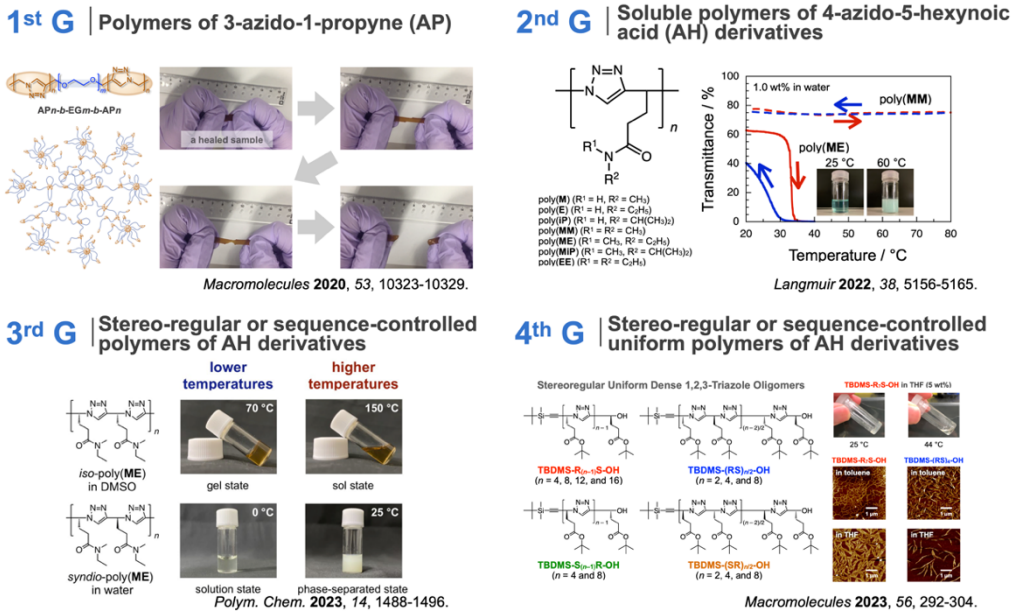

Figure 1. Four generations of dense 1,2,3-triazole polymers.

References

[1] Y. Yang, et al., *Macromolecules*, **53**, 10323 (2020). [2] S. Yamasaki, et al., *Polymers*, **13**, 1627 (2021). [3] K. Okuno, et al., *Langmuir*, **38**, 5156 (2022). [4] K. Okuno, et al., *Polym. Chem.*, **14**, 1488 (2023). [5] L. Xu, et al., *J. Polym. Sci.*, **62**, 937 (2024). [6] T. Omae, et al., *Synlett*, **35**, 1301 (2024). [7] T. Yamamoto, et al., *Langmuir*, **40**, 7178 (2024). [8] Y. Kamon, et al., *Macromolecules*, **56**, 292 (2023).

Submitting Author: hashidzume@chem.sci.osaka-u.ac.jp

Conformational studies on arabinogalactan by SAXS

Hai Huang[a], Wenqing Zhang[b], and Ken Terao[a*]

[a] Department of Macromolecular Science, Graduate School of Science, Osaka University, 1-1 Machikaneyama-cho, Toyonaka, Osaka 560-0043, JAPAN
[b] School of Chemistry and Molecular Engineering, East China University of Science and Technology, Shanghai, 200237, CHINA

Arabinogalactan (AG) is a variety of polysaccharides commonly found in plants or microorganisms. It is rich in galactose and arabinose residues but with high structural complexity because of multiple linkages on the galactan backbone, high possibility of branch substitution, and diversity of residues on the branches, etc. Many AGs from several plant materials have been studied over years in terms of their primary structures and functionalities. However, its conformation-related studies did not receive much attention probably because of obstacle to scattering technique choices since the molecular size of AGs is relatively small due to its low molar mass and high branching degree. This makes small-angle X-ray scattering (SAXS) become a suitable choice for studying the conformation of AGs in dilute solutions.

In recent years, we isolated a 1,6-linked galactose-dominant AG from jasmine tea post-treatment waste (JSP-1a) [1]. Meanwhile, a larch tree arabinogalactan with a 1,3-linked galactan backbone (LAG60) and a linear 1,4-linked galactan with few arabinose residues (LG) were chosen for comparative analysis. The form factor $P(q)$ was evalualted as a function of the magnitude q of the scattering vector with the aid of the Berry plots. The resulting $P(q)$ data were analyzed with the Kratky plot (Figure 1) to estimate their conformations in different solvents, including 0.1 M NaCl aqueous, HBSS(-), and dimethylacetamide/0.1 M LiCl. Furthermore, the corresponding triphenylcarbamates (LAGTPC and LGTPC) in tetrahydrofuran were also studied.

Each polysaccharide could maintain similar conformation in different solvents or after derivatization, which was indicated by using the same fitting model but different parameters. JSP-1a, LAG60, and LAGTPC could be fitted by the perturbed hyperbranched chain model, showing high flexibility of backbones and highly branched features. LG and LGTPC showed obvious linear flexible chain features, which could be fitted by the touched-bead worm-like chain model. Besides, the Flory viscosity factor in 0.1M NaCl aq of three polysaccharides proved their branched degree (LAG60: 6.42×10^{23} mol^{-1}; JSP-1a: 4.42×10^{23} mol^{-1}; LG: 1.70×10^{23} mol^{-1}).

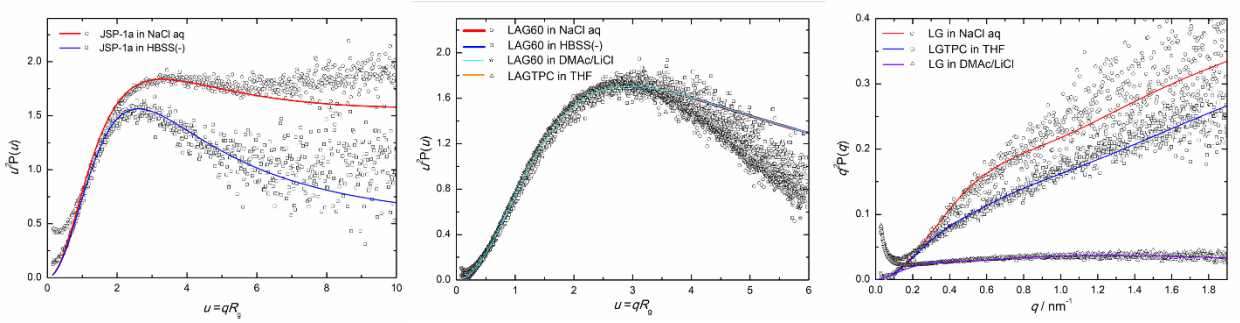

Figure 1: Kratky plots of JSP-1a, LAG60, LG, and corresponding triphenylcarbamates in solutions

References

[1] H. Huang, W. Zhang, *et al*., *Int. J. Biol. Macromol.*, **235**, 123816 (2023).

Submitting Author: huangh23@chem.sci.osaka-u.ac.jp

Analysis of Multiscale Structure of Epoxy Adhesive with Various Crosslink Density in the Single-lap Joint

Kakeru Obayashi[a], Rasha Bayomi[b] and Ken Kojio[a-e*]

[a]Graduate School of Engineering, [b]Institute for Materials Chemistry and Engineering, [c]Research Center for Negative Emissions Technologies, [d]Center for Polymer Interface and Molecular Adhesion Science, and [e]International Institute for Carbon-Neutral Energy Research, Kyushu University, Nishi-ku, Fukuoka 819-0385, JAPAN

Cured epoxy resin (CEP) is mainly synthesized by the polyaddition reaction of epoxy and amine, and are widely used as structural adhesives for automobiles, aircraft, and other applications. To create adhesives with higher adhesive strength, it is important to understand the failure mechanism of adhesive including the structure changes in the microscale from the microscale to the macroscale. In this study, the mechanical properties of single-lap joints (SLJ) with low-crosslinked CEP and the structure changes of multiscale of the adhesive layer during lap shear deformation process are analyzed using lap shear test, digital image correlation (DIC) analysis and synchrotron μ-beam small-angle X-ray scattering (SAXS) mapping measurements.

A commercially available epoxy resin (Epon828, Polysciences, Inc.) with a chemical structure of diglycidyl ether of bisphenol A, and 2-phenyl-ethylamine (2-PEA, f = 2), a primary monoamine, were used for polymerization of CEP. [Amine] / [Epoxy] = 1 and adhered two stain-less steel (SUS304) substrates. SLJ was prepared by curing at 100 °C for 24 hours. The sample name was denoted as CEP-2-PEA-SLJ. The macroscopic and microscopic structure changes during the lap shear deformation process were evaluated using DIC analysis and synchrotron radiation μ-beam SAXS mapping measurements.

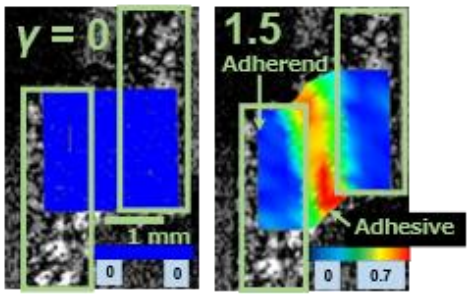

Figure 1 : Strain maps in CEP-2-PEA-SLJ.

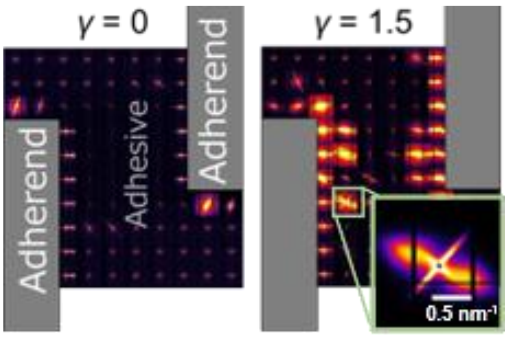

Figure 2 : SAXS patterns of CEP-2-PEA-SLJ during lap shear deformation.

Figure 1 shows the strain maps of CEP-2-PEA-SLJ obtained from the DIC analysis. With increasing strain, the local strain in the adhesive layer also increased and large deformations occurred at the edge positions. This suggests that stress concentration occurred at the edge of the adhesive layer.

Figure 2 shows SAXS patterns of the CEP-2-PEA-SLJ adhesive layer at various positions during lap shear deformation process. In the initial state, streaks from the substrate were observed near the adherend region. At γ = 1.5, a new scattering pattern near the adherend corners, possibly originating from the craze and fibrils, was observed in a direction tilted from perpendicular to the adherend. It is considered that internal structure changes occurred in the stress concentration region and crazes were formed. Furthermore, the stress values decreased during the SAXS mapping measurements. It is suggested that stress relaxation occurred due to the formation of crazes in the adhesive layer and plastic deformation.

Submitting Author: Kakeru Obayashi, obayashi.kakru.749@s.kyushu-u.ac.jp

Nanostructure Formation Behavior of Branched Poly(*N*-isopropylacrylamide)s in Water

Ken Terao[a], Masahiro Abe[a], Masafumi Nagase[a], Tatsuki Nagao[a] and Shota Shimazu[a*]

[a]*Department of Macromolecular Science, Graduate School of Science, Osaka University, 1-1 Machikaneyama-cho, Toyonaka, Osaka, 560-0043, JAPAN*

The thermoresponsive behavior of star-branched poly(*N*-isopropylacrylamide) (sPNIPAM) in an aqueous solution has been investigated using synchrotron-radiation small angle X-ray scattering (SAXS) and electrophoretic light scattering. The temperature-induced formation of spherical nanoparticles with narrow size distribution in sPNIPAM solutions at different temperatures (15 - 55°C) was investigated. The samples contained different end groups: carboxyl, hydroxyl, and benzyl. Unlike linear PNIPAM, sPNIPAM solutions remained transparent even at high temperatures, above the phase separation temperature of linear PNIPAM.

At elevated temperatures (45 °C and above), the formation of nano-sized spherical particles with aggregation numbers between 10 and 50 was observed, regardless of the end group. The stability of these particles was attributed to electrostatic repulsion, as indicated by the negative ζ potential measured at high temperatures. Interestingly, this stability was reduced in the presence of NaCl, resulting in turbidity of the solution.

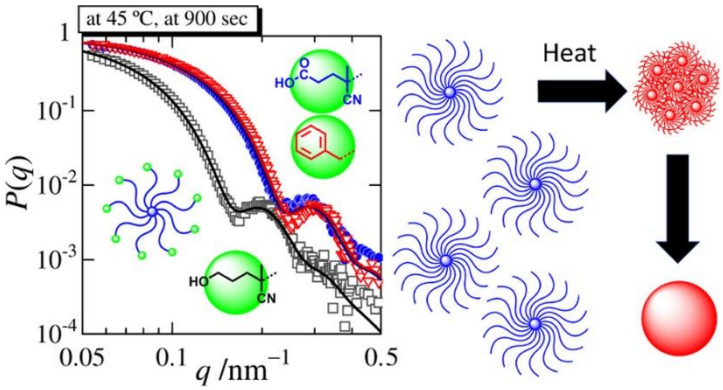

Figure 1. Double logalithmic plots of the form factor $P(q)$ of sPNIPAM in water after rapidly heated in water and shcematic representation of formation of nanoparticles from star branched polymer in water.

Comparative studies between constant and rapid heating processes showed that rapid heating resulted in more uniform nanoparticle formation, probably due to spinodal decomposition, a dominant mechanism under such rapid heating conditions (Figure 1). This process produced narrower size distributions compared to constant heating. The resulting internal polymer mass concentrations (c_{in}) of the nanoparticles were calculated to be between 0.14 and 0.36 g cm^{-3}.

These results suggest that the star-shaped structure of sPNIPAM plays a critical role in temperature-induced nanoparticle formation, providing a method for controlled nanoparticle fabrication. Similar behaviors have recently been observed for comb-branched PNIPAM and star-like PNIPAM micelles. We will also present our recent results on the nanoparticle formation behavior of these polymers.

References

[1] K. Terao *et al.*, *Macromolecules*, **56**, 5635–5641 (2023).

Submitting Author: terao.ken.sci@osaka-u.ac.jp

Deformation Behavior of Body-Centered Cubic Lattice Formed in ABA-type Triblock Copolymer

Aya Fujimoto[1], Ayumi Hamada[1], **Ken Kojio[1-3]**

[1]Institute for Materials Chemistry and Engineering, Kyushu University, Fukuoka, Japan
[2]Graduate School of Engineering, Kyushu University, Fukuoka, Japan
[3]International Institute for Carbon-Neutral Energy Research, Kyushu University, Fukuoka, Japan

A body-centered cubic (BCC) lattice is a crystal unit cell structure observed in various materials including metals, inorganics, and polymers. The deformation behavior of the BCC lattice in metals has been well elucidated, whereas that of polymers remains unclear. We used a microphase-separated copolymer with randomly oriented grains wherein spherical phases are packed in the BCC lattice. The strain value of polymer showed much larger than for metals and inorganics. Small-angle X-ray scattering measurement revealed that the copolymer showed affine deformation under a strain of 1.8. Atomic force microscope revealed that spectacular rearrangement as shown below and "push-and-shove" deformation occurred localy. To the best of our knowledge, these structural changes have not yet been observed in other materials with the BCC lattice. These differences in the behavior of metals

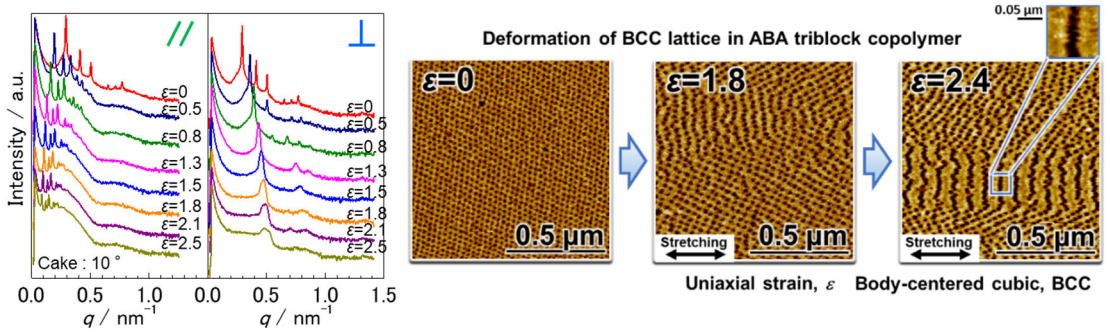

Figure 1. SAXS profiles and AFM images of SEBS films at various strains.

Acknowledgements

Japan Science and Technology Agency (JST) CREST Grant Number JPMJCR17J4 JST, PRESTO Grant Number JPMJPR2194, Japan.

References

1. Fujimoto, A.; Hamada, A.; Kojio, K. Deformation behavior of Body-Centered Cubic lattice in Polymers, *J. Phys. Chem. Lett.* **2023**, 14(44), 10019-10024.
2. Dechnarong, N.; Kamitani, K.; Cheng, C.; Masuda, S.; Nozaki, S.; Nagano, C.; Amamoto, Y.; Kojio, K.; Takahara, A. In Situ Synchrotron Radiation X-ray Scattering Investigation of a Microphase-Separated Structure of Thermoplastic Elastomers Under Uniaxial and Equi-Biaxial Deformation Modes. *Macromolecules* **2020**, 53 (20), 8901– 8909.
3. Dechnarong, N.; Kamitani, K.; Cheng, C.; Masuda, S.; Nozaki, S.; Nagano, C.; Fujimoto, A.; Hamada, A.; Amamoto, Y.; Kojio, K.; Takahara, A. Microdomain Structure Change and Macroscopic Mechanical Response of Styrenic Triblock Copolymer Under Cyclic Uniaxial and Biaxial Stretching Modes. *Polym. J.* **2021**, 53 (6), 703– 712

Time Evolution of the Inner Structure of Colloidal Nanosheets Developing Structural Color

Emiko Mouri[a], Takashi Fukumoto[a], Riki Kato[b], Nobuyoshi Miyamoto[b], Teruyuki Nakato[a]

[a] Department of Applied Chemistry, Kyushu Institute of Technology, 1-1 Sensui-cho, Tobata, Kitakyushu, Fukuoka, 804-8550, JAPAN
[b] Graduate School of Engineering, Fukuoka Institute of Technology, 3-30-1 Wajiro-higashi, Higashi-ku, Fukuoka 811-0295, JAPAN

Two-dimensional nanosheets obtained by layered materials can possess liquid crystalline nature and some of them also develop structural coloration by periodic structuring in liquid [1]. One of the classical nanosheet systems that develop structural coloration is the antimony phosphate nanosheet system reported by Gabriel *et al* [2].

However, the stability of the inner structure and coloration have scarcely been investigated. In this study, we investigate the time evolution of structures in the suspension of antimony phosphate nanosheet systems using UV-visible spectrometry and small-angle X-ray scattering [3].

We noticed the color of antimony phosphate colloid changes with time; The color of the 10 g L^{-1} antimony phosphate colloid is green as prepared and it turns to blue 1 month later. The structural change in the colloid was trucked by SAXS. Figure 1 is a representative SAXS profile series of time evolution of antimony phosphate colloid, which shows a peak shift to a wider angle with time. This indicates that the basal spacings between nanosheets decrease with time. A similar tendency was confirmed for other samples at lower concentrations (isotropic or biphasic region). The sample at lamellar phase did not show the time evolution of the inner structure. Thus antimony phosphate nanosheet systems re-organize their inner structures, especially in isotropic or biphasic regions.

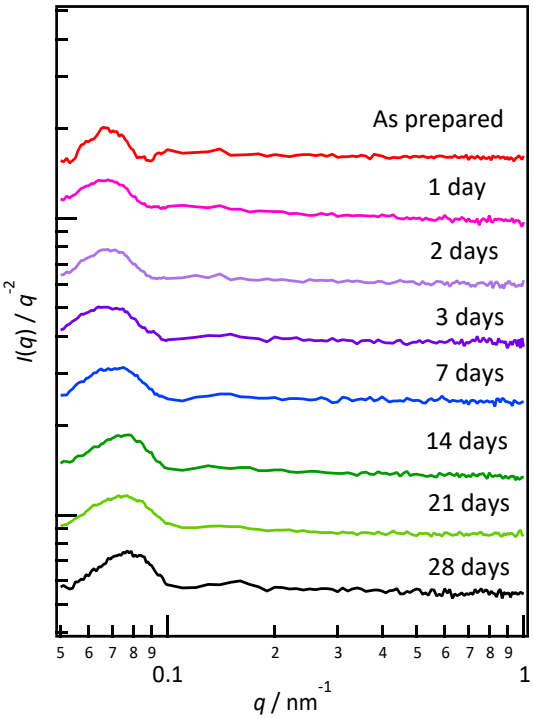

Figure 1. Time evolution of SAXS profiles after sample dilution of nanosheet colloids of 10 g L^{-1}.

References

[1] E. Mouri, C. Ogami, T. Fukumoto, T. Nakato *Chemistry Letters* 49, 717–720 (2020).
[2] J.-C.P. Gabriel, F. Cameral, B. J. Lemaire, H. Desvaux, P. Davidson, P. Batail, *Nature* 413, 504-508 (2001).
[3] E. Mouri, T. Fukumoto, R. Kato, N. Miyamoto, T. Nakato *Soft Matter* 20, 6353-6360 (2024).

Submitting Author: mouri@che.kyutech.ac.jp

Revealing the Solution Conformation and Hydration Structure of Type I Tropocollagen using X-ray Scattering and Molecular Dynamics Simulation

Ying-Jen Shiu[a], Bradley W. Mansel[b], Kuei-Fen Liao[a], Ting-Wei Hsu[a], Je-Wei Chang[a], Orion Shih[a], Yi-Qi Yeh[a] and U-Ser Jeng [a,c*]

[a] National Synchrotron Radiation Research Center, Hsinchu 300092, Taiwan.
[b] Fonterra Research and Development Centre, Dairy Farm Road, Fitzherbert, Palmerston North 4442, New Zealand.
[c] Department of Chemical Engineering & College of Semiconductor Research, National Tsing Hua University, Hsinchu 300044, Taiwan.

Hydration plays a crucial role in regulating the dispersion behavior of biomolecules in water, particularly in how pH-sensitive hydration water network forms around proteins. This study investigates the conformation and hydration structure of type-I tropocollagen using small- and wide-angle X-ray scattering (SWAXS) and molecular dynamics (MD) simulations. SWAXS data for type-I tropocollagen in a pH 2 solution were collected at the 3.0 GeV Taiwan Photon Source -National Synchrotron Radiation Research Center, employing an integrated online size exclusion chromatography (SEC) system alongside UV-Vis absorption and refractive index spectrometers. [1]. The SWAXS data in the range of 0.002 – 0.1 Å^{-1} were fitted using the worm-like chain (WLC) model in conjunction with power law scattering (q^{-2} and q^{-1}), as illustrated in Figure 1. The results reveal that tropocollagen exhibits a significant softening conformation in solution, transitioning from its rod-like structure in tissues to a worm-like conformation, characterized by a reduced radius of gyration of 50 nm and a persistent length of 34 nm. The higher q data in the range of 0.06 – 2.5 Å^{-1}, characterized by two humps at q_0 and q_1, were calculated using the GROMACS-SWAXS with the MD simulation of a truncated tropocollagen (~ 13 nm in length) [2]. The SWAXS calculations further establish a hydration water network characterized by a 2.8Å free-water exclusion zone where water molecules are all hydrogen-bonded to the densely distributed polar groups on the tropocollagen surfaces. These first-layer water molecules are bridged by outer water molecules extending up to 4 Å from the protein surfaces, forming an extensive hydration shell that encapsulates the protein.

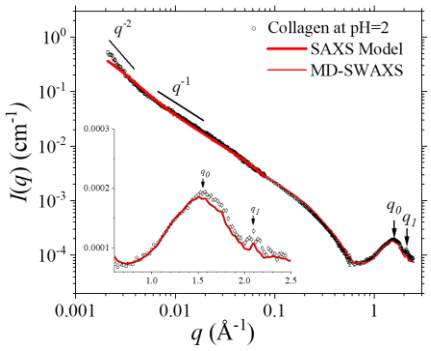

Figure 1: The experimental SWAXS data for the tropocollagen solution at pH 2 are well characterized by power law scattering, fitting to the worm-like chain (WLC) model, and GROMACS-SWAXS calculations across a wide q range (0.002 - 2.5 Å^{-1}). The inset highlights the two humps of q_0 and q_1.

References

[1] O. Shih *et al.*, *J. Appl. Cryst.*, **55**, 340–352 (2022).
[2] P.-C Chen *et al.*, *Biophys. J.* **107**, 435–447 (2014).

Submitting Author: cesms2024@gmail.com

Double Hydrophilic Nano-Scale Compartment Produced by Microphase Separation of Zwitterionic Block Copolymers

Yuji Higaki[a*], Masaya Takahashi[b], Takumi Masuda[b] and Haruna Shiroi[b]

[a]Faculty of Science and Engineering, Oita University, 700 Dannoharu, Oita, 870-1192, JAPAN
[b]Graduate School of Engineering, Oita University, 700 Dannoharu, Oita, 870-1192, JAPAN

Block copolymer solutions yield ordered lattice structures through microphase separation. The morphology depends on the volume fraction of the two phases which is modulated by the polymer concentration and selectivity of the solvents. We reported a lyotropic microphase separation in concentrated aqueous solutions of a double zwitterionic diblock copolymer (PCB2-*b*-PSB4), which is composed of a poly(carboxybetaine methacrylate) (PCB2) and a poly(sulfobetaine methacrylate) (PSB4) (**Figure 1**).[1)] The morphology depended on the polymer concentration due to the limited water capacity of the PSB4 phase. This copolymer can be regarded as a new type of molecular compartment that is valid for biomedical platforms. In this paper, the phase behavior of the double zwitterionic PCB2$_n$-*b*-PSB4$_m$ diblock copolymer aqueous solutions was mapped out to address the insights into the unique microphase separation due to the specific interactions of zwitterions.

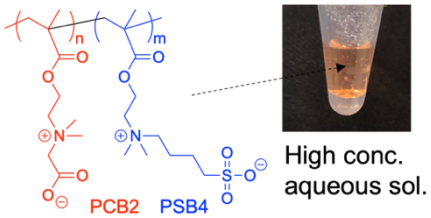

Figure 1. Chemical structure of PCB2$_n$-*b*-PSB4$_m$ and the aqueous solution.

The phase assignment and determination of the lattice structure geometry were conducted by small angle X-ray scattering (SAXS). The SAXS profiles of the PCB2$_n$-*b*-PSBX$_m$ aqueous solutions exhibits multiple peaks, and the scattering vector of peaks depended on the polymer concentration (f) and volume fraction of PSB4 chain (f_{PSB}). The lattice structure transformed from periodic two phase lamellar to hexagonal packed columnar due to the volume expansion of PCB2 phase. The f vs f_{PSB} phase diagram showed order-order transition boundaries with vertical above f = 0.44 while with negative slope below indicating that water exhibited polymer concentration-dependent selectivity, which is neutral above threshold polymer concentration but selective towards PCB2 below the threshold (**Figure 2**). This work advanced our understanding of the microphase separation of zwitterionic block copolymers and it was valid for novel molecular design of aqueous functional materials.

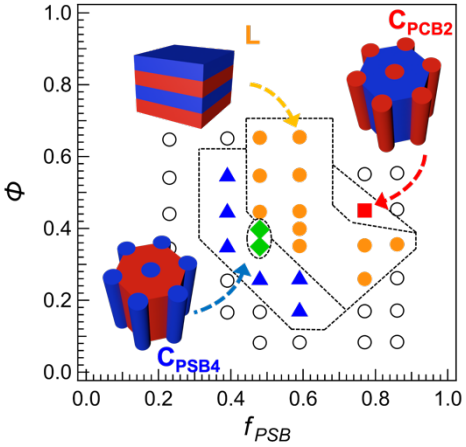

Figure 2. Polymer concentration, ϕ, vs volume fraction of PSB4 in the block copolymers, f_{PSB4}, phase diagrams for (A) PCB2$_n$-*b*-PSB4$_m$ diblock copolymer aqueous solutions at 25°C.

References:

1) M. Takahashi, Y. Higaki *et al.*, *Macromol. Chem. Phys.* **222**, 2000377 (2021).
2) Y. Higaki *et al.*, *Macromol. Chem. Phys.* **224**, 2200416 (2023).

Yuji Higaki: y-higaki@oita-u.ac.jp

Monodisperse Nanosheet Mesophases

Nobuyoshi Miyamoto[a], Hiroyuki Iwano[a], Hiroyuki Nonaka[a]

[a] Department of Life, Environment and Applied Chemistry, the Graduate School of Engineering, Fukuoka Institute of Technology, 3-30-1, Wajirohigashi, Higashiku, Fukuoka 811-0295, JAPAN.

Inorganic nanosheets obtained by exfoliation of layered crystals are known to form intriguing colloidal liquid crystals (LCs). They have been applied for fabrication of anisotropic polymer composite materials, structural color materials, etc. However, large polydispersity in lateral size of the nanosheets limited precise design of self-assembled structures and materials design.

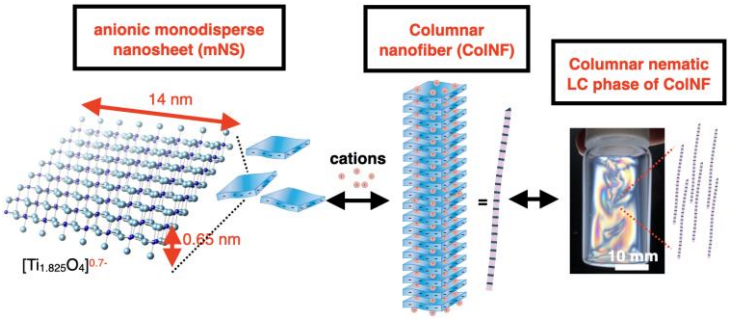

Figure 1 Schematic drawings of mNS and ColNF and crossed polarizer image of the ColNF dispersion that formed nematic LC phase.

Here, we demonstrate that very unusual mesophases are reversibly formed by self-assembly of anionic *monodisperse* nanosheets (mNS) in combination with various cationic species (Fig. 1).[1] In an as-prepared tetramthylammonium (TMA)/mNS aqueous dispersion, mNSs with the thickness of 0.65 nm and the lateral size of 14 nm were isotropically and uniformly dispersed. As [mNS] and [TMA] increased, one-dimensional columnar nanofibers (ColNF) formed; the ColNF was composed of alternating stacking of TMA and mNS with the periodic distance of 1.7 nm as revealed by small angle X-ray scattering (Fig. 2) and transmission electron microscopy. The ColNFs formed fluid columnar nematic LC phase as observed by crossed polarizer observation. Crystalline fibrous bundles of ColNF were also formed. The formation and dissociation of these mesophases were reversible and controllable by many factors such as solvent composition, kind of interlayer cations, and temperature.

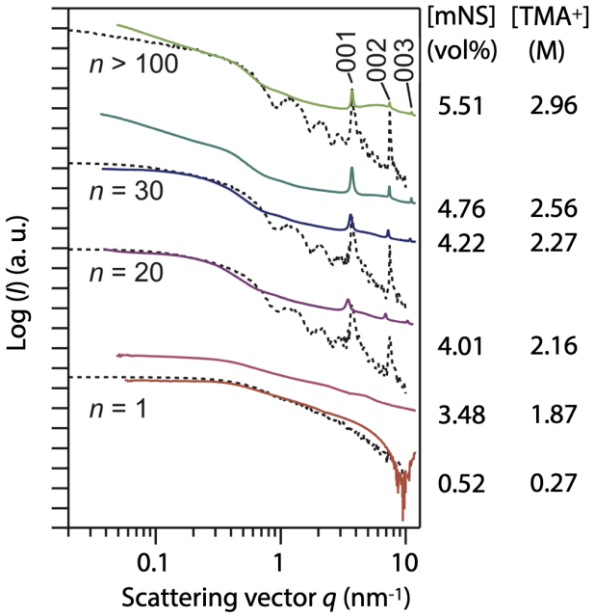

Figure 2 SAXS patterns of the aqueous mNS dispersion with varied concentrations of mNS and TMA. The dotted lines are simulated data.

References

[1] N. Miyamoto, M. Miyoshi, R. Kato, Y. Nakashima, H. Iwano, H. Nonaka, T. Kato, *Sci. Adv.*, **10**, eadk6452 (2024).

Submitting Author: miyamoto@fit.ac.jp

Theory and simulations of branched gels

Filip Uhlík[a], E. B. Zhulina[b] and O. V. Borisov[c]
[a]*Department of Physical Chemistry, Charles University, Prague, Czech Republic*
[b]*Institute of Macromolecular Compounds, St. Petersburg, Russia*
[c]*Institut des Sciences Analytiques et de Physico-Chimie Pour l'Environnement et les Matériaux, Pau, France*

Let us consider polymer gels based not on cross-linked linear chains but molecular brushes. They can be described by three parameters, namely degree of polymerization (or length for brevity) of the backbone strand *M*, length between side-chains *m*, and length of side-chains *n*. Having two more adjustable parameters over simple gels we can hope for a possibility to adjust gel properties, *e.g.* swelling ratio and osmotic modulus, as needed for applications.

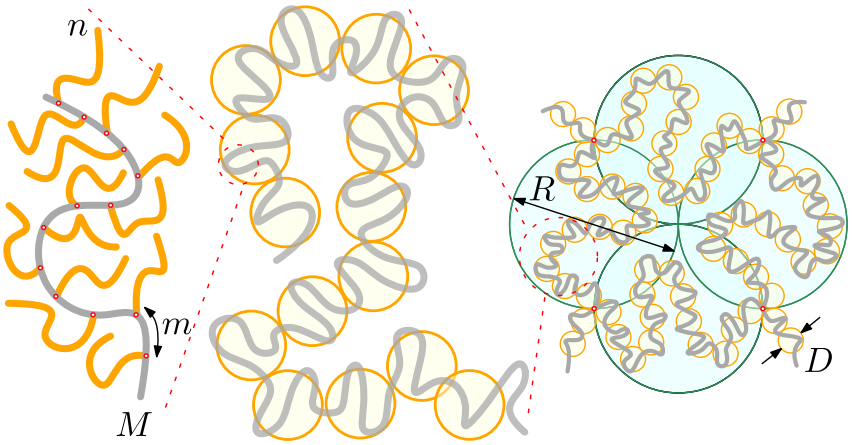

Figure: Geometry parameters of a branched gel.

In this contribution we review predictions of a scaling theory of branched gels in a good solvent and their comparison with Monte Carlo simulations [1–2]. Four interesting regimes according to {*n*,*m*} values are expected, namely either hollow or filled gel mesh and each either with partially or fully stretched spacers of length *m*. The scaling exponents with respect to geometry parameters {*M*,*n*,*m*} are predicted for each regime. The swelling ratio is predicted to pass thru a maximum and osmotic modulus thru a minimum as *n*/*m* ratio increases at fixed *M*. The simulations used Hamiltonian Monte Carlo method with up to 10^5 coarse-grained particles in *NPT* ensemble. The agreement of simulations and scaling theory predictions is fair despite the limited range of accessible {*M*,*n*,*m*} parameters for simulations as theory assumes all of them going to infinity.

References

[1] E. B. Zhulina, F. Uhlik, O. V. Borisov, *Macromolecules* **57**, 6860 (2024).
DOI: 10.1021/acs.macromol.4c00594
[2] F. Uhlik, O. V. Rud, O. V. Borisov, E. B. Zhulina, *Gels* **8**, 793 (2022).
DOI: 10.3390/gels8120793

Submitting Author: filip.uhlik@natur.cuni.cz

Evaluating crosslinking structures by small-angle neutron scattering measurement of sulfur crosslink-controlled rubber

Satoshi Sawada[1,2], Hiroaki Kondo[2], Yohei Nakanishi[3], Motoki Shibata[4], Ryuhei Motokawa[5], Takayuki Kumada[5], So Fujinami[4], Tsukasa Miyazaki[4], Mikihito Takenaka[3]

[1]*Graduation School of Engineering, Kyoto University, Gokasho, Uji, Kyoto 611-0011, JAPAN*
[2]*Chemicals Evaluation and Research Institute, Japan, 1600 Shimotakano, Sugito-machi, Kitakatsushika-gun, Saitama 345-0043, JAPAN*
[3]*Institute for Chemical Research, Kyoto University, Gokasho, Uji, Kyoto 611-0011, JAPAN*
[4]*Office of Institutional Advancement and Communications, Kyoto University, Yoshida-honmachi, Kyoto 606-8501, JAPAN,*
[5]*Materials Sciences Research Center, Japan Atomic Energy Agency, Tokai, Naka-gun, Ibaraki 319-1195, JAPAN*

Improving the physical properties of rubber products requires controlling the homogeneity of the network structures. However, the crosslinking structures of sulfur cross-linked rubber are typically inhomogeneous. In our experiment, two types of rubber samples, an effective vulcanization (EV) system (SBR1, SBR 100/ZnO 3/stearic acid 1/tetramethylthiuram disulfide 4) and a conventional vulcanization (CV) system (SBR2, SBR 100/ZnO 3/stearic acid 1/sulfur 2/1,3-diphenylguanidine 4), with controlled sulfur crosslinking structures were prepared. We evaluated the changes in the inhomogeneous structure and network structure of each rubber sample swollen by toluene-d_8 upon each sulfide bond cleavage using small angle neutron scattering (SANS) measurements and fitting of their profiles. SANS measurement was performed at the SANS-J spectrometer at JRR-3[1]. Fig. 1 shows SANS profiles of sample rubber. For CV system, sulfur bond cleavages—disulfide bonds and polysulfide bonds—resulted in a stepwise decrease in the highly crosslinked domain size and a stepwise increase in the network mesh size. In contrast, the network mesh size did not change much due to the bond cleavage for EV system. This is consistent with the results of crosslinking density measurement by the swelling method. This work will enable the development of rubber products with precisely controlled network structures.

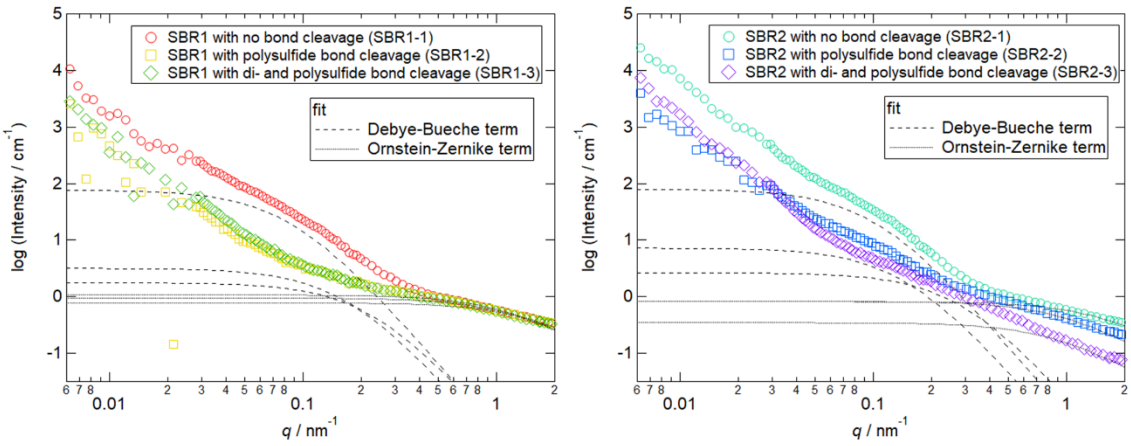

Fig. 1. SANS profiles of rubber samples; (left) SBR1, (right) SBR2. Dashed lines indicate Debye-Bueche term and dotted lines indicate Ornstein-Zernike term, which are obtained by curve fitting of SANS profiles.

References

[1] Kumada *et al.*, *J. Appl. Cryst.*, **2023**, *56*, 1776.

Satoshi Sawada: sawada.satoshi.38r@st.kyoto-u.ac.jp

Synthesis and Function of Artificial Ion Channels Based on Thermoresponsive Amphiphilic Block Copolymers

Shunji KOSAKA[a], Tomoki NISHIMURA[b]

[a] Graduate School of Science and Technology, Shinshu University,3-15-1, Tokida, Ueda, Nagano, 386-0018, JAPAN
[b] Department of Chemistry and Materials Science, Shinshu University,3-15-1, Tokida, Ueda, Nagano, 386-0018, JAPAN

Ion channels are integral membrane proteins that regulate ion permeation across cell membranes. Recently, synthetic ion channels have gained attention for their potential as substitutes for natural ion channels and as anticancer agents. [1] However, conventional synthetic ion channels, typically small molecules, face several challenges, including rapid clearance through renal filtration when administered intravenously.[2] Additionally, their poor water solubility often necessitates the use of organic solvents for membrane incorporation, limiting their practical in vivo applications. Therefore, the development of novel artificial ion channels that differ from peptide- or supramolecular-based systems is urgently needed.

We have previously reported that amphiphilic polymers with poly(propylene oxide) (PPO) as the hydrophobic segment enable the permeation of small water-soluble molecules when incorporated into liposomes in aqueous solvents.[3] Despite the hydrophobic nature of PPO, the hydrophobic PPO layer retains a certain amount of water,[4] which enabling the permeation of water-soluble compounds. Based on this, we hypothesized that this structure could also allow ions to partition within the hydrophobic layer, thus functioning as an artificial ion channel.

In this study, we synthesized an amphiphilic block polymer (OGlu-*b*-$PPO_{2.5K}$) consisting of pegylated oligo(glutamic acid) as the hydrophilic segment and PPO as the hydrophobic segment to develop an artificial ion channel suitable for in vivo applications. The self-assembly behavior of OGlu-*b*-$PPO_{2.5K}$ was examined using transmission electron microscopy, and small-angle X-ray and neutron scattering, revealing the formation of spherical bilayer vesicles with 22.5 vol% water content in the PPO layer. The HPTS and potassium green assays demonstrated that the polymer, when incorporated into DOPC liposomes or cancer cells, facilitates ion permeation across membranes. Moreover, the incorporation of this polymer into cancer cells induced apoptosis (Figure 1).

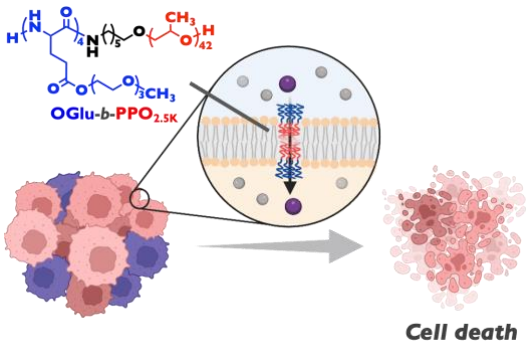

Figure 1: Schematic illustration of OGlu-*b*-$PPO_{2.5K}$ incorporated into cancer cells inducing cell death due to ion permeation.

References

[1] J. Liu et al., Adv. Mater., 2024, 2312352.
[2] N. Bertrand, J-C. Leroux, J. Controlled Release, 2012, 161, 2, 152-163
[3] a) T. Nishimura et al., J. Am. Chem. Soc., 2020, 142, 1, 154–161. b) N. Ozawa et al., Polym. Chem., 2023, 14, 2198–2204.
[4] T. Nishimura et al., Macromolecules, 2020, 53, 17, 7546–7551

Shunji KOSAKA: 23fs506g@shinshu-u.ac.jp

Poster Presentation

A microdomain Structure of Polystyrene-*b*-polyisoprene-*b*-polystyrene Copolymers Prepared by Shear Press and Injection Molding during Mechanical Deformation

A. Fujimoto[1], A. Hamada[1], K. Obayashi[3], M. Ito[4], K. Nakajima[4], K. Kojio[1,2,3]

[1]IMCE, [2]Ctr. Polym. Int. Mol. Adhe. Sci., [3]Grad. Sch. Eng., Kyushu Univ.,
[4]Sch. Mater. & Chem. Tech., Tokyo Inst. Tech.
[1,2,3]Motooka, Nishi-ku Fukuoka 819-0395, [4]Ookayama, Meguro-ku Tokyo 152-8552, Japan
[1]Phone: +81-92-802-2515, Fax: +81-92-802-2518, E-mail: kojio@cstf.kyushu-u.ac.jp

The influence of the preparation method on the initial structure and deformation behavior of polystyrene (PS) - polyisoprene (PI) - polystyrene (SIS) triblock copolymer elastomers was investigated using small-angle X-ray scattering (SAXS) and wide-angle X-ray diffraction (WAXD). Shear pressing (SP) and injection molding (IM) were used as the preparation methods. Two PS contents of 18 and 30 wt% were used.

Figure 1 shows SAXS profiles of shear-pressed (SP) and injection molded (IM) SIS18 and SIS30 sheets. The peaks were observed at $q^*/q_1 = \sqrt{1} : \sqrt{3} : \sqrt{4} : \sqrt{7}$ for SP SIS18 and SIS30. This indicates that a microdomain structure in which PS cylinders were packed in the hexagonal lattice was formed. Furthermore, period and diameter of PS cylinder domains of SIS30 were smaller and larger than those of SIS18. In contrast, for the I-M SIS18 and SIS30, they did not show strong diffracted peaks but broad peak, indicating that the ordering of injection molded SIS were quite low.

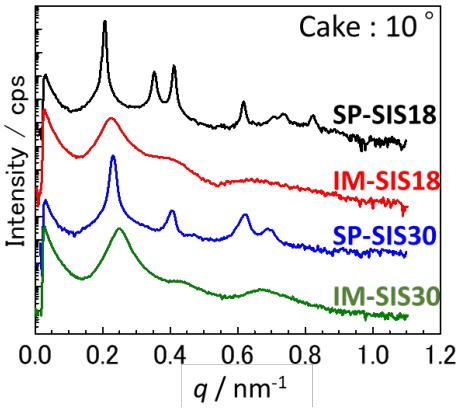

Fig. 1 SAXS profiles of shear-pressed and injection molded SIS18 and SIS30 sheets.

Figure 2 shows stress-strain curves of (a) SP and (b) IM SIS18 and SIS30 sheets along stretching parallel to the PS cylinder axis. Young's modulus of SIS30 is larger than that of SIS18, and IM SIS30 exhibited yielding. The strength of SP SIS30 was above 20 MPa and those of others were below 10 MPa. The ordering and degree of the microphase-separated structure of SP specimens is quite high. This is the reason for large strength of SP SIS30. On the other hand, for the IM specimens, SIS30 exhibited higher tensile strength than for SIS18. Since the diameters of these two sample are almost the same and the degree of microphase separation of injection molded specimens is low, the effect of the PS content was not clear like the shear-pressed ones.

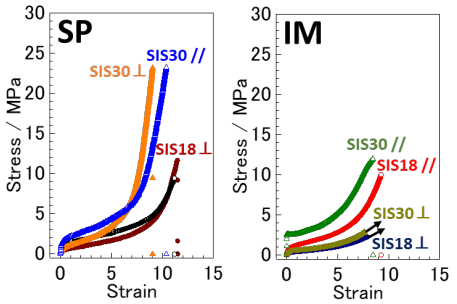

Fig. 2 Stress-strain curves of shear-pressed and injection molded SIS18 and SIS30 sheets along stretching parallel to the PS cylinder axis.

Evaluating Skin Permeation Mechanisms of Microemulsions Dispersed in Thymol-based Deep Eutectic Solvents

Shotaro Shinoda [a] and Sakuragi Mina [a]

[a] Division of Applied Chemistry, Graduated School of Engineering, Sojo University,4-22-1, Ikeda, Nishi-ku, Kumamoto, Kumamoto,860-0082, JAPAN

Introduction The stratum corneum (SC), the outermost layer of the skin, plays a crucial role in maintaining the skin's barrier function, which in turn affects the efficiency of transdermal drug delivery systems. The water content within the SC significantly influences these lamellar structures. Studies using small-angle X-ray scattering (SAXS) have demonstrated that increased water content leads to an expansion of the spacing in S-La[1]. Additionally, the introduction of deep eutectic solvents (DES), such as those composed of thymol and decanoic acid, can disturb the lamellar structures of both L-La and S-La, thereby promoting drug penetration through the skin[2]. To explore these structural changes in detail, advanced techniques like SAXS and wide-angle X-ray scattering (WAXS) are employed, providing precise insights into the molecular structure of the SC. Moreover, small-angle neutron scattering (SANS), utilizing H/D isotope substitution, allows for selective observation of the drug carrier's inner phases. In this study, we focused on the SC penetration mechanism of a drug carrier. As a drug carrier, water-in-oil (W/O) type microemulsions add hydrophobic DES in the oil phase.

Methods **Preparation and structural evaluation of DES and ME:** The components of DES were a mixture of thymol and decanoic acid in a molar ratio of 3/2. The ME was dispersed in a solvent containing a mixture of DES and isopropyl myristate (IPM) in two different weight ratios, 1/9 and 1/6, and was named 1/9 ME and 1/6 ME. The weight ratio of ME components was fixed at solvent/surfactant/water = 76/20/4 (wt%). Rutin, a poorly soluble drug, was used as a model drug. SAXS and SANS were used for the structural analysis of MEs.

Skin permeation test: Hairless mouse skin was kept under 90% RH humidity for 2 h in the hydration condition and under 10% RH for 1 h in the dry condition. 50 µl of ME, including rutin, was added to the skin surface under each condition. After 48h, rutin that penetrated the skin was quantified by HPLC.

Structural changes in ME: The inner water of ME was replaced with the D_2O(d-MEs), then SANS measurement was carried out to observe the structural changes of the inner phase of MEs when penetrating the SC.

Results and discussions The SAXS profile of 1/6 ME and 1/9 ME indicated the presence of spherical structures with a radius of 5.1 nm and 4.8 nm, respectively. For SANS, we can obtain information about the inner D_2O phase of d-MEs.Results showed that 1/6 d-MEs and 1/9 d-MEs have an inner radius of 4.3nm and 4.0 nm, respectively. Next, we evaluated the skin permeability of MEs. As a result, the skin penetration amounts of 1/6 ME and 1/9 ME were almost the same for dry conditions. On the other hand, for high humidity conditions, 1/9 ME permeated the skin more than 1/6 ME. Additionally, we investigated the structural changes of d-MEs when penetrating dry SC or hydrated SC using SANS measurements. For dry SC, the structural change of 1/6(a) and 1/9(b) d-MEs did not occur for three hours. On the contrary, the inner phase sizes of 1/6(c) and 1/9(d) d-MEs increased over time in the hydrated SC. The sizes of 1/6 MEs increased more than 1/9 MEs(Fig.1).

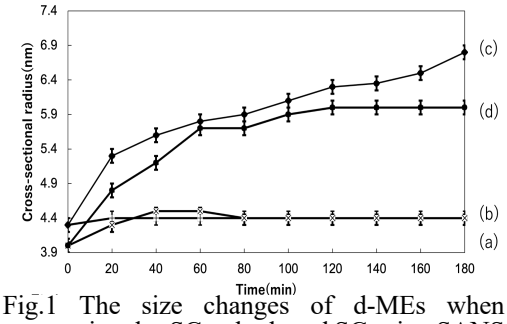

Fig.1 The size changes of d-MEs when penetrating dry SC or hydrated SC using SANS measurements

References

[1] Hatta, I., Ohta, N., Inoue, K. & Yagi,N. *Biochim Biophys Acta Biomembr* **1758**,1830–1836 (2006).
[2] Araki, Y., Hamada, Y., Imamura, N., Yamasaka, K. & Sakuragi, M. JJAP **62**,1-30(2022).

Shotaro Shinoda: g2314m04@m.sojo-u.ac.jp

Analysis of structural change of the skin lamellae induced by bicelle using small-angle X-ray scattering

Yusuke Hayashida[a], Mina Tanigawa[a], Mina Sakuragi[a*]

[a]*Division of Applied Chemistry, Graduate School of Engineering, Sojo University, 4-22-1, Ikeda, Nishi-ku, Kumamoto, Kumamoto 860-0082, JAPAN*

Transdermal drug delivery systems (TDDS) are a technology for delivering drugs through the skin. They are attracting attention as a new method of drug delivery as an alternative to oral or injection administration. However, a challenge to using TDDS is the presence of the stratum corneum (SC). It has a barrier function and hydrophobic property, which means that transdermal delivery is limited to hydrophobic and low molecular weight drugs.

This study focuses on bicelles, which are disc-like structures composed of phospholipids. L. Rubio et al reported that a skin permeability of a hydrophilic anti-inflammatory drug improved by the application of the drug to the skin after application of the bicelles [1]. However, it has not been reported about the detailed structural changes of the skin after the application of the bicelles. In this study, we examined the skin penetration-enhancing effect of bicelle and clarify structural change of the SC by X-ray, to achieve highly efficient transdermal delivery.

Skin penetration tests were conducted to find the best application time and concentration for the bicelles. The results showed that skin pre-treated with bicelle at higher concentrations and for longer periods improved the penetration of a hydrophilic substance, fluorescein sodium. On the other hand, did not improve the skin penetration of a hydrophobic substance, meloxicam. The fact showed that bicelles can improve the skin penetration of hydrophilic substances but they do not work as well for hydrophobic substances.

To elucidate the mechanism of pre-treatment effect by bicelles, we performed structural analysis of the SC after applying the bicelles using small-angle X-ray scattering (SAXS). We focused specifically on the structure of the SC intercellular lipid, which is the main pathway for drug permeation. This intercellular lipid consists of two types of lamellar structures: long-period lamellae with a repeat distance of 13.6 nm(L-La) and short-period lamellae with a repeat distance of about 6 nm(S-La). The short-period lamellae has water phases. The results showed that when Bicelle was applied to the SC, new peaks appeared that were not present in the original SC (Fig1). On the other hand, the peak position derived from long-period lamellae did not change after applying bicelles. This fact indicated that a new periodic structure had formed by the interaction between short-period lamellae lipids and bicelle lipids. These new structures are close to the periodic spacing of the short-period lamellae, suggesting that the lipids of the short-period lamellae interacted with the lipids of the bicelle. This structural change may have improved the permeability of hydrophilic drugs.

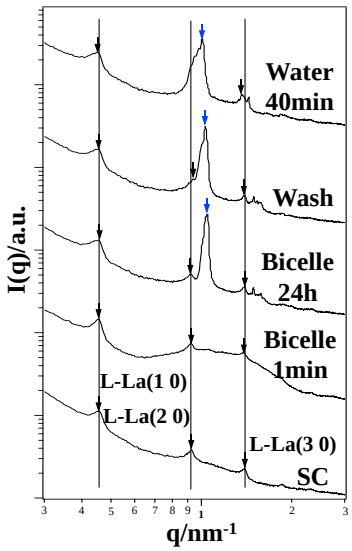

Fig.1 SAXS profiles of the SC lamellar structures over time with Bicelle applied. Vertical lines indicate the peak positions of long-period lamellae of the SC.

References

[1] L. Rubio et al. *International Journal of Pharmaceutics*, 2010, 386, 108-113

Yusuke Hayashida: g2414m03@m.sojo-u.ac.jp

Structural analysis of PEG-modified bicelles and their stratum corneum penetration mechanism

Mina Tanigawa[a], Sabrina Binti Mohamed Hasnol[a], Takuya Matsunaga[b], Mina Sakuragi[a*].
[a] Division of Applied Chemistry, Graduated School of Engineering, Sojo University, 4-22-1, Ikeda, Nishi-ku, Kumamoto,kumamoto 860-0082, JAPAN [b] The University of Kitakyusyu, 1-1 Hibikino, Wakamatsuku, Kitakyushu, Fukuoka, 808-0135, JAPAN

Introduction

Bicelles are discoidal nanostructures formed by long and short-chain phospholipids in an aqueous solution. Previous study has shown that applying DPPC/DHPC bicelles (Bic) to the skin before drug application significantly improved the percutaneous absorption of the drug [1]. The results suggest that Bic plays an important role in skin penetration enhancer. Introducing PEG to the drug carriers can improve skin penetration due to its hydration effect. Accordingly, PEG chain-induced Bic was prepared in this study to further improve skin penetration of the drugs. PEG units were introduced to the rim or face of the Bic (PEG-Bic). PEGylated cholesterol with varying PEG length (CS-10,20,30) was used for the introduction to the rim (Bic-CS10,20,30) and Tween60 was used for the introduction to the face. (Bic-Tw60) This study aims to propose the structural property of Bic suitable for skin permeation and to elucidate the interaction mechanism between PEG-bicelles and the stratum corneum (SC).

Sample Prepration

Bicelles were prepared by mixing appropriate amounts of DPPC, DHPC, Tween60, and Polyoxymethylene Cholesteryl Ether 10,20,30 (CS-10,20,30). The molar ratios of DPPC / DHPC (Bic), DPPC / DHPC / Tween60 (Bic-Tw60) and DPPC / DHPC / CS-10,20,30 (Bic-CS10,20,30) was fixed with 2 / 1, 7 / 4 / 1, 8 / 3 /1 respectively.

Result and discussion

Small Angle X-ray Scattering (SAXS) showed more PEG units on the rim of bicelles for CS-10, 20, and 30 and on the face for Bic-Tw60.

Next, skin permeation tests were using Franz cell. Bic samples were applied to the skin and removed after 24 hours. Then, fluorescein sodium solution was applied. Skin penetration of fluorescein sodium after application of PEG-Bic increased more than Bic without PEG. Bic-CS20 with PEG units on the rim achieved the highest skin penetration.

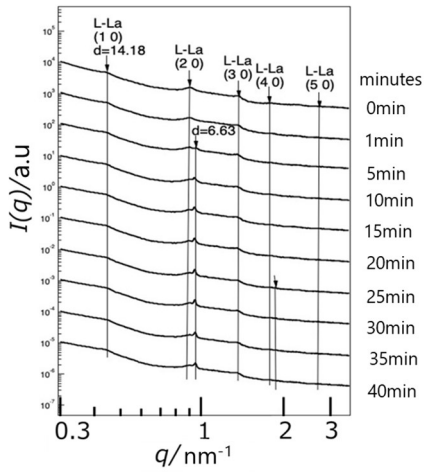

Fig. 1 SAXS diffraction profiles of SC penetrated by Bic-CS20 over time.

Subsequently, we investigated lamellar structural changes when bicelles were applied to the SC using SAXS. X-ray irradiation of SCs detects lamellar structures of intercellular lipids, composed of long-period lamellar (L-La) structures with a repeat distance of 13.6 nm and short-period lamellar (S-La) structures with a repeat distance of around 6 nm, where only S-La has water layers. Applying the PEG-Bic to the SC did not change the L-La peak position, indicating no interaction with hydrophobic L-La. For Bic and Bic-CS20, new lamellar peaks with repeat distances from 6.6 to 7.42 nm appeared 5 minutes after application, suggesting interaction with the lipids of S-La (Fig.1). For Bic-Tw60, no peaks appeared until 20 minutes, indicating that bicelles with PEG units on the rim interact more easily with lamellar lipids. The fact showed that Bic creates a new pathway for hydrophilic substances to penetrate, and Bic-CS20 is the most suitable for the enhancement of skin permeation.

References

[1] *Int.J Pharm* 2010,386,108.

Mina Tanigawa: g2314m05@m.sojo-u.ac.jp

Physical property evaluation of a polysaccharide-nucleic acid complex containing two DNA molecules by Small-Angle X-ray Scattering (SAXS)

Y. Hata, K. Sumiya, S. Yoshitake, and K. Sakurai*

Faculty of International Environmental Engineering, The University of Kitakyushu, 1-1 Hibikino, Wakamatsu-ku, Kitakyushu, Fukuoka 808-0135, JAPAN

Introduction

Our laboratory is conducting research using complexes composed of schizophyllan (SPG) and polydAdenine (dA_X). Recent studies have revealed that SPG, with adjusted molecular weight, forms complexes containing 1 to 3 molecules of dA_X.[ref.1]. The relationship between the radius of gyration and molecular weight of this complex follows the Kuhn segment length (λ-1) of 42 nm in accordance with the Kratky-Porod semiflexible chain model. However, based on molecular weight, composition, and microscopic observations, it is believed that the complex composed of dA60S adopts a "broken-rod" structure, in which a rigid rod formed by complexation using a 17.5 nm-long DNA template is linked to an uncomplexed polysaccharide portion through near-free junctions (see Fig.1, with DNA shown in red and SPG in green) [ref.2]. If this were the case, the relationship should follow λ-1 = 17.5 nm. To investigate the cause of this discrepancy, we conducted small-angle X-ray scattering (SAXS) measurements on the complex containing two molecules of $dA_{60}S$.

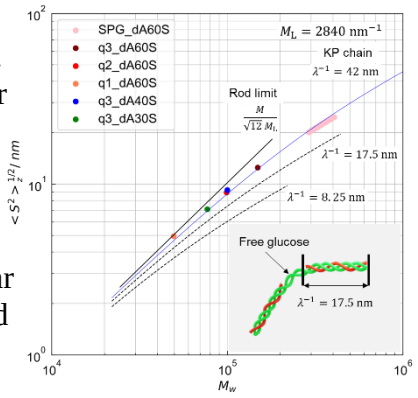

Figure 1. "Log-log plot of the radius of gyration against the molecular weight for all dA_X complexes."

Experimental Methods

The complex containing 1 to 3 molecules of dA60S was fractionated by HPLC into a complex containing 2 molecules of dA60S (q2_dA60S) and a complex containing 1 molecule of dA60S (q1_dA60S). The obtained q1 and q2 complexes were evaluated using small-angle X-ray scattering (SAXS).

Results and Discussion

Fig. 2 shows the results of small-angle X-ray scattering (SAXS) measurements. The complex containing one molecule of dA60S (q1_dA60S) exhibited scattering characteristic of a rigid rod with a diameter of 1.2 nm and a length of 17.5 nm (labeled as "Rigid rod" in the figure). On the other hand, the complex containing two molecules of dA60S (q2_dA60S) deviated from the rigid rod calculation at low angles and showed behavior very close to the calculation for a "Once-Broken Rod." The fit improved further by introducing a constrained connecting segment, where the probability of occurrence decreases as the bending angle increases. This suggests that q2_dA60S adopts a molecular conformation in which two rigid rod segments, nearly identical to q1_dA60S, are connected in series at a junction without sharp bending.

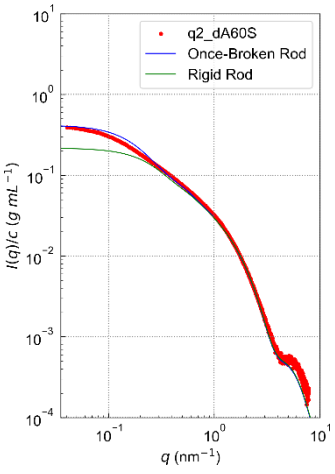

Figure 2. Comparison of q2_$dA_{60}S$, the 17.5 nm Rigid Rod, and the Once-Broken Rod.

References

[1] Sumiya, K., Matsunaga, T., Tanaka, M., Mochizuki, S. & Sakurai, K. Biomacromolecules 21, 4823-4834 (2020).

[2] Pecora, R. Macromolecules 2, 31-34 (1969).

Submitting Author: f4mab020@eng.kitakyu-u.ac.jp

Defect-Free Block Copolymer Self-Assembly Facilitated by Structural Coloration for Providing Solar Cell Distributed Bragg Reflectors.

Mingeun Park[a], Suhyeon Park[a], Ding Shangxian[a], Kyungkon Kim[b*], and Du yeol Ryu[a*]

[a]*Department of Chemical and Biomolecular Engineering, Yonsei University, 50 Yonsei-ro, Seodaemun-gu, Seoul 03722, Korea*
[b]*Department of Chemistry and Nanoscience, Ewha Womans University, 52 Ewhayeodae-gil, Seodaemun-gu, Seoul 03760, Korea.*

Straightforward method for fabricating high-reflectance distributed Bragg reflectors (DBRs) was proposed by creating defect-free one-dimensional lamellar microdomains in polystyrene-*b*-poly(2-vinylpyridine) (PS-*b*-P2VP). By optimizing the thermal annealing process, thermal equilibrium of the block copolymer (BCP) eliminated dislocations and disclinations, ensuring that the lamellar structures are oriented parallel to the substrate across the entire film. The dehalogenation of 1,4-dibromobutane induced a crosslinking reaction within the P2VP blocks, leading to the ionization of nitrogen atoms. Subsequently, the ionic P2VP networks were swollen in a solvent mixture of methanol/methanesulfonic acid (MSA), where the swelling ratio governed by the cross-linking density of the P2VP block (Figure 1). This results in the domain spacing of the swollen films aligning with visible wavelengths, produced strong (> 68%) reflection of various visible wavelengths. When the films were applied to silicon solar cells, these DBR films caused only minor reductions in power conversion efficiency while maintaining vivid and intense colors. This approach for photovoltaics minimizes optical loss and facilitates the integration of zero-energy buildings with their surrounding environment.

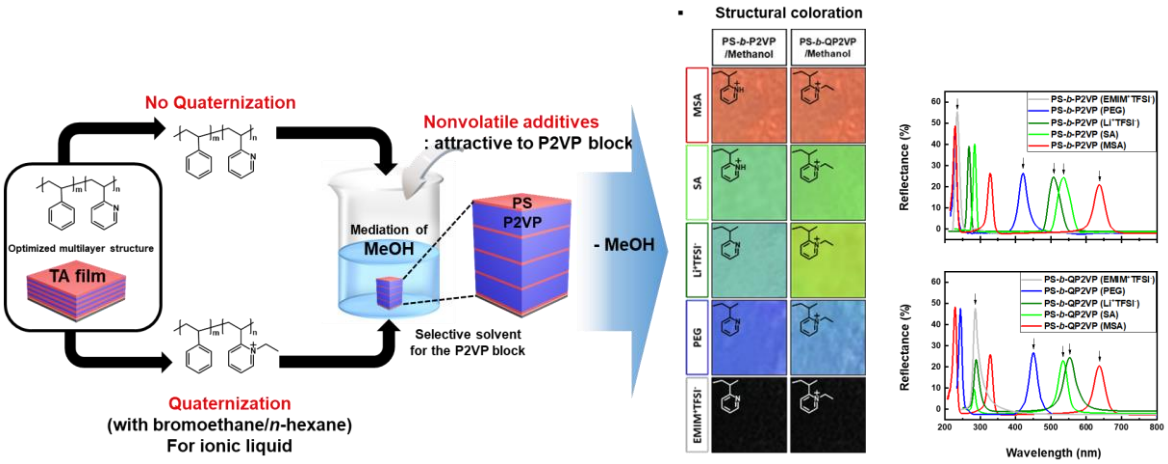

Figure 1 : Quaternization scheme and Optical properties of PS-b-(Q)P2VP films with FT-IR analysis

Submitting Author: mpark@yonsei.ac.kr

Phase behavior of aqueous solution of poly(N-vinylpyrrolidone-co-acrylic acid)

Miyu Sato, Isamu Akiba
Department of Chemistry, The University of Kiatakyushu, 1-1 Hibikino, Wakamatsuku, Kitakyushu, Fukuoka, 808-0135, JAPAN

Phase behavior of aqueous solutions of poly(*N*-vinylpyrrolidone-*co*-acrylic acid) (P(NVP-*co*-AA)) was investigated. The aqueous solution of P(NVP-*co*-AA) showed upper critical solution temperature (UCST) type phase behavior in low pH region, even though both NVP and AA are water-soluble monomers. It was considered that the UCST phase behavior was caused due to intramolecular hydrogen bonding between NVP and AA in P(NVP-*co*-AA).

1. Introduction

Water-soluble polymers are generally dissolved in water due to attractive interaction between water and polymers, so-called hydration. Since the hydration is weakened as temperature rises, aqueous polymer solution generally exhibits lower critical solution temperature (LCST) type phase behavior. Hence, introducing attractive interaction that competes with or is stronger than hydration into the polymers is expected to drastically change the phase behavior of aqueous polymer solutions due to the significant change in the balance of interaction. Thus, in this study, we investigate the phase behavior and interaction of poly(*N*-vinylpyrrolidone-*co*-acrylic acid) (P(NVP-*co*-AA)), in which both NVP and AA are strongly hydrated and NVP is strongly hydrogen-bonded with AA.

2. Experiment

P(NVP-*co*-AA)$_x$ was synthesized by radical copolymerization of *N*-vinylpyrrolidone (NVP) and *tert*-butyl acrylate (*t*BA) and then hydrolysis. Here, subscript *x* is the molar fraction of NVP in the copolymer. The characterization of the obtained P (NVP-*co*-AA)$_x$ was performed by ^{1}H-NMR and GPC-MALS / RI.

An aqueous solution was prepared by dissolving P (NVP-*co*-AA)$_x$ in ion-exchanged water adjusted to various pH using hydrochloric acid so as to achieve a predetermined concentration. The obtained aqueous solution was analyzed by state observation at a predetermined temperature, small-angle X-ray scattering, electron microscopy observation, and dynamic light scattering.

3. Results and Discussion

Fig. 1 shows the appearance of a 6.25 mg/mL aqueous solution (pH < 4) of P(NVP-*co*-AA)$_{0.25}$ at 93 °C and 80 °C. Although P (NVP-*co*-AA)$_{0.25}$ was uniformly dissolved in water at 93 °C, the aqueous solution became cloudy and generates precipitates ar 80 °C. This change in state of the aqueous P (NVP-*co*-AA)$_{0.25}$ solution was thermoreversible. This result means that the aqueous P (NVP-*co*-AA)$_{0.25}$ solution (pH < 4) shows upper critical solution temperature (UCST) type phase behavior. The lower the temperature, the stronger the hydrogen bonding between NVP and AA. Therefore, it is considered that phase separation of aqueous P(NVP-*co*-AA)$_{0.25}$ solutions during coolong from 93 to 80 °C was caused due to the formation of intramolecular hydrogen bonding between NVP and AA.

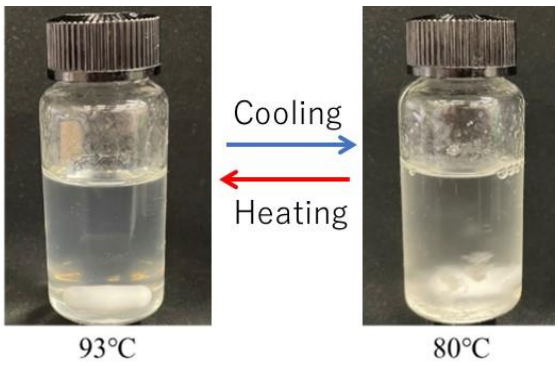

Fig. 1. P P(NVP-*co*-AA)$_{0.25}$ State change with temperature change of aqueous solution.

References

1) Akino, Y.; Morimoto, K.; Tsuboi, K.; Kanazawa, S.; Akiba, I. *Polymers* **2019**, *11*, 382.

下余白 30mm

Solvent Induced Chain Orientation of Cyclo Olefin Polymer Film

Yuki Nakama[a], Yuki Tamura[a] and Toshiyuki Awano[a]

[a]Zeon Corporation, Shin Marunouchi Center Building 14th Floor, 1-6-2 Marunouchi, Chiyoda-ku, Tokyo 100-8246, JAPAN

Cyclo Olefin Polymer (COP) has been used for optical applications such as lenses and films since 1990s. In the early 2000s, the discovery of the syntheses of stereoregular COPs paved the way to design new materials with attracting properties not found in conventional COPs[1]. Among those, syndiotactic poly(dicyclopentadiene) is a crystalline polymer which has excellent thermal durability and chemical resistance.

Recently, a unique method using dipping into solvent process that induced out-of-plane retardation(R_{th}) strongly was found[2]. The unique optical behavior was thought to correspond to the change of molecular chain orientation. In this research, we investigated the chain orientation behavior induced by the interaction with solvent using X-ray scattering measurement.

First, the COP film was prepared by the extrusion process. In this process, the film was amorphous and isotropic since the cooling rate was very rapid and no extension was applied. Next, the film was dipped into limonene bath and then dried in vacuum oven at 353K. We analyzed the molecular chain orientation by measuring 2-dimensional wide angle X-ray scattering (2-D WAXS). Figure 1 shows the 2-D WAXS images of the film taken from through and edge view. As seen in through view (Figure1(a)), the scattering was isotropic, meaning there was no in-plane orientation. On the other hand, the anisotropic scattering was observed in edge view (Figure1(b)), which can be attributed to chain alignment in thickness direction. It is considered that limonene doesn't dissolve the COP but induces chain orientation in thickness direction.

The effect of the type of solvent, the crystallization by post annealing and the control of optical properties will be presented. The estimated mechanism therein will be discussed.

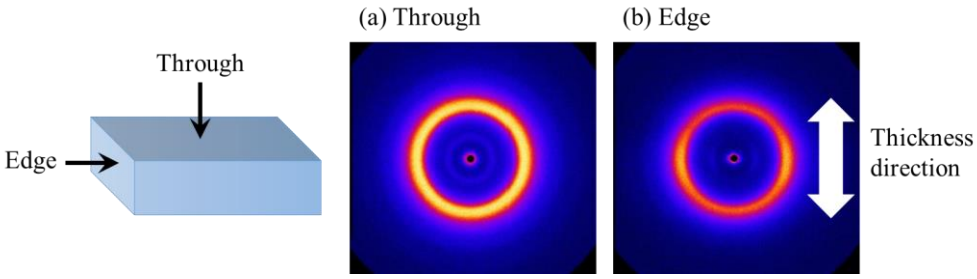

Figure 1: 2-D WAXS images of COP film after immersion in limonene and vacuum- dry. (a) Through and (b) edge view.

References

[1] H. Hayano *et al.*, *Macromolecules*, **36**, 7422-7431 (2003).
[2] K. Inoue *et al.*, IDW '22 FMC2-4 (2022).

Yuki Nakama: y.nakama@zeon.co.jp

Preferential Solvation of Lysozyme in Aqueous Solutions of Sugars or Polyols Studied by Small-Angle X-ray Scattering

Yasuyuki Maki[a*], Masahiko Annaka[a]

[a]Department of Chemistry, Faculty of Science, Kyushu University, 744 Motooka, Nishi-ku, Fukuoka, 819-0395, JAPAN

Sugars and polyols stabilize proteins in aqueous solutions. The stabilizing effect of these cosolvents is related to the preferential interaction of proteins with water or cosolvents; sugars and polyols are preferentially excluded from the vicinity of the proteins and therefore the proteins are preferentially hydrated. The strength of the preferential interaction has been represented by a preferential interaction parameter $\xi_3 = (\partial g_3/\partial g_1)_{T,\,\mu 1,\,\mu 3}$ calculated from densimetric data [1-3], where g_i, μ_i, and T is the concentration of component i, the chemical potential of component i, and temperature, respectively, and in a three-component system, water is designated as component 1, protein as component 2, and the cosolvent as component 3 . Recently, a simple method using small-angle X-ray scattering (SAXS) to quantify the preferential solvation of proteins in aqueous solutions of sugars or polyols was presented, in which the cosolvent concentration in the "solvation shell" around the protein was estimated from the scattering intensity [4-6]. In the present study, we measured SAXS of lysozyme in aqueous solutions of glucose, sorbitol and glycerol, and obtained the concentration of these cosolvents in the "solvation shell," from which the preferential interaction parameter ξ_3 was estimated using the relation $\xi_3 = A_3 - (g_3/g_1)A_1$, where A_i is the total amount of component i bound to the protein [1].

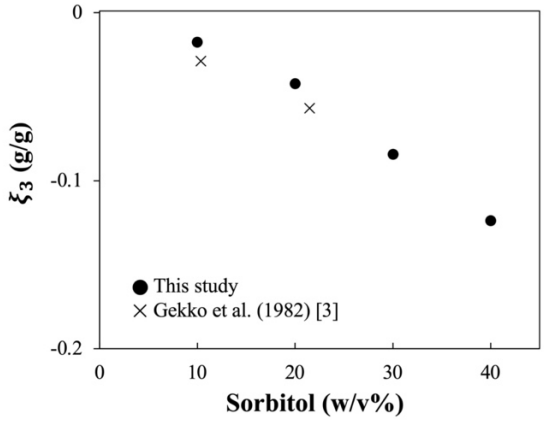

Figure 1: Preferential interaction parameter ξ_3 of lysozyme in sorbitol-water mixtures as a function of sorbitol concentration calculated from the SAXS data (this study, ●) and the densimetric data (Gekko et al. [3], ×).

References

[1] T. Arakawa *et al.*, *Biochemistry* **21**, 6536–6544 (1982).
[2] K. Gekko *et al.*, *Biochemistry* **20**, 4667-4676 (1981).
[3] K. Gekko, *J. Biochem.* **91**, 1197-1204 (1982).
[4] M. Hirai *et al.*, *Biophys. J.* **115**, 313-327 (2018).
[5] S. Ajito et al., *J. Phys Chem. B* **122**, 8685-8697 (2018).
[6] I. Kuroiwa et al., *J. Phys Chem. B* **128**, 676-683 (2024).

Yasuyuki Maki: maki@chem.kyushu-univ.jp

Fractionation analysis of micelles composed of polyglycerol mono fatty acid esters by field flow fractionation and small-angle X-ray scattering

Nanako Shimada[a], Hikaru Nonobe[b], Ryo Yamashita[b], Kenzi Murashima[b], Isamu Akiba

[a]Department of Chemistry & Biochemistry, The University of Kiatakyushu, 1-1 Hibikino, Wakamatsuku, Kitakyushu, Fukuoka, 808-0135, JAPAN
[b] Sakamoto Yakuhin Kogyo Co, 1-2-6 Awazi-mati, Chuo-ku Osaka 541-0047, JAPAN

Introduction Polyglycerol (PG), a nonionic water-soluble polymer, is attracting attention as an alternative to poly(ethylene glycol), and hydrophobically modified PGs, such as fatty acid esters of PG (PGFE), are widely used in cosmetic products. Since PGFE is amphiphilic and used as cosmetics in aqueous media, the structure of PGFE micelles determines the characteristics of the products. However, due to polydispersity of PGFE, structural characteristics of PGFE micelles, such as shape, size, and aggregation number, are also polydisperse. This makes it difficult to control the properties of PGFE solutions. Thus, in order to characterize the polydisperse PGFE micelles, we examined to perform a fraction-by-fraction analysis of PGFE micelles using a combination of field flow fractionation (FFF) and small-angle X-ray scattering (SAXS).

Experiment Polyglycerol monofatty acid esters (G*x*C*y*) with different degrees of polymerization and carbon numbers of fatty acids were used as samples. Here, *x* is the degree of polymerization and *y* is the carbon number of fatty acid. G*x*C*y* was dispersed in pure water at a desired concentration, and the resulting aqueous solution was homogenized using ultrasonic waves. The prepared sample solution was fractionated by FFF combined with multi-angle light scattering (FFF-MALS), and SAXS measurements were performed on each fraction. In order to characterize the G*x*C*y* molecules in the fractionated micelles by GPC, each fraction was dried and the obtained materials were dissolved in THF.

Result and Discussion FFF-MALS elugram for G10C12 micelles shows two peaks. The fractions at the short and long elution times are designated as F7 and F9, respectively. For the F7 and F9 micelles SAXS measurements were performed at SPring-8 BL-40B2. Figure 1 shows the SAXS profiles from F7 and F9 micelles. The SAXS intensity ($I(q)$) of F9 micelles in $q < 0.2$ nm^{-1} is proportional to q^{-2}, where q is the absolute value of the scattering vector. This indicates that the micelles in F9 have a planar structure. The solid lines in the figure are the results of fitting analyses with scattering functions of a ellipsoidal oblate for F7 and a plate-like particle for F9. Because the calculated SAXS curves are in good agreement with the experimental data, F7 and F9 micelles form ellipsoidal oblate and plate-like forms, respoectively. The GPC measurements for the components in F7 and F9 showed that *x* of F9 components are lower than than that of F7. A smaller *x* of PG corresponds to a relatively larger volume of the hydrophobic chains. The volume ratio of hydrophilic to hydrophobic groups strongly aggects the curvature of the micelle interface. Therefore, it can be considered that F9 composed of components with lower *x* formes plate-like micelles with small interfacial curvature.

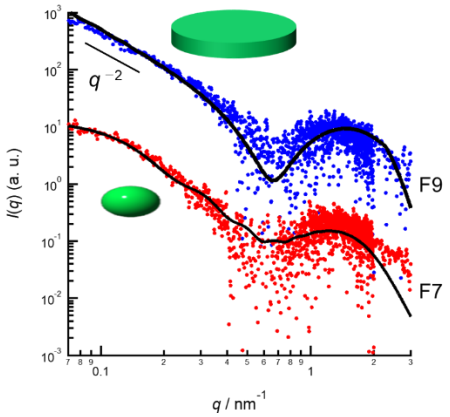

Figure 1 SAXS profiles G10C12 micelles fractionated by FFF.

Submitting Author: f4maa013@eng.kitakyu-u.ac.jp

Characterization of drug-loaded monodisperse nanoparticles using small-angle X-ray scattering (SAXS)

Takuma Kojima[1], Shin Takano[1] and Kazuo Sakurai[1*]
[1]*Faculty of International Environmental Engineering, The University of Kitakyushu, 1-1 Hibikino, Wakamatsu-ku, Kitakyushu, Fukuoka 808-0135, JAPAN*

Introduction

Spherical polyacrylic acid particles (SPAA) with a narrow particle size distribution can be prepared by precipitation polymerization in acetonitrile [1]. Their distribution, expressed as a molecular weight distribution, is less than 1.05 [2]. Monodispersibility provides consistent physical and chemical properties throughout the particles, which is a great advantage in designing drug carriers.
In this study, the anticancer drug doxorubicin (DOX) was encapsulated in SPAA and the structure of the complex (SPAA/DOX), including drug inclusion rate and drug inclusion state, was analyzed.

Experimental

SPAA was synthesized by precipitation polymerization in acetonitrile based on previous studies [1,2]; DOX was used to calculate the drug inclusion rate by UV-vis measurements due to its UV absorption properties; the structures of SPAA and SPAA/DOX were characterized by dynamic light scattering (DLS) small-angle X-ray scattering (SAXS) and transmission cryo-electron microscopy (Cryo-TEM).

Results and discussions

Fig. 1.A shows a Cryo-TEM image of SPAA/DOX, which clearly shows that DOX is encapsulated in the center of SPAA forming a core. The relationship between the electrostatic interaction between SPAA and DOX is shown in Fig. 1.B. Since the complexation efficiency decreases as the salt concentration of the solvent is increased, the electrostatic interaction is considered to contribute to this complexation.
Fig. 1.C shows the SAXS profile of SPAA, which is in good agreement with the theoretical curve of the rigid sphere model indicated by the black line, indicating that the particles are monodisperse and spherical.
Detailed structural analysis of SPAA/DOX will be discussed in the presentation.

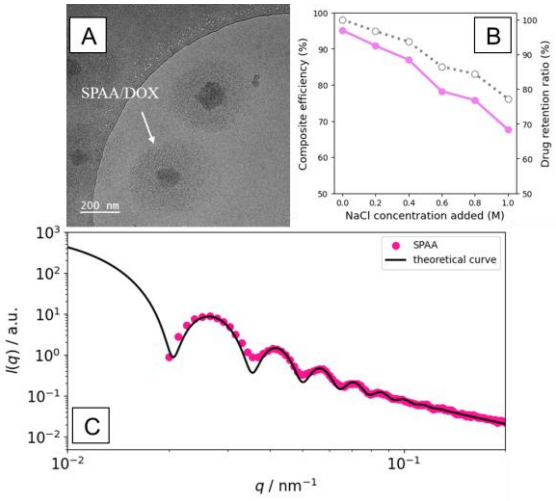

Figure 1. (A) Cryo-TEM image of SPAA/DOX (B) Complexation (pink) and drug retention efficiency (gray) due to electrostatic interaction (C) SAXS profile of SPAA in PBS. Dots and solid line indicate the experimental data and theoretical curve, respectively. This measurement was performed at the BL40B2 beamline of the SPring-8 facility, Hyogo, Japan.

References

[1] H. Minami et al., *Langmuir* 2020, 36, 11957−11962
[2] S. Takano et al., *Polymer Journal*, 1-5, 2023

Submitting Author: f4mab006@eng.kitakyu-u.ac.jp

Microphase Separation of Dual Polysulfobetaine Diblock Copolymer Aqueous Solutions

Yasuhiro Eguchi[a], Yuji Higaki[b] *

[a]Graduate School of Engineering, Oita University, 700 Dannoharu, Oita, 870-1192, JAPAN
[b]Faculty of Science and Technology, Oita University, 700 Dannoharu, Oita, 870-1192, JAPAN

Introduction

Zwitterionic block copolymers produce ordered lattice structure in concentrated aqueous solutions through the zwitterion-specific intermolecular interactions. The mesoscale phase separation is expected as a novel biocompatible molecular compartment that is valid for molecular containers [1]. The phase-separation behavior of diblock copolymers composed of poly(sulfobetaine methacrylate)s with different charged group spacer length (CSL), PSB2-*b*-PSB4, in water was investigated (**Figure 1**).

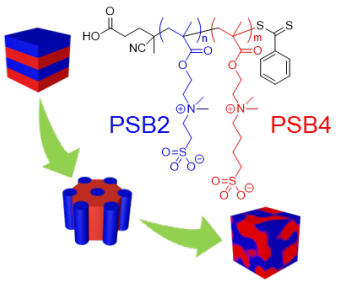

Figure 1. Morphology transitions of PSB2-*b*-PSB4 aqueous solutions.

Experiment

Sulfobetaine monomers of SB2 and SB4 were synthesized following previous report [2]. PSB2, PSB4, and PSB2-*b*-PSB4 were prepared by reversible addition-fragmentation chain transfer polymerization. The aggregation state of PSB2 and PSB4 in water was verified by the hydrodynamic radius of gyration (R_h) determined by dynamic light scattering (DLS), and the ordered lattice morphology produced in the PSB2-*b*-PSB4 concentrated solutions was figured out using small-angle X-ray scattering (SAXS).

Results and discussion

The degree of polymerization (DP) for PSB2 macro-CTA was 104, and the molecular weight distribution (M_w/M_n) was 1.11. Block copolymers with PSB4 DP of 76, 102, 164, 278, 443, and 554 with narrow M_w/M_n were prepared. $PSB2_{104}$ exists in water as a single chain with R_h of 7.9 nm, while $PSB4_{103}$ was insoluble to water. SAXS profiles of the 60wt% PSB2-*b*-PSB4 aqueous solution showed scattering peaks, indicating the mesoscale ordered lattice structures (**Figure 2**). The lamellar structure transformed to a columnar structure as the volume fraction of PSB4 (f_{PSB4}) increased. The PSB4 phase volume expansion leads to the interfacial curvature modulation, resulting in the morphology transition. The scattering peaks were broad over $f_{PSB4} = 0.84$, indicating the structure disordering with a lack of periodic lattice. The cohesive interaction is pronounced as the DP of PSB4 increased, and the excess aggregation disrupts the phase ordering. Thus, the microphase separation of dual sulfobetaine diblock copolymers was induced by zwitterion-specific interactions due to the difference in CSL, and that the morphology transition depended on the f_{PSB4}.

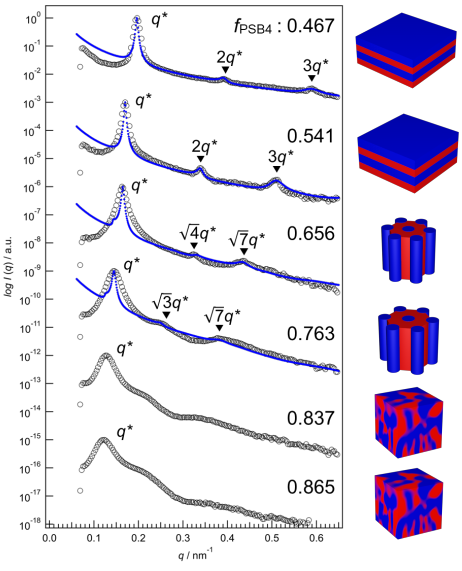

Figure 2. SAXS intensity profiles of 60wt% $PSB2_{104}$-*b*-$PSB4_m$ aqueous solutions with $f_{PSB4} = 0.47$, 0.54, 0.66, 0.76, 0.84, 0.87..

References:[1] Takahashi, M.; Shimizu, A.; S. Yusa.; Higaki, Y.; *Macromol. Chem. Phys.* **2021**, *4*, 20000377. [2] Kratzer, D.; Barner, L.; Friedmann, C.; Bräse, S.; Lahann, J.; *Chem. Eur.* **2014**, *36*, 8064-8071.

Yasuhiro Eguchi: v23e4006@oita-u.ac.jp

Sample Abstract of CeSMS2024: Information for Authors

Yuri Tanimura[a], Kazuki Sumiya[a], Hiroto Izumi[b] and Kazuo Sakurai[a]

[a]*Department of Chemistry and Biochemistry, The University of Kiatakyushu, 1-1 Hibikino, Wakamatsuku, Kitakyushu, Fukuoka, 808-0135, JAPAN*
[b] *The University of Occupational and Environmental Health, 1-1 Iseigaoka, Yahatanishiku, Kitakyushu, Fukuoka, 807-8556, JAPAN*

In our laboratory, schizophyllan (SPG), a polysaccharide β-1,3-glucan, is used as a drug carrier by taking advantage of its ability to form complexes with nucleic acids and to be recognized and internalized by Dectin-1 expressed on the cell surface.
Recent studies have led to the discovery of a complex with no molecular weight distribution (q1 quantized complex) consisting of a single nucleic acid molecule and an SPG appropriate for the chain length of the nucleic acid. We have devised a method to synthesize antisense nucleic acids that inhibit the proliferation of two target genes at the ends of the q1 quantized complex, and to expect further growth inhibition effects on genes whose proliferation is not well inhibited by a single target gene alone.
In this study, we evaluated the expression ratio of GLUT1, a gene related to glucose metabolism, in macrophages after administration of nucleic acid drugs, using siRNAs (siVHL and siNF-κBIA) of two genes that inhibit glucose metabolism, by real-time PCR and Western blotting. The expression levels of GLUT1 were evaluated, respectively. In subsequent experiments, macrophage-like cells treated with SPG and nucleic acid (siRNA) complexes showed increased expression of GLUT1 in both experimental systems. These results suggest that the administration of siRNA-based complexes to macrophage-like cells may be a way to activate glucose metabolism in macrophages.

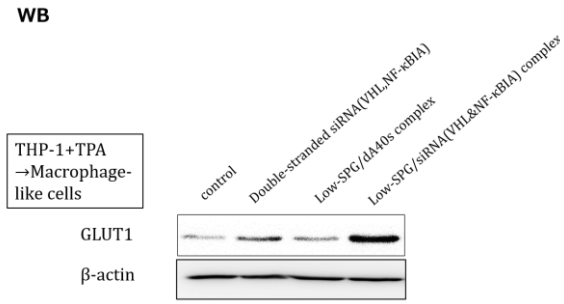

Figure 1: Expression levels at the protein level.

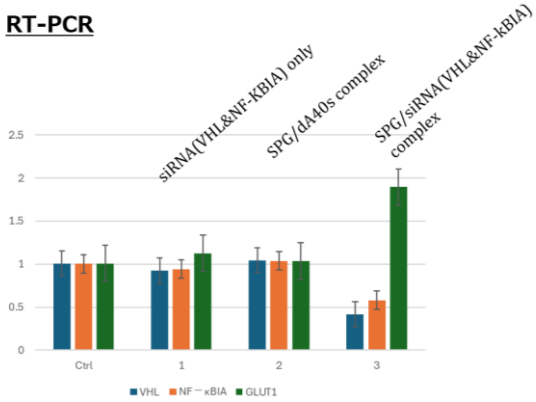

Figure 2: Expression levels at the gene level.

References

[1] K. Sumiya et al. *Chem lett* (2021).

Yuri Tanimura : e3mab013@eng.kitakyu-u.ac.jp

Development of Nanoparticles Capable of Encapsulating Large Amount of Drugs and Elucidation of the Encapsulation Mechanism.

T. Kosugi, K. Sakurai*

Department of Chemistry and Biochemistry, The University of Kiatakyushu, 1-1 Hibikino, Wakamatsuku, Kitakyushu, Fukuoka, 808-0135, JAPAN

Polymeric nanoparticles tend to accumulate in tumor tissues more than in normal tissues through the enhanced permeability and retention (EPR) effect, making them potential drug carriers in drug delivery systems. Our group developed a hyperbranched polymer made from cyclodextrin (CDNP), which has hydrophobic cavities that can encapsulate hydrophobic drugs.[1] [2] CDNP was synthesized through the reaction between the hydroxyl groups of cyclodextrin and the epoxy groups of epichlorohydrin (ECH). This structure enhanced cyclodextrin's encapsulation ability by over 100 times, demonstrating CDNP's potential as a carrier for the anticancer drug α-mangostin (MGS). However, CDNP's small size (<10 nm) limited its efficiency in EPR-based drug delivery, where particle sizes of 10 to 200 nm are preferred.

To address this, we synthesized a new CDNP using polyethylene glycol diglycidyl ether (PEGDE) instead of ECH to achieve a more suitable size for the EPR effect. This new CDNP successfully encapsulated MGS at a loading capacity nearly five times higher than that of ECH-based CDNP. The synthesis of CDNP involved reacting the hydroxyl groups of cyclodextrin with PEGDE under alkaline conditions. MGS was encapsulated in the CDNP, and unbound MGS was removed by centrifugation and dialysis. The amounts of MGS were quantified using UV spectroscopy, and the drug loading rate was calculated. The structural properties of drug-loaded CDNP were evaluated using dynamic light scattering (DLS) and small-angle X-ray scattering (SAXS).

The hydrodynamic radii of CDNP prepared with PEGDE and ECH were compared, showing that PEGDE significantly increased the particle size. PEGDE-based CDNP was five times larger than ECH-based CDNP, likely due to the excluded volume effect of the polymer crosslinking agent.

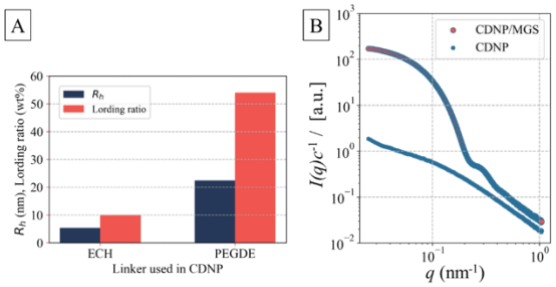

Fig.1 (A) The comparison of the hydrodynamic radius and MGS loading ratio when changing cross-linkers. (B) SAXS profile of PEGDE-based CDNP and its MGS complex.

The loading capacity for MGS also dramatically increased in PEGDE-based CDNP. Using synchrotron SAXS at the SPring-8 facility, we further analyzed the PEGDE-based CDNP/MGS complex structure. The SAXS profile of PEGDE-based CDNP indicated a Gaussian chain scattering, while the profile of the PEGDE-based CDNP/MGS complex exhibited scattering typical of spherical structures. This structural change likely explains the high drug-loading capacity of PEGDE-based CDNP.

References

[1] V. T. H. Doan, S. Fujii, K. Sakurai *et al.*, *Polymer Journal* 52, 457-466(2020)
[2] V. T. H. Doan, S. Fujii, K. Sakurai *et al.*, *Polymer Journal* 53, 481-492(2021)

Tomoki Kosugi: sakurai@kitakyu-u.ac.jp

Silicon- and Fluorine-containing Block Copolymer Films featuring sub-10 nm perpendicular lamellae and Electric-field induced Directed Assembly

Junsu Kim[a], Seungbae Jeon[b], Seungjae Lee[a], and Du yeol Ryu[a*]

[a]*Department of Chemical and Biomolecular Engineering, Yonsei University, 50 Yonsei-ro, Seodaemun-gu, Seoul 03722, Korea*
[b]*Advanced Materials Division, Korea Research Institute of Chemical Technology (KRICT), Daejeon 34114, Korea*

Lamellar-forming block copolymer (BCP), polydimethylsiloxane-*b*-poly(2,2,3,3,3-pentafluoropropyl acrylate) (PDMS-*b*-PPeFPA), was designed to provide high-χ, low-N, low-T_g, and similar surface energies between the two blocks, eliminating the need for top-coat materials. We observed that the lamellar structures in BCP films transitioned from parallel to perpendicular orientation by varying the substrates, including standard Si with a native oxide layer, H-passivated Si, and physically adsorbed layers. Detailed analysis revealed that physically adsorbed copolymer layers promote perpendicular lamellar orientation due to compositional randomness on the substrates. Additionally, the significant dielectric contrast between the blocks led to unidirectional alignment of perpendicularly oriented lamellae under a lateral electric field. To facilitate nanoimprint lithography, we fabricated an inorganic-based (oxidized-PDMS) nano-template using O_2 plasma treatment (Figure 1).

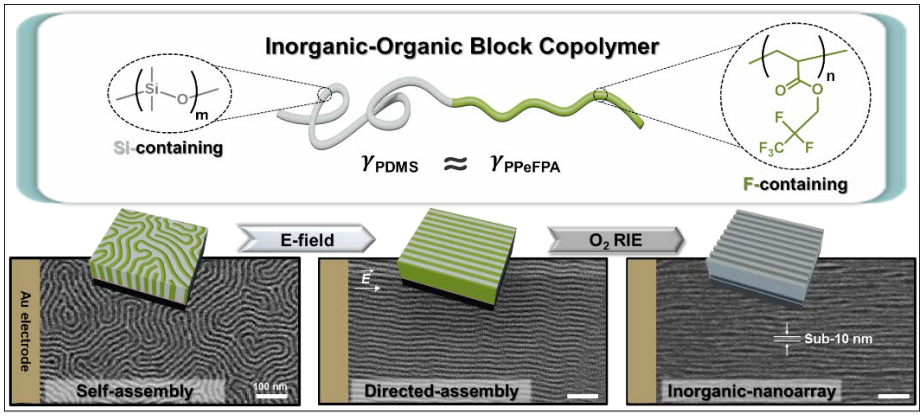

Figure 1: molecular scheme of the BCP and electric-field application

Submitting Author: dyryu@yonsei.ac.kr